A STUDY ON THE SPLIT HOPKINSON BAR TESTING IN COLD ENVIRONMENTS

Frank Gronwald & Emily Asenath-Smith
US Army Corps of Engineers

INTRODUCTION

The split Hopkinson bar is a current method that is primarily used to determine the material properties of a specimen at very high strain rates. With this technique, the impact and blast resistance of materials can be assessed.The split Hopkinson bar name is often interchanged with the Kolsky bar but there is one important distinction between them. The Kolsky bar is used for compression and tension experiments while the split Hopkinson bar is just focused on testing compression material performance (Hong et al, 2016).The initial motivation to create the modern Hopkinson bar system stemmed from the desire to measure the pressure-time curves produced by a detonation or a bullet impact. Conventional load frames apply loads under quasi-static conditions with strain rates only up to a range between 10^{-4} to 0 s^{-1}. Thus they have limited utility for impact scenarios. Ge et al (2017) found that split Hopkinson bars would produce valid data provided two conditions are met:

1) 1-D elastic wave theory is valid in pressure bars
2) Stress and strain rates within specimen are uniaxial and uniform.

They made sure the first was met by both limiting the impact velocity to ensure pressure bars were elastically deformed *and* using proper length to diameter ratios for bars and striker to eliminate wave dispersion. The second condition was met by eliminating friction restraints and axial inertia and using lubricant.

PREVIOUS HISTORY

In 1872, John Hopkinson conducted rupture tests of an iron wire by the impact of a drop weight to prove the existence of stress waves in the wire. While the stress waves could be seen indirectly, there was not yet a way to measure the magnitude of stress waves using what was available in the 19th century. His son, Bertram Hopkinson, in 1914, invented a pressure bar to measure the pressure produced by high explosives or high speed impact of bullets. Bertram Hopkinson then attempted to further improve upon his father's work by introducing a technique for determining the pressure – time relations due to an impact produced by a bullet or explosives.

Hopkinson's initial apparatus consisted of: a long steel rod, a short steel billet, a ballistic pendulum, and a means of developing impact like pressures. **Error! Reference source not found.**displays his experimental design (Chen and Song, 2012). The machine worked byhaving a known object impact one end of the rod (A), which would generate a compressive pressure wave of finite length inside the rod. At the other end of the rod, a short steel billet was attached by a thin layer of grease (C). Hopkinson's theory was that the compressive wave travelled down the bar, through the greased joint, and into the billet. The wave would be then reflected at the far end as a pulse of tension. Since the grease could not withstand any appreciable tensile loads, the billet would fly off with a definite momentum, measured with a ballistic pendulum (D). The time over which this momentum acted was the round trip time of the longitudinal wave in the billet. By running several tests of identical magnitude but using different length cylindrical billets, he was able to generate a series of pressure–time curves. Hopkinson proved to be excellent in the determination of both the maximum pressure and total duration of these impact events, but the pressure-time curves produced were always slightly inaccurate.

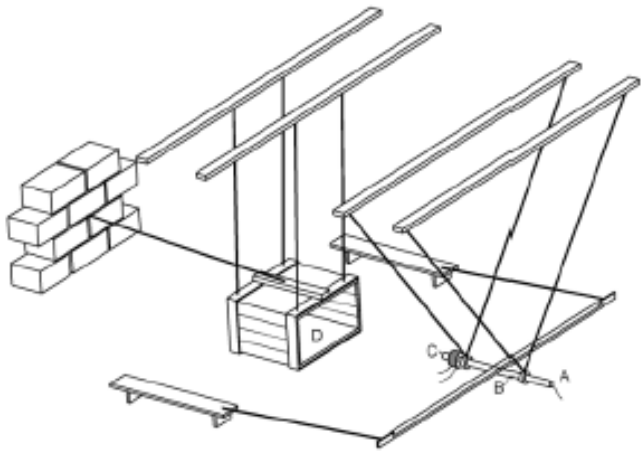

Figure 1. Hopkinson experimental design

Davis (1948) performed a critical study of Hopkinson's technique using parallel plate and cylindrical condenser microphones to electrically measure the axial and radial movements of a bar loaded by detonation. These electrical measurements have proven to be more accurate than Hopkinson's method. Davis also discussed the dispersion of stress waves when propagating in a long rod. Davies, in the next phase of his research, developed a technique using condensers to measure the strains existing in the pressure bar. The output from the condenser is proportional to the displacement–time relations that are proportional to the pressure-time relations assuming the pressures in the bars are under the elastic limit of the material. Using condensers to measure strains greatly improved the accuracy of Hopkinson's original apparatus, which relied on measuring the momentum of a steel billet flying off the end of the pressure bar. One main reason for this is that Hopkinson attached these billets with a film of grease, which introduced uncertainty regarding to the forces required to break the greased joint.

In 1949 Kolsky added a second pressure bar to Hopkinson's original apparatus and changed the name to split Hopkinson bar. Instead of attaching a billet at the far end of a bar, Kolsky placed the specimen between the two bars. He developed many of the equations for calculating specimen properties based on strain histories in the bars. The strains were measured using similar condensers as those used by Davies. Of course the two bar apparatus now required calibration measurements for both bars. This two bar technique has become the most widely used testing procedure today.

The more advanced theory governing the specifics of Hopkinson bar testing has been around for decades. Dennison Bancroft solved the principle equation for the longitudinal wave velocity in cylindrical bars in 1941. Bancroft expressed the velocity of longitudinal waves in cylindrical bars in terms of a wave of infinite wavelength, Poisson's ratio, and the ratio of the bar diameter to the wavelength of interest. It has only been in the last decade or so, that Bancroft's work has been applied towards Hopkinson bar testing due to the rapid calculations that can be made using the that significant data processing advancements in computer software.

There have also been several enhancements to the split Hopkinson bar in the mid to late 20th century. The primary alterations were to adapt it for testing of other modes. The first modification was in the interest of conducting tensile tests (Harding et al. 1960, Hauser 1966, Lindholm and Yeakley 1968, Christman et al. 1971, Nicholas 1981, Harding 1983, Ross et al. 1984). Duffy et al. (1971) then modified the split Hopkinson bar to achieve high strain rate in torsional loading. They found that the main benefit of the torsional mode was the fact that the wave propagation was constant in all directions, and thus would not be subject to the radial inertia effects. Nicholas (1975) went further in the Kolsky bar redesign, enabling it to conduct a dynamic three-point bend test similar to the impact tests performed using Charpy machines. That was performed with only a single bar instrumented with a strain gauge. Klepaczko (1980) used a wedge-loaded specimen in a conventional split Hopkinson bar of the Hopkinson bar method toobtain dynamic load-displacement data. This method is still used today in thestudyof dynamic fracture-initiation properties of materials.

Types of Data Produced

The splitHopkinson bar operates out of the principles of unidirectional stress wave propagation. The impact produced by the striker bar on the Hopkinson bar lasts for a few hundred microseconds, and then a small but finite time passes. The impact force will then generate a compressive wave that travels down the incident bar. It then proceeds to enter the specimen at the opposite end of the bar. Upon entering the specimen, a portion of the incident stress wave is propagated

into the transmitter bar and another portion is reflected back into the incident bar due to an impedance caused by the specimen and the bars having different material makeup and structure. These incident, reflected, and transmitted stress waves are measured by strain gaugesthat are placed in various locations on the bars as shown in Figure 2. Some of the energy from the incident wave may be absorbed by the specimen as heat.These internal reflections build up the stress level in the specimen gradually and work to further compress the specimen. Generally the sums of the magnitudes of the transmitted and reflected waves should equal or be very close to that of the incident wave.

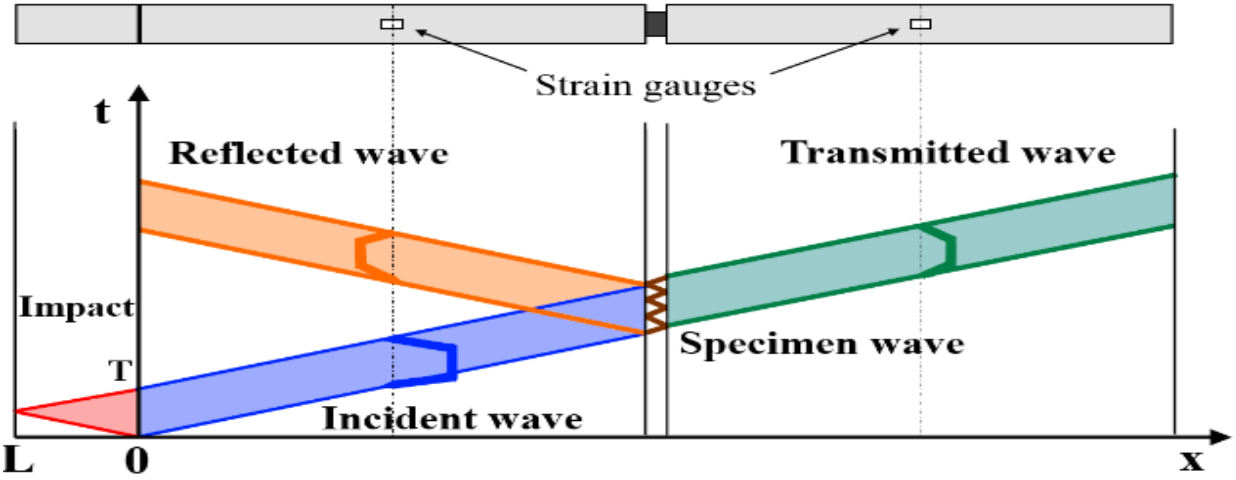

Figure 2. Waveforms produced by Hopkinson Bar

Figure 3 shows the expected results of a typical Hopkinson experiment. The time between the incident, transmitted, and reflected waves appearing is dependent on the type of material being tested, the material and length of the bars, and the speed that the striker was launched.

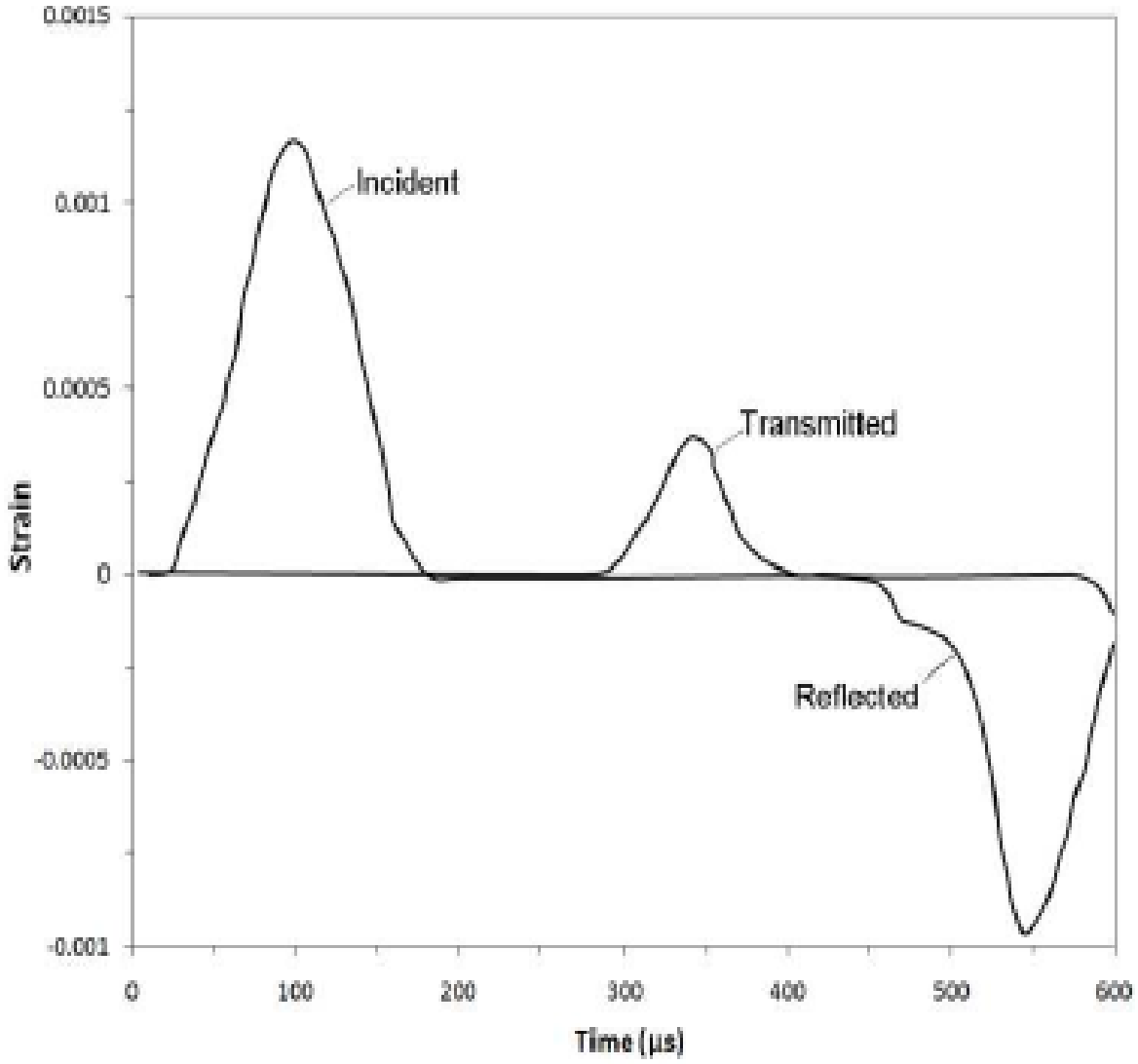

Figure 3. Waves made by Hopkinson Bar

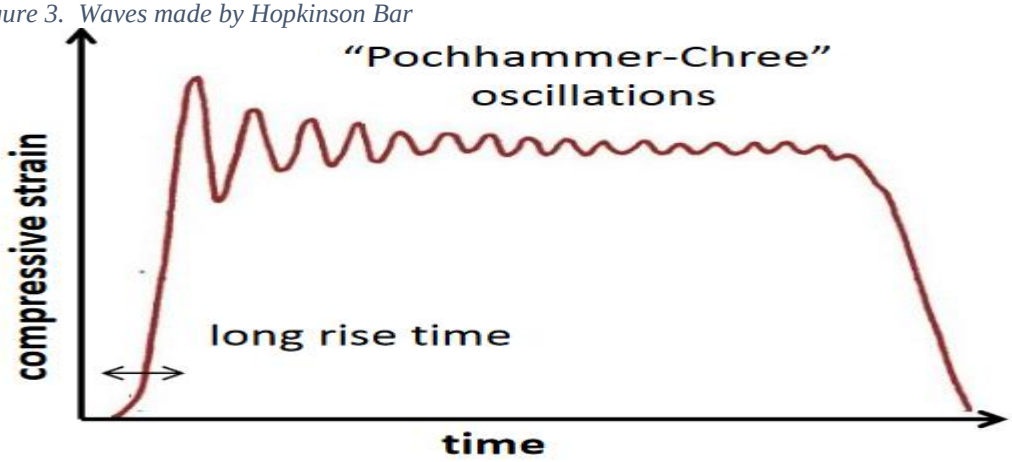

Figure 4. Pochammer-Chree Oscillations

Relevance Today

Laboratory instrumentation can record the stress waves in the incident bar propagating towards the specimen and being reflected back from the specimen and the wave in the transmission bar. Under this arrangement the impact event is controllable and quantitative. The impact velocity and specimen size may be varied to achieve different strain rates. Further analysis on the waves recorded in the impact event will result in information regarding the loading conditions and deformation states in the specimen. Much of the recent work involving the Hopkinson bar testing has been focused on finding new materials that can expand their capabilities. Clarke et al. (2016) created adaptive housing for the strain gauges so that they can be placed far enough on the incident bar to avoid being damaged by munitions blasts while still giving accurate measurements. Field and Walley (2013) applied the split Hopkinson bar to study shock physics and perform experiments on brittle materials such as ceramics and glass. This is now being applied to find other types of materials that contain a region in their makeup where the shock impedance is lower. Rosenberg et al. (1990) found that there was an increase in penetration depth when glass specimens were struck by a flattened projectile. Such research will assist in planning against near field explosions such as those from an IED. This general change in research is due to the focus of designing structures that can withstand greater amounts of forces from explosions and natural disasters such as hurricanes and earthquakes.

CRREL Bars

The split Hopkinson bar that was operated at CRREL was composed of three major subsystems: the stress generating system, the specimen cooling system, and the stress measurement system. Figure 1 displays a schematic produced by Dutta et al (1987). The stress generating system consisted of a reservoir with a quick opening solenoid valve, launch cylinder, striker, incident bar, transmitter bar, and shock absorbing system. One important thing to keep in mind is that before each test the compressed air reservoir will need to be recharged to the desired pressure with the compressor. The firing stage is then implemented, and the compressed air gets released through a quick-opening valve. This burst of air accelerates the striker down the launch cylinder. This process essentially converts the potential energy of the gas into the kinetic energy for the striker. Dutta et al (1987) found that the impact between striker and incident bar should occur on a plane normal to the desired direction of stress propagation. That means that it is vital that the striker and the bars must be properly aligned. Proper alignment is also important to ensure that the bending waves generated due to the reaction are kept to a minimum. Otherwise these waves will be sensed by the strain gauges and disrupt the true uniaxial compression or tension signals.

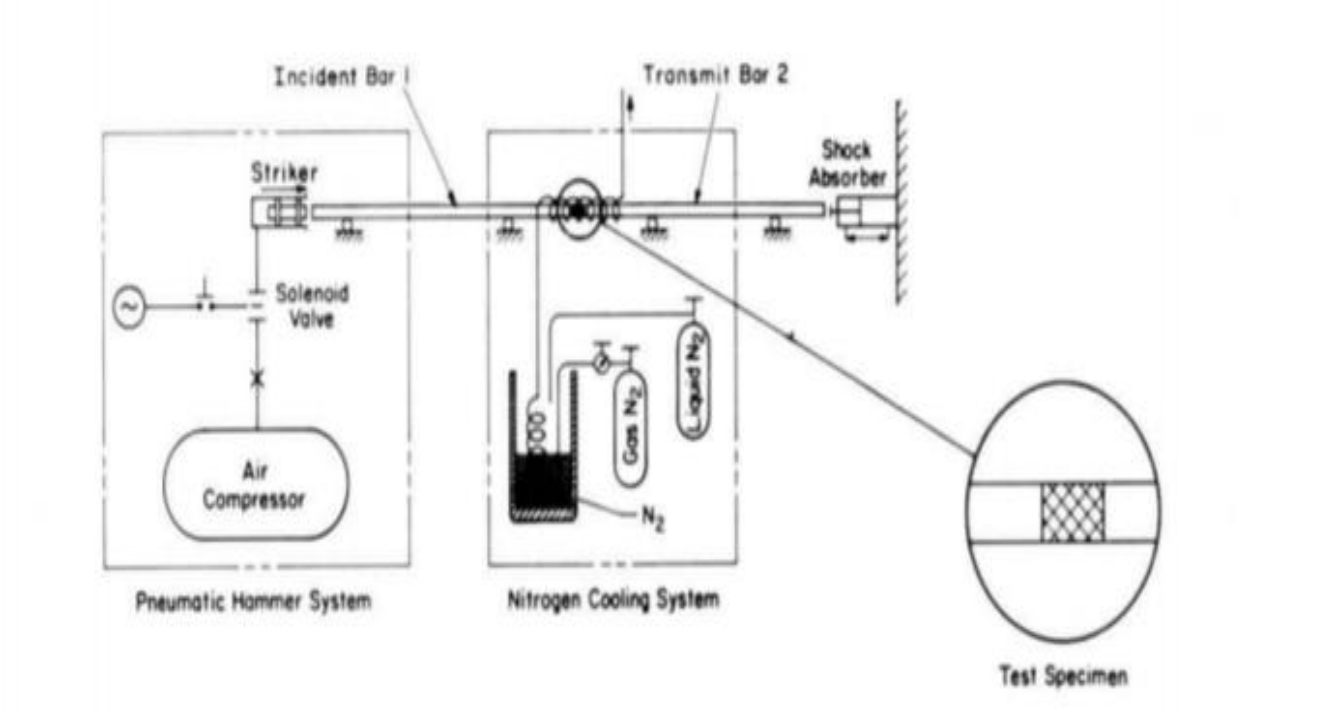

Figure 5. Hopkinson bar system designed for CRREL lab

Each bar is then guided through a set of three support blocks with low friction ball bearings to maintain proper alignment and prevent the creation of stress waves. The support blocks were designed withlow-friction ball bearings to help reduce the spreading of stress waves. These support blocks as well as the launch cylinder are then mounted on a long rigid table. One of the benefits of the design are that the blocks and the impactor can be adjusted to ensure adequate alignment through testing. It is vital for the consistency of the measurements that the striker, incident bar, specimen, and transmitter bar are all in alignment.

In the CRREL system the striker, the incident bar, and the transmitter bar are made of 303 stainless steel. These stainless steel bars were chosen in part for their low corrosivity. Dutta et al (1988) found that the stress developed in the bar needs to be kept below its yield stress (462 MPa) to maintain the integrity of the system. It was also advised to limit the stress level to 50% of the yield stress, thus the striker velocity should not exceed 11.6 m/s. The yield strength of the bars must be about four times stronger than the materials being tested. By using the kinetics of the striker motion, Dutta et al (1987) found that at 100 psi a 2 inch striker stroke was sufficient to reach this velocity. The striker was created with a 12 in. length and the same diameter as the incident bar and the transmitter bar 1.5 in. Both the incident bar and the transmitter bar had a total length of 8 ft. The striker, incident bar, transmitter bar, and the support blocks were designed to test materials with yield strengths below 231 MPa. The dynamic yield strength values for many materials typically will be two to three times greater than those found in quasi-static testing.

The specimen cooling system was devised out of a requirement to test material performance at cold temperatures. The system worked by essentially surrounding all of the ends of both bars by two copper-coiled enclosures through which cooled nitrogen gas is circulated. The nitrogen gas temperature is then further reduced via the process of circulating it through a liquid nitrogen bath. Reinhardt et al ((1985) were the first to design a testing apparatus that could test the effects of extreme cold on concrete. The cold box used had a 210mm height and 270 mm outside diameter with a layer of 5mm thick glass fiber epoxy resin with insulated foam between the outer and inner walls for insulation. A major problem found during testing was the creation of thermal stresses due to the difference of thermal expansion coefficients of the aluminum bars and the concrete samples. This was fixed by gluing 30mm thick steel plates to the ends of the specimen and the bars. Liquid nitrogen was used as the cooling solution which enabled temperatures to fall as low as -196 C and a Commodore 64 microcomputer was used to regulate the temperature with a thermal resistor.

Dutta et al. (1987) designed the cold box so that even the coils were kept insulated by being enclosed in a Styrofoam container. The specimen temperature was monitored with a thermocouple. Temperature is controlled by the level of immersion of the cooling coil in the liquid nitrogen and the flow rate of the nitrogen gas through the coils. It was found that if the coils were operated continuously, the temperature of the ends of the Hopkinson bars would decrease. This meant that there could be rapid re-stabilization of specimen temperatures. This cooling system helped Dutta et al (1987) achieve a stable temperature as low as -90 °F over the period of a couple of hours. Figure 2 shows one of the cold boxes used at CRREL and Figure 3 displays an aerial view of its contents. They were designed so that they could contain the specimen and keep the immediate air environment at the needed constant temperature.

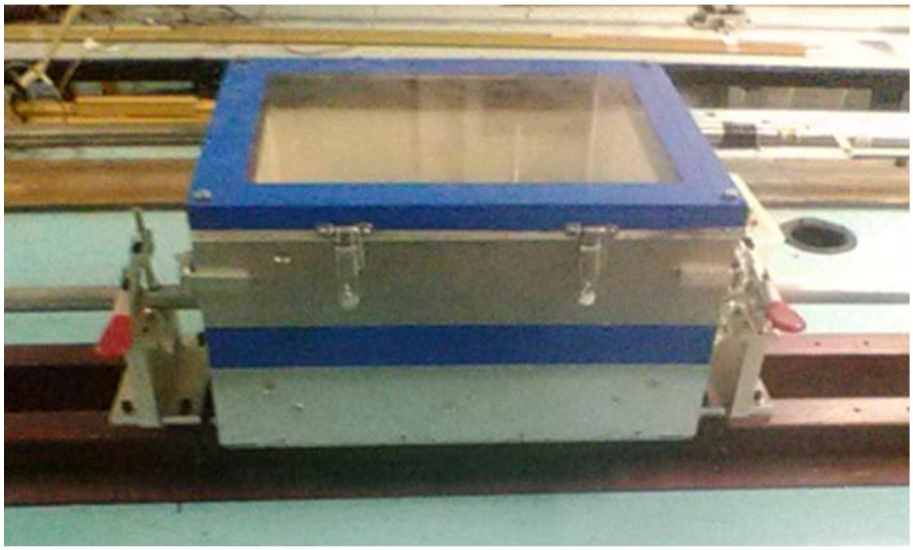

Figure 6. Side image of the cold box

Figure 7. A top view of cold box

TYPES OF MATERIALS TESTED

The main focus of the Hopkinson bar testing at CRREL wason several specimen materials including brass, Teflon, and polycrystalline ice.Many studies have been undertaken in recent history. Lau et al (2001) explored the effects of the cold on Fiber reinforced plastic materials and how they are impacted by being bonded with a concrete beam. Dutta (2001) was able to pinpoint the process composites undergo when they begin to fracture at extremely cold temperatures. There are three sets of bars available for testing (tension, compression, and torsion). Dutta et al (1996) was able to display their layout and it is shown in Figure 4.Other studies have altered Hopkinson barsto provide confinement testing for rock, ceramics, and concrete (Heard et al, 2014; Dutta and Kim, 1993; Dutta et al, 1991). In some cases mechanical sleeves were used to provide additional lateral confining pressureas discovered by Nwosu et al, (2002). Sand from the Ottawa region was tested for its compressive strength and how it is affected by the degree of saturation by Lin et al (2016). A lot of these studies are driven by the desire to obtain data on a wide range of materials for impact modelling purposes. Examples include polymer foams (for crash dummies) (Zhao 1997), metal foams (for blast mitigation) (Yi et al. 2001, Hanssen et al. 2002, Lopatnikov et al. 2003), polymer-bonded explosives (Gray III et al. 2000, Siviour et al. 2003), and semi-brittle materials such as concrete (Albertini et al. 1999). Soft materials such as muscles, tendons, and brain matter have also been tested. Johnson et al (2016) used the split Hopkinson bar to evaluate the strength of the keratin found in big horn sheep.

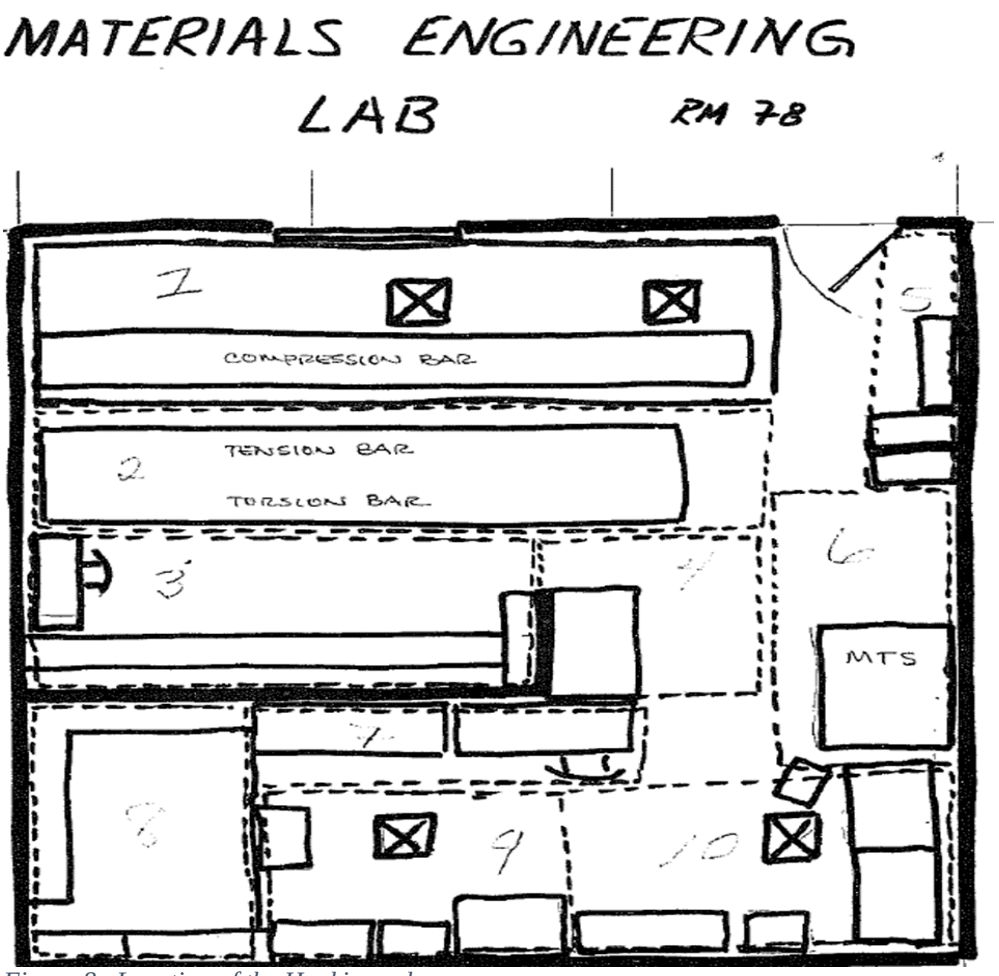

Figure 8. Location of the Hopkinson bar

NOTEWORTHY RESEARCH OUTCOMES

One of the first projects at CRREL using the Hopkinson bar was to study the shock wave attenuation in frozen soil by developing a novel polymeric piezoelectric shock gauge. This was deemed necessary due to the potential for hardening of military structures built on frozen soil and also an evaluation of frozen soil responses due to weapon explosions from either nuclear or conventional explosives. A methodology for measuring the shock Hugoniot response of frozen soil using the Hopkinson Bar data was developed and new equipment for producing air-bubble-free frozen soil cylindrical specimens were designed and optimized (Dutta et al, 1993). A new piezoelectric material, polyvinylidene fluoride (PVDF), was created for use as a hook gauge, and a techniques for using it as a shock sensor and an interface for other electronic instrumentation were developed. The project yielded two successful results. First, the piezo-polymer sensor was turned into a patentable product. Also, when embedded in a laminate, the soil was found to have the potential for controlling stresses by developing localized moments. This made it an excellent vibration attenuator that is still being used today in many applications including space structures.

Southwest Research Institute (SHRI) developed a 2 inch diameter split Hopkinson bar system to test soil in confined laboratory tests (Liu et al, 2013). Their results showed that all of the soil tested, even those of varying particle size and moisture content, produced considerable scatter in the data. However, they did see signs of increased wave speed and stress transmission for saturation levels up to 70%. This was most prominent in consistently dry and higher density soils. They also used the split Hopkinson bar to test the following materials: balsa wood, polystyrene, and graphite composite laminates. They found that each different material experienced a shift in mechanical properties when tested dynamically instead of statically that led to a large shift in yield strength.

Dutta et al (1993) also performed a study of energy absorption within graphite/epoxy composite plates using a split Hopkinson bar test apparatus. The laminate specimens consisted of 30 plies of AS4/3502 graphite epoxy with the following

stacking sequence: [(±4 /50 2)2/90/± 45 / 0 2/± 45]. This study also found that the plate's energy absorption was accurately measured using the recorded incident, reflected, and transmitted stress waves. This allowed for an accurate determination of velocity, force, and energy absorption information in the entire impact duration. This meant that the setup methodology could be altered such that it was capable of determining the energy absorption of impacted composite specimens. The only limitation that Dutta et al (1993) found was that the impactor was forced into the laminate at relatively low velocities.Compression bars are nearly all of the dynamically loaded type. However there is no reason why in principle a 'statically' loaded compression SHPB could not be built. Tension SHPBs have been designed of both types (Nemat-Nasser, 2000). Torsion SHPBs are nearly always statically loaded (Gilat 2000). Tension and torsion systems have the advantage that friction between the bars and the specimen is not a problem. They have the disadvantage that the specimens are of more complex geometry and hence harder to fabricate. Also tension specimens usually have to a large length to diameter ratio so that issues of stress equilibrium and longitudinal inertia have to be carefully considered. Torsion specimens are usually thin-walled tubes which raises the issue as to how many grains or crystals they contain within the wall thickness and hence how representative they are of bulk material.

COMPRESSION BAR

The split Hopkinson bar tests specimens in compression by producing short incident pulses lasting less than 0.3 ms which creates small displacements. It is most suitable for small-sized homogeneous specimen where these small displacements can easily be measured and their corresponding strains can be calculated.

ASSEMBLY

Rhorer et al (2002) suggested that the Hopkinson bar system should be mounted on some base structure. Their setup was 5 m long, made in five sections. Each of their sections consisted of an H-beam (200 mm wide by 225 mm deep), that had steel plates welded on the ends. They used precision machining for both ends. At the top Rhorer et al (2002)bolted each section together to form a flat surface for holding up the bar supports. Two A-frames with casters and screw pads for leveling were used to support each of their individual base sections. The benefit to this system is that sections can easily be assembled and broken down to form a mobile bar base structure

COMPONENTS

The split Hopkinson bar is typically composed of three components: the launch system, the stress generation system, and the data acquisition system. The launch system is composed of a pressurized tank, valves, striker, and the launch tube. Typically, the launch tube is bored out from a solid bar of steel. This is done to keep a strict tolerance on the inside diameter of up to ± 0.001 inch (Christman et al, 1971). The striker is usually machined to fit very snugly inside the launch tube. A tight fight is usually necessary to ensure to restrict pressure loss around the outside of the bar when it is fired. A fast acting solenoid valve can also be used to release the pressure from the tank to accelerate the striker bar and to help generate an instantaneous release of pressure. However, due to the cost of machining and integrating a solenoid valve, a ball valve is often used instead. The downside of the ball valve is that it cannot be opened as quickly as the solenoid valve but good results can still be obtained. Figure 4 shows the launch system used for one of the CRREL systems. In their design the launch tube is supported on a sub-plate for its protection and to support its weight. Iron u-bolts are used to hold it in place and compressed air is sent through the attached tube to fuel the system.When firing the striker,Lindholm and Yeakley (1968) found that some pressure is lost due to the flow around the bar and the ball valve is slightly undersized. One the striker has been fired and is in motion it will transition towards the stress generation system when it impacts the incident bar.

The material of the bars is chosen so that they remain elastic (small strains) even though the specimen itself may be taken to large strains. This means that strain gauges can be used repeatedly to measure the signals in the bars (strain gauges normally have small failure strains). Dynamic loading is produced either by striking one end of one of the bars (the input bar) or by statically loading a section of the input bar held at some point by a clamp and then releasing the clamp so that the load propagates to the specimen.

Figure 9. Launch system for Kolsky bar

A key requirement for getting accurate results from the Hopkinson bar system is that it must be well aligned and remain firmly in place without causing any vibrations. This is accomplished by a series of bolting connections. Typically the Hopkinson bar is bolted to a pair of support railings which are bolted into the surface that the Hopkinson bar is on. Figure 5 shows one of the bracket systems used at CRREL. That bracket system also includes a metallic clamp shown in the picture which restricts the incident and transmission bars from rotation and producing forces parallel to the axial direction.

Figure 10. Brackets for bar alignment

One aspect for the design of the mounting bracket is that it would make the Hopkinson bar system more useful and versatile if incident and transmitted bars could be substituted. Different sized bars will produce different strain rates in materials. This means that for a system able to test a wide variety of materials it will need to be able to incorporate different size bars. Thus the bracket design must be wide enough to enable the largest bars to slide in and have some method of keeping smaller bars in place to avoid noise and vibrations. Figure 6 displays one of the methods in the CRREL design. This is a silver metallic square which bolts into both sides of the bracket to give further stability. Another factor is both bars should be manufactured in such a way that they are perfectly straight and covered with some sort of low friction coating to ensure that a one dimensional wave is produced.

Figure 11. Side view of brackets

Because the dimensional tolerances of the launch tube and striker can allow for some leaking of gas pressure when the system is fired, the pressure tank must be charged to an even higher pressure to produce the appropriate velocity. Nicholas (1981) found that the launch tube needs to have its inner diameter be held to a very tight tolerance level. The striker should also be manufactured so that its diameter is slightly smaller than the inner diameter of the launch tube to ensure it wouldn't bind when it was fired.Since the launch system design may be difficult to create in house, Shin et al. (2015) also looked at other possible manufactures to produce the launch tube such as companies that specialize in producing rifle gun barrels. The striker bar should also be properly manufactured so that it will fit inside the launch tube with minimal clearance. The striker impact can be further optimized by machining the striker and polishing the surface to minimize friction. Another approach that Klepaczko (1980) used involves incorporating nylon sealing features such as O-rings that get imbedded into the striker bar.

The length of the pressure bars are chosen to ensure there is only one dimensional wave propagation for the given specimen. The length of the bars must be long enough that the data acquisition system will be able to detect the incident wave and reflected wave. However if the bars are too short, the data acquisition system will not be able to distinguish the end of the incident wave and the start of the reflected wave. It is suggested by Panowicz et al.(2017) and Dutta and Hui (1991) that in each of the bars should have a minimum of length to diameter (l/d) ratio of around 20.

The bar material composition is also important. Solid steel bars have been employed with much success in the testing of metals, ice, and rock, however there is the potential for strong impedance mismatch in testing aluminum foams and specimens made of soft materials. This impedance can sometimes makes it difficult to interpret the different pulses during testing. The use of plastic bars to obtain stronger strain signals potentially causes other problems including marked wave dispersion due to high internal damping and non-linear elastic behavior. These issues can dramatically increase the complexity of data processing required. The bars are mounted in bearings to allow only pure axial motion.Rhorer et al (2002) found several items were necessary to generate accurate measurements from the Hopkinson bar, including straightness of the bars, freedom of the bars to move without binding, and mounting along the axial plane.Chakraborty et al (2015) discovered that there is an overlap in the capabilities of aluminum and steel. However, they also have their unique applications. This means that materials with high elongations, low strengths or lower strain rates aluminum bars allow for pulse generation with larger displacements. Lower striker velocities can be run with a higher sensitivity on transmitted load strain gauges. One issue with using aluminum is that under higher strain rates and stronger samples the aluminum is likelyto get overworked. There are several forms of overworking are possible. Higher strain rates require higher striker bar velocities which can plastically deform the ends of aluminum bars. Stronger samples also require more energy to fail and need longer and heavier strikers which can yield aluminum bars. At this point steel bars become more attractive. Maraging C350 has phenomenal strength to take high velocity impacts with lots of energy. However, it requires these conditions to generate usable strain signal levels due to the higher stiffness of steel.

The main problem is that there are no definite velocities, loads or strain rates that define their capabilities or fully differentiate between the two. It just depends on each material response at a specific strain rate. We test a large variety of materials here at REL and do have some rules of thumb, but often we have to adjust our bar selections during calibration testing for each new material.

Experimental Set Up

Calibration and Initial Parameters

Rhorer et al (2002) theorized that their incident signal was weaker than expected and____ suggested there was probably some reflection being generated from the bearings supporting the bars. However, they have so far been unable to prove this condition due to the difficulty of quantifying the error generated.There could possibly be other sources of waves that generated in this time period. When it comes to the alignment of the bars, Malvern (1984) found that the level of signal on the incident bar gage between the time of the end of the incident pulse and the return of the reflected pulse is the most important measurement. When there areno constraints from the bearings, the bearings needed to be perfectly aligned and the bars kept perfectly straight. This must be maintained so that there should be no oscillations especially prior to the return of the reflected pulse. An observed signal at that point will indicate there is probably some reflection from the bearings supporting the bars. However Kang et al (2017) found that this problem is difficult to isolate and quantify as there may be other sources of waves. Alignment of the mounting brackets is performed by pointing a laser down the center of the launch tube. The mounting brackets are then individually adjusted until the laser passes strait through the center of the brackets to the end.

It is currently suggested that the bearings of the Hopkinson bar apparatus appear to do some straightening of the bars over time but as of now no one has come up with a quantitative method of measuring the amount of this straightening or its long term effects. After the individual bearings get precisely aligned, the incident and transmitted bars are slid through the bearings and placed into position. Kruszka et al.(2014) discovered this optical tooling method led to an ultimate precision of on the order of one arc second. This roughly translates into an ultimate straightness of about 25 m for the support bearings. However, Al-Juaid and Othman. (2016) found that the overall deviation of the bearing centers from a perfect line needs to be on the order of 100m when taking into account other uncertainty sources such as the target fit into bearings and the ability to align crosshairs to the target center hole, air disturbances and optical distortions of the scope. Song et al. (2015) set up their split Hopkinson system so that the bearings were machined with a clearance of 75m for the 15 mm diameter bars. Their bars were fabricated from 350-maraging steel, hardened and center less ground so that they are straight within approximately 0.5 mm when placed on the flat surface of a coordinate measuring machine, In their conclusion, Rhorer et al (2002) proposed an interesting study of intentionally misaligning the bars to various degrees. They would then compare the strain gauge results to a previously known measurement, thus determining the magnitude of the effect from a misalignment.

At CRREL two 0.125 in long, 350 ohm strain gauges were compensated for stainless steel and attached at the midpoint of each half of the split Hopkinson bar. They were aligned diametrically opposite each other to compensate for the bending moment. Type CEA-09-125 Ur-350 gauges were bonded using AE-10 epoxy and cured at room temperature and were kept at .60 in width so the strain averaging would only occur on a small area of the bar. A bridge configuration was used to

connect the gauges via a three wire technique. This helped to shield each individual gauge cable and form opposite sides of a two active arm, four arm bridge. The benefit of this configuration is that it offers twice the voltage output of a two gauge, one active arm, four arm bridge with a reduction of nonlinearity and a minimal loss of bending. Dutta (1988) used Micro Measurement M Coat D to insulate the gauges and prevent moisture. Each gauge was then connected to the bridge completion and balance circuit by 15 ft of Belden 8723 cable.

A 500 kohm potentiometer was used to bring the bridge into balance according to previous research by Stien (1967). Bridge exitiation was kept at 15V and was created by a set of Hewlett Packard HP 6218PB power supplies which were kept at each end of the bridge. The amplifiers were set for a gain of ten to give a bandwidth of 100 KHz and 120 dB of rejection at the inputs. Each amplifier output was single ended and connected to the oscilloscope's positive input terminal for each scope channel. 100 mV settings were used with a 0.5r us per point digitization rate to keep the record length at a reasonable 4 ms. Channel 1 on the scope was used to record the incident and reflected strain and Channel 2 records the transmitted strain. The oscilloscope was triggered to begin recording when the hammer contacts the first bar of the split Hopkinson bar by adding a 3V battery signal to the external trigger input of .the oscilloscope. A gauge shunt technique was used to calibrate both the strain gauges and bridge circuits.

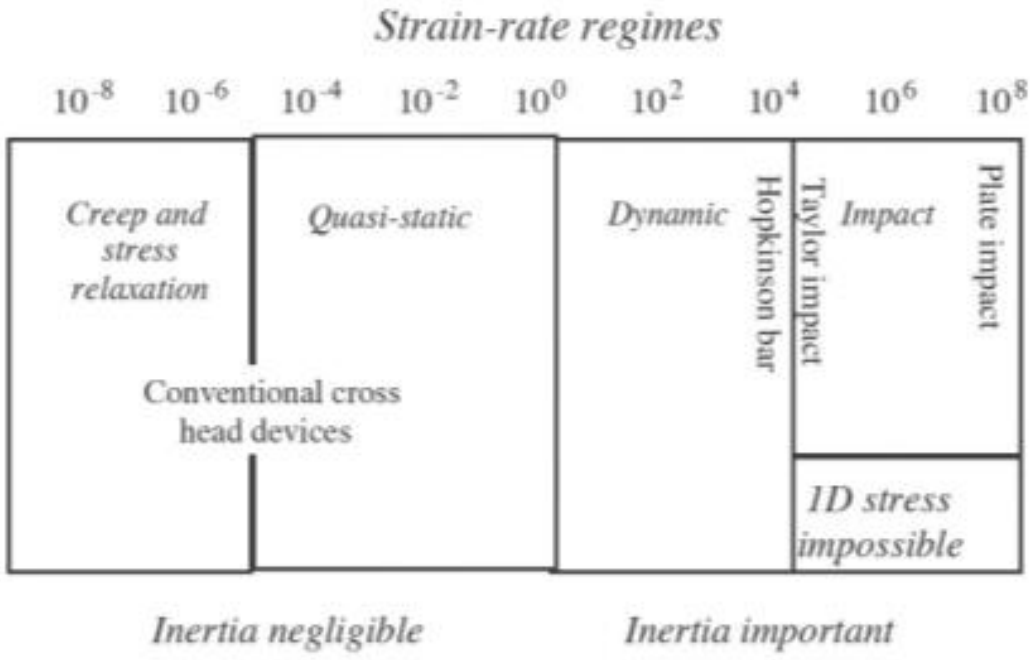

Figure 12. Stress levels and loading

Sample Preparation

The specimen is most often placed between the incident bar and the transmitter bar. A small amount of preloading is necessary to hold the cylindrical specimen in position between the two bars. Duffy et al. (1971) found this could be performed using two rubber bands to provide tensioning for the two bars to close on the specimen. Dutta and Hui (1991) found that two Teflon collars could mate the ends of the specimen to both bars. Each collar is lightly cut lengthwise to allow a modest flexibility in diametrical expansion when required for mounting the specimen.

Placement of strain gages

In order to minimize the strain caused by the bending of either of the bars, two strain gauges will need to be wired in parallel and on opposite sides of the bars. The purpose of this is so that if the bar bends one gauge will show an increase in resistance and the other gauge will show a decrease in resistance. This produces a cancelation of the strain caused by bending and allows the strain gauge to only measure pure axial strain.

All three of the pulses (incident, reflected, and transmitted) are measured using strain gauges. How the strain gauges work is that when the energy reading from a wave is registered by the strain gauge, the voltage is written to an output file that also writes the time associated with the value. Since all three waves begin at different times, each will have a different time

linked with it. Through looking at the readings and the times they are released, the shape and strength of each pulse can be determined. In order to develop a dynamic stress-strain cure all three of these waves must be used. A measure of the transmitted strain calculation is that the incident wave magnitude must be subtracted from the magnitude of the reflected wave. Since both waves occur at different times the initiation of the wave is reset to zero and the time scales are adjusted. Once the two waves are on a matching time scale, their magnitudes can simply be subtracted from one another to determine the strain in the specimen as a function of time. The same procedure of resetting the zero value also needs to be applied to the reflected wave as well. Once all of the wave times have been reset to zero, a dynamic stress strain curve can be produced by using the transmitted wave to calculate the stress. This stress is also a function of time and thus can be plotted against the difference in magnitude in between the Incident wave and the reflected wave to generate a dynamic stress strain curve.

Pulse shaping tool application

A pulse shaper made of a different material such as copper can modify the incident wave from a rectangular shape to some other shape. These new shapes can include a ramp, half sine wave, or triangular. Another additional feature can be obtained by inserting a small rubber disc in front of the copper shaper. That acts to further reduce the magnitude of the rising portion of the slope of rising portion of the pulse and/or limit it to a desired value Ross et al, 1984). The purpose of the pulse shaper is to guarantee constant strain rate during the loading and to maintain force equilibrium across the sample. The shape and loading needed for testing is dependent on the materials being tested.

This pulse shaping and reduction is necessary due to some brittle materials having small failure strains of below 1%. If the loading is too fast from a compression SHPB test, the specimen may fail in a non-uniform manner. One case of this would be the front of the sample may be shattered while the back remains intact. The loading pulse in the compression SHPB system has a trapezoidal shape accompanied by high level of oscillations(Kruszka et al, 2014). These oscillations are induced by the sharp rising portion of the incident wave and make it extremely difficult to achieve either dynamic stress equilibrium state or constant strain rate in the sample. That becomes significant because the stress equilibrium is a prerequisite for valid SHPB tests. The constant strain rate is mainly dependent on the rise of the incident pulse which can induce premature failure long before dynamic stress equilibrium could ever be reached in the sample. As a rule of thumb, the loading stress wave needs approximately 3 to 4 rounds to travel within the specimen for the stress to achieve an equilibrium (Kang et al, 2017). For the split Hopkinson bar to obtain accurate measurements, the dynamic loading must be slow enough so that the specimen is experiencing an essentially quasi-static load. That will make the deformation of the specimen uniform.

Another way to change the shape of the incident pulse and to slow it down is to modify the geometry of the striker. Christensen et al. (1972) used striker bars with a truncated-cone on the impact end in an attempt to produce ramp pulses. Frantz et al. (1984) used a striker bar with a large radius on the impact face to generate a slowly rising incident pulse. Li et al. (2000) and Zhou et al. (2012) used a fully formed cone-shaped striker to generate a half-sine loading waveform. Information about the continuing deformation of the specimen is contained within the waves that reverberate up and down the length of the bar system, and this information can be accessed with suitable analysis and software (Zhao and Gary 1997, Zhao and Gary 2001, Othman et al. 2001b). Another way of addressing this problem is to use the direct impact Hopkinson (or 'block') bar (Deshpande and Fleck 2000, Reid et al. 2001, Abdennadher et al. 2003). As with granular materials, the question may be raised as to how representative a foam specimen is of the bulk. This may not be such a severe problem for foams as evidence is accumulating that the mechanism of rate sensitivity is due to mechanical inertia of the cell walls so that even foams made from rate insensitive metals can exhibit substantially higher resistance to deformation under impact compared to quasistatic rates of loading (Abdennadher et al. 2003, Abdennadher and Zhao 2003). Ideally high-speed or flash photography should be used when deforming foams or cellular materials so that the mechanisms of deformation may be identified. Some optical techniques are particularly useful for these non-standard materials as they allow displacement data to be obtained from the whole of the field of view. One of the first optical techniques to be used in the SHPB was a diffraction grating ruled on the specimen (Bell 1966). However, this is an extremely time-consuming technique to use on a regular basis and requires very skilled technicians. This author and his co-workers are the only ones ever to use this method. Speckle techniques are much easier to implement experimentally (Chiang and Asundi 1979) but can require the implementation of complex algorithms and lengthy numerical calculations on a computer to obtain the displacement and strain fields (Sjödahl 9 and Benckert 1993). Speckles can be formed by the interference of reflected coherent (laser) light from a surface (Chiang 1978) or by the application of spray paint (optical) (Asundi and Chiang 1982) or fine smoke (for electron microscopy studies) (Huntley et al. 1990). Alternatively the microstructure of the material itself can be used if it is sufficiently granular (Rae et al. 2004). In the last case, staining techniques may have to be used to increase the contrast between the various components. Examples of the application of this technique to the deformation of specimens in a

compression SHPB in our laboratory are given in refs (Grantham et al. 2003, Grantham et al. 2004).These methods appear to be more valid if there is an ample supply of extra strikers. The downside is that one a striker is modified, it cannot be changed back.

Operating Split Hopkinson Pressure Bar

There are two approaches that have been used to determine the pressure required to accelerate the striker to a given velocity: Newton's method and the Energy method. Newton's method applies the second law (F=mA) to relate the forces acting on the striker to the striker's acceleration (Kim and Young, 2015). It assumes that the force acting on the striker bar is constant until leaving the launch tube so that the pressure is constant. It also assumes that the friction and the air resistance inside the tube are so low they can be considered negligible. The conservation of energy method was devised to relate the potential energy of compressed air to the kinetic energy of the moving striker (Kim and Young, 2015). This approach also assumes that the friction and air resistance are negligible. It then further assumes that all of the potential energy of the gas gets transferred to the striker, and that the gas undergoes an isentropic expansion.

It has been found that using these two methods to determine the velocity of the striker will produce different results. This is due to the calculations based upon Newton's method being less accurate than the energy method. The main reason for this is due to the Newton method assuming that the sum all of forces acting on the striker bar will be constant when a majority of the time they are not (Kim and Young, 2015). Studies have indicated that as the striker bar travels down the launch tube the pressure in the tank is decreasing because the overall volume of the system is increasing (Christman et al. 1971, Nicholas 1981, Harding 1983, Ross et al. 1984, Duffy et al, 1991). Thus the assumptions made by the energy method approach more accurately represent the likely conditions than the assumptions made in Newton's method.

A split Hopkinson bar is not considered to be a one size fits all test rig for materials testing. Depending on the materials that require testing, the bars needed for that testing can change substantially in diameter and length (Zon et al, 2016). Thus a SHPB facility should allow for a range of bar diameters and the support bed should be as long as could fit into the allowable area. Another aspect that needs quite specific planning is the gas gun or launcher. Li et al. (2016) found that most of the commercial gas guns were for projectile impact and or penetration which produced velocities in the range of hundreds of m/s whereas a SHPB would require the striker velocity of < 25 m/s. For a materials testing facility the area of most use will be the data capture system for the strain gauges on the HPB. It is necessary to make sure the amplifiers used for the strain gauge bridges have sufficient bandwidth - anything less than 50kHz is going to distort HPB signals. Li et al. (2016) suggested getting amps with bandwidth of 100kHz minimum, and A/D capture card with sampling rate of about 5MHz, 12 bit resolution.

Data Acquisition System

A data acquisition system (DAQ) is typically composed by strain gauges that are attached to the center of incident and transmission bar, a signal amplifier such as an oscilloscope, and a computer with an analog to digital data acquisition card. The strain generated in the bar is measured in the terms of voltage signal through strain gauges. The output voltage of the active strain gauges must then be amplified in order for the data acquisition system to accurately measure the signal. Most systems use an oscilloscope that are run on two channels: one channel shows readings from the strain gauge on incident bar and the other shows the results for the transmission bar (Panowicz and Janiszewski, 2016). These signals are displayed on the oscilloscope and then sent to the PC for permanent storage. Generally a software logging program such as LabView is used for recording the data.

The DAQ this lab had been using was the Laboratory Computer System (LABCOM). It was developed to be used in conjunction with the Nicholet 4094A oscilloscope, the PAC 3300 Acoustic Emission Analyzer, and the Delta Design 9064 Environmental Chamber (Hadjuck, 1987). The system is controlled by several files: HPKINSON.BAS was used for receiving and analyzing data from the Hopkinson bar, THERMAL.BAS was used for controlling the environmental chamber, PLOTDATA.BAS, and ACOUSTIC.BAS which processed the results of the acoustic tests.

The goals of the data acquisition system are to sample the voltage produced by the strain gauges, amplify these voltage measurements, adjust these measurements according to the gauge factor to convert the strain gauge voltage to strain, and finally record the strain measurement to an output file or device Kang et al, 2017). One main issue of this is that by performing all of these operations within a short period of time, the data acquisition system slows down the rate at which the strain voltage can be sampled. Panowicz and Janiszewski (2016) suggest that the data acquisition system should be redesigned to be capable of performing dynamic data operations. A new dynamic data acquisition system should only sample the strain voltage and save/write the voltage to a file. By making these adjustments the system would theoretically be capable of working with at least 100,000 samples per second. That means the gauges to sample the voltage would also need to be capable of sampling at least 100,000 samples per second. Typically, voltage amplification is done by an external Wheatstone bridge. Figure 7 displays a Wheatstone bridge circuit used on one of the CRREL bars. The strain voltage

output needs to be converted to strain in a post processing calculation so that the stress strain curves can then be produced (Diemand and Moritz, 1990). By moving these data operations to a post processing application, it will significantly improve the rate at which the signal can be sampled.

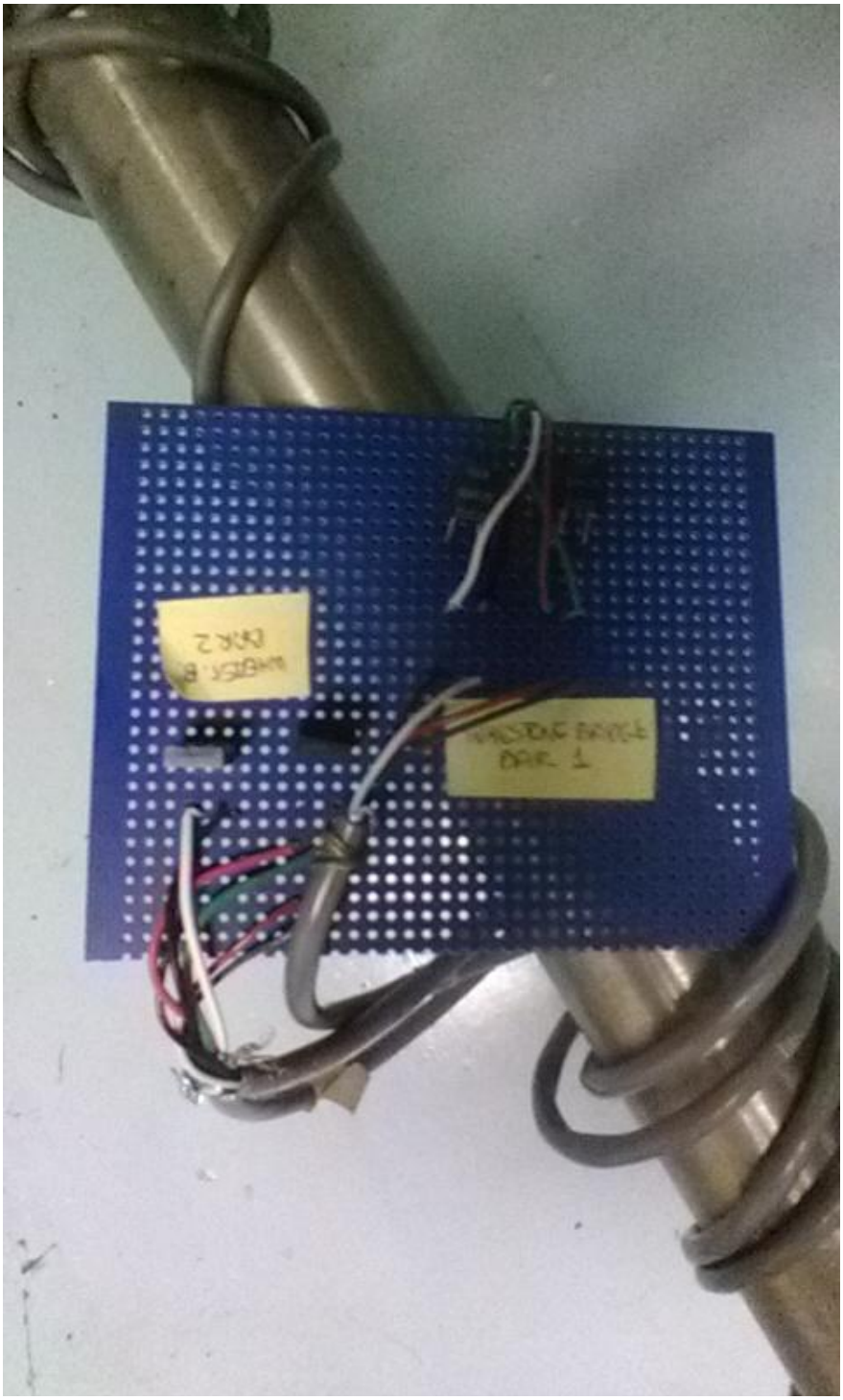

Figure 13. Wheatstone bridge circuit

Nitrogen Liquid and Gas cooling and freezing processes.

Several chemical processing companies use nitrogen in either a liquid or gas form. Beteta and Ivanova, (2015) found that nitrogen gas (GAN) can enter vessels and purge lines to eliminate explosion hazards and prevent oxidation reactions that can reduce product quality. Liquid nitrogen (LIN) is an effective and convenient refrigerant due to its availability, low cost, and inert properties. It is also a practical cryogen for most low-temperature activity because of extremely low boiling temperature (–195.8°C) and high refrigeration capacity at atmospheric pressure. For elevated pressures, thermal properties of liquid nitrogen make it an effective refrigerant to rapidly cool processes to low temperatures.

LIN refrigeration methods

There are several cooling techniques that use LIN's refrigeration capabilities in batch or continuous processes.

- Direct surface (semi-indirect) cooling - LIN provides cooling via a single conductive wall, the cold surface of which freezes or cools liquid or gas streams.

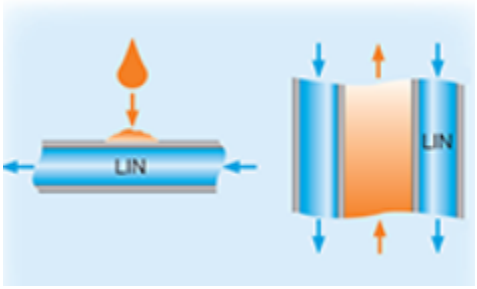

Figure 14. Direct surface cooling

- Secondary circuit (indirect) cooling - The boiling temperature of LIN is buffered with an intermediate heat-transfer fluid (HTF) to enhance temperature control. The HTF temperature can be tuned to the desired process temperature, as low as the boiling point of LIN. The HTF then provides refrigeration through a conductive wall to freeze materials or cool fluids.

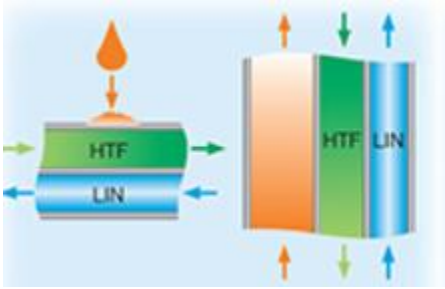

Figure 15. Secondary circuit cooling

- Cold GAN cooling - LIN vaporizes, and the sensible heat capacity of the cold GAN is used for refrigeration. Additional LIN is injected to control the temperature. Cooling occurs via a conductive surface, or by blowing the cold GAN directly onto the materials to be cooled.

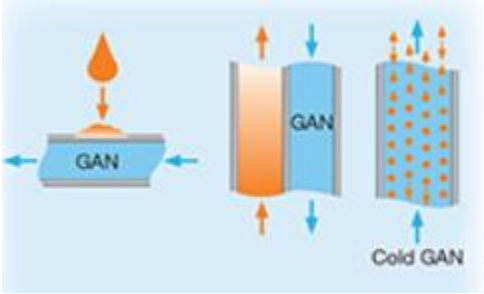

Figure 16. Cold GAN cooling

- Direct LIN injection or spray cooling - LIN is injected or sprayed directly onto materials or into processes. Materials and processes are cooled by the latent heat of vaporization of LIN; depending on the design of the cooling system, the sensible heat capacity of the cold GAN may also contribute to the cooling. This one of the most efficient uses of LIN's refrigeration capability.

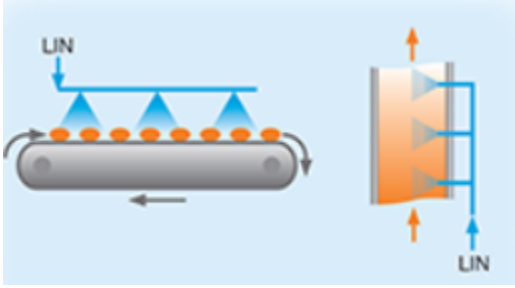

Figure 17. Direct LIN injection cooling

- Immersion cooling - Direct immersion in LIN cools or freezes a material. The rate of cooling depends almost entirely on the latent heat of vaporization of LIN. The overall heat transfer rate is generally lower than that of direct LIN injection or spray cooling, because the GAN has a blanketing effect. This means the bubbles generated by the turbulent boiling of the LIN will create a vapor boundary layer around the immersed material, thus lowering the overall heat-transfer coefficient.

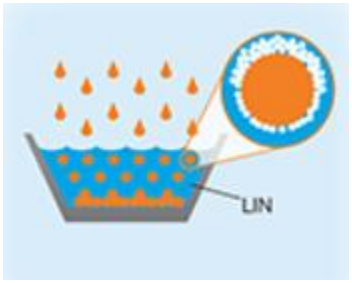

Figure 18. Immersion cooling

The suitability of a particular cooling method is dependent on the cooling method and nature of the materials or processes to be cooled. For example, Cold GAN cooling is an attractive option for cooling delicate materials, when compared to either direct LIN injection/spray or immersion cooling which could damage the structure of the material. Cold GAN and secondary-circuit cooling should also be used when it is critical to operate above the freezing point of materials or fluids to avoid freezing that could damage the material or plug the process. Direct LIN injection/spray cooling or immersion cooling would be preferable for instances when rapid or flash cooling was required.

Cryogenic milling and grinding

LIN refrigeration may also necessitate cryogenic milling and grinding to pulverize some materials into a powder that would otherwise be difficult to mill at ambient temperature. This process is most suitable for materials that have high viscoelasticity, adhesive properties, or thermal sensitivity. Materials like rubber and elastomeric gels have high viscoelasticity and can resist shear flow, stretch when impacted, and return to their original state when stress is removed.

Viscoelastic properties are directly proportional to temperature so lowering the temperature makes the material more brittle. This makes milling easier and more effective. Adhesive properties are composed of sticky materials like waxes and oily biological samples that have a tendency to cling to other materials and surfaces. When milled at ambient conditions, they often build up inside the mill and lowering the mill throughput. That causes a spike in power consumption and eventually plugs up the process. Low temperatures inhibit the adhesion mechanisms responsible for stickiness and increase cohesive intermolecular forces, making the materials more brittle and less sticky and thus easier to mill. Thermal sensitivity is where some materials lose their chemical, biological, or electrochemical activity at elevated temperatures. In one case heat may damage protein-based pharmaceuticals. Due to the heat that the milling processes generates, refrigeration is then needed to control the temperature when processing these sensitive materials. The heat generated by milling also makes it more difficult to process viscoelastic and adhesive materials. Therefore, it is critical to control the temperature of the mill as well as the temperature of the material being milled. Cryogenic milling involves cooling the materials and the

mill, generally through direct LIN injection. This process also expunges its excess to the atmosphere, which prevents undesired oxidation reactions.

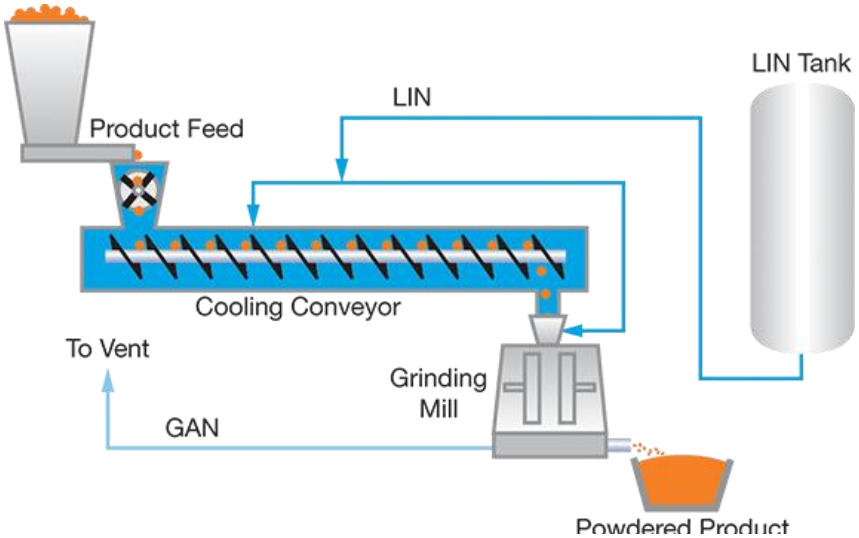

Figure 19. Cryogenic milling and grinding

Lyophilization

Lyophilization, or freeze-drying, is the process of dehydrating thermally sensitive materials such as proteins by freezing the material with LIN, followed by controlled sublimation under vacuum. Materials may be freeze-dried to preserve their microscopic cellular structures and to enhance stability for prolonged storage and transportation. Mechanical refrigeration by compressors has been used for freeze-drying applications, but LIN is becoming more widespread due to enabling better control of the freezing process and a broader range of operating parameters. For small-scale operations, materials may be frozen through LIN immersion or direct surface cooling prior to being placed in a vacuum chamber. In larger-scale operations, LIN secondary circuit cooling via a heat-transfer fluid is the most economic and effective method of freezing. This is due to offering quick, cryogenic-temperature freezing and flexible temperature control to speed up vacuum drying. After freezing, a vacuum pump will then cause sublimation of most of the frozen solvent in the primary drying step. A cryogenic condenser, cooled via LIN direct surface cooling, maximizes the rate of mass transfer of solvent from the frozen material to the condenser surface. Any remaining solvents from primary drying will be removed during secondary drying, where the material temperature and vacuum are increased. If the material being freeze-dried is oxygen-sensitive, an inert gas backfill breaks the vacuum while maintaining an inert atmosphere.

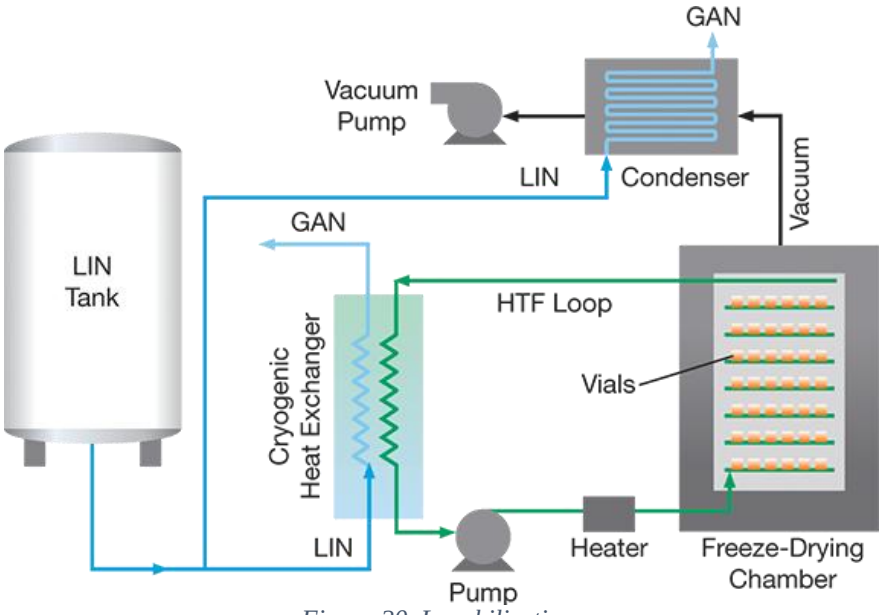

Figure 20. Lyophilization

Cryopelletization

Cryopelletization is a low-temperature technique for manufacturing pellets that are most often spherical or semi-spherical and range from 0.5 mm to 5 mm in diameter. It is often used to pelletize heat-sensitive materials, such as bacterial cultures and probiotics. Because cryopelletization effectively flash-freezes materials, it is used to prevent phase separation of components in solutions, colloids, or suspensions, as well as to form pellets with a high degree of homogeneity. The three common forms of LIN-cooled cryopelletization are direct surface freezing, LIN immersion freezing, and cold GAN freezing.

Direct surface freezing

Causes droplets to freeze on a cold surface, such as a rotating stainless steel drum that is cooled by direct LIN injection inside of the drum. The pellets formed are consistently semi-spherical with a flat base. The size and shape can be modified by adjusting process variables, such as the distance the droplets fall and the rate of freezing.

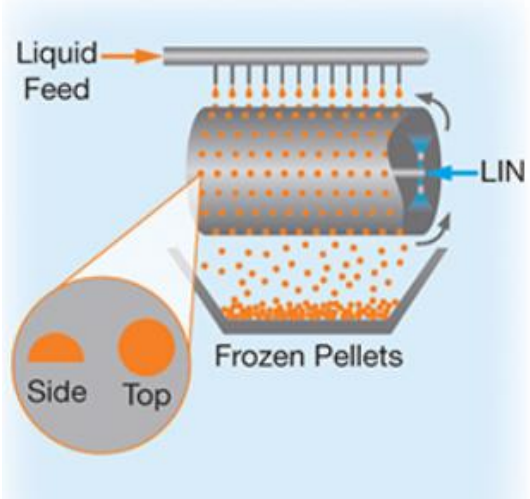

Figure 21. Cryopelletization

LIN immersion freezing

Freezes the droplets as they are immersed in LIN. As droplets are immersed, the LIN boils turbulently, which makes it more difficult to control the size distribution and the shape of pellets. Nevertheless, this method generally produces a high percentage of spherical pellets.

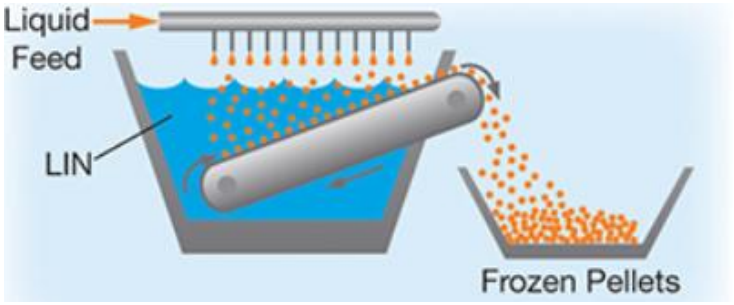

Figure 22. LIN immersion freezing

Cold GAN freezing

Cold GAN freezes droplets as they free-fall, producing spherical pellets with a narrow size distribution. However, it is critical to control process variables, such as droplet size, GAN temperature, and freezing chamber geometry, to prevent droplets from agglomerating or sticking to sidewalls as they fall.

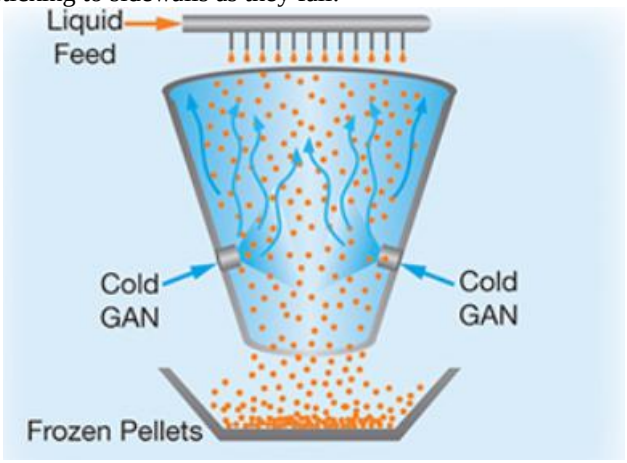

Figure 23. Cold GAN freezing

Pelletization

This method is considered to be advantageous because it improves flowability and blendability. Flowability makes downstream conveying and packaging easier. Pellets can be easily and accurately blended or mixed to form products with a variety of properties. Additionally, pelletization minimizes the creation of fines and dust, reducing the risk of dust explosions and respiratory health effects.

Cryogenic spray freeze-drying

Cryogenic spray freeze-drying (SFD) creates fine dry powders that are usually smaller than 100 µm and have low-density at low temperatures. It combines the principles of lyophilization and spray drying. The process works by creating fine droplets from a solution, suspension, or colloid, and then rapidly freezing them by either direct LIN spraying or LIN immersion. Single-fluid or two-fluid atomizing and ultrasonic piezoelectric nozzles create the micro- or nano-sized droplets. The liquid-product formulation, atomizing parameters, and freezing rate can be modified to control dry particle characteristics, such as shape, size, size distribution, and overall morphology. The frozen powder may be the final product, but typically a gentle drying process, such as vacuum (lyophilization) or atmospheric drying, follows the freezing step. Atmospheric drying introduces temperature-controlled, cold, dry GAN to dry the frozen powder through convective mass transfer under atmospheric pressure. The moist, cold GAN is then vented from the process or dehumidified and recycled.
The dry powder particles produced by SFD are spherical, light, and highly porous, and they have attractive aerodynamic properties, making them well-suited for inhalable powdered drugs that are administered through the nasal or pulmonary

pathways. Additionally, the dry powders can be reconstituted faster than materials dried by traditional lyophilization and spray drying methods, which is important for pharmaceuticals with low water solubility.

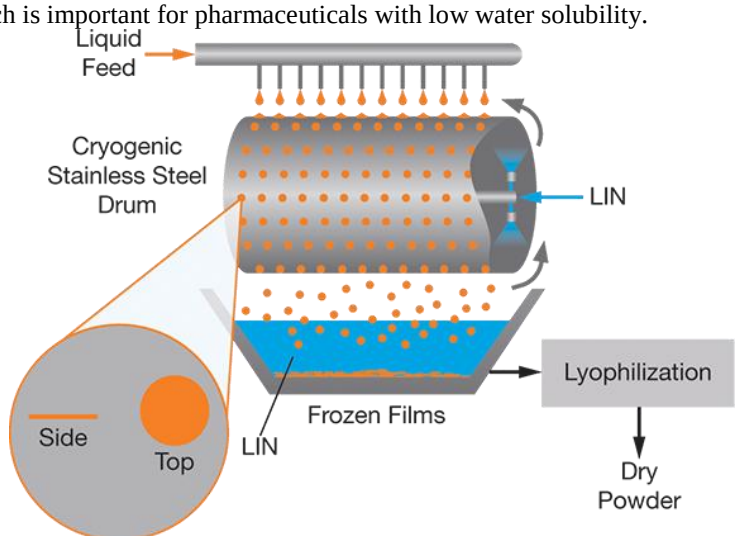

Figure 24. Cryogenic spray freeze-drying

Cryogenic thin-film freezing

Cryogenic thin-film freezing (TFF) is a relatively new low-temperature process that produces highly porous, micron- and submicron-sized dry particles of heat-sensitive materials, such as proteins, that are suitable for pulmonary and parenteral drug-delivery applications. The process is similar to cryogenic pelletization by direct surface cooling using a rotating stainless steel drum. Drops of a solution, suspension, or colloid fall onto a cold stainless steel surface from a distance that allows the droplets to collapse into flat, thin (micron- or submicron-thick) films as they rapidly freeze. The film thickness can be modified by adjusting the free-fall distance and the physical properties of the liquid feed. The frozen films are freeze-dried to produce dry powders.

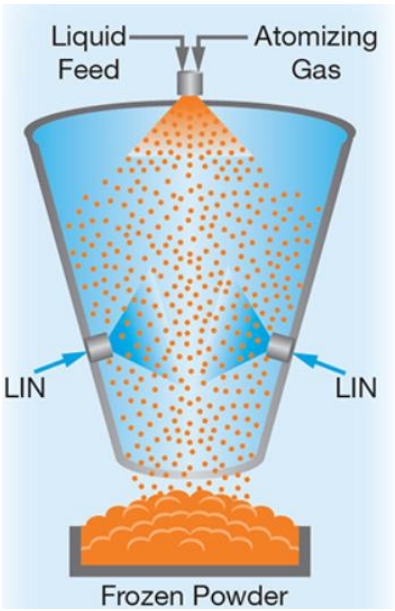

Figure 25. Cryogenic thin-film freezing

In TFF processing, the gas-liquid interface is minimized during freezing (in contrast to SFD), which reduces protein denaturation. TFF is used at the laboratory scale, especially for research on the reconstitution of insoluble drugs. It is not clear whether it will be a cost-effective solution for large-scale manufacturing.

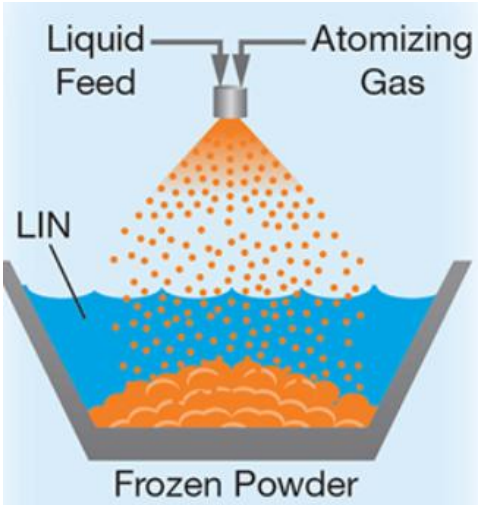

Figure 26. Standard thin-film freezing

Cryogenic reaction cooling

Cryogenic reaction cooling provides refrigeration and low-temperature control for temperature-sensitive processes, such as highly exothermic and cold-chemistry reactions. In organic synthesis, low temperatures are important to balance reactivity, selectivity, and yield. For highly exothermic reactions, cooling is critical to control heat release and avoid runaway reactions. Direct injection cooling, semi-indirect cooling, and indirect cooling with HTF are the three primary options for cooling reaction vessels with LIN.

Direct injection cooling

In this method the LIN is injected directly into the reaction. This method achieves maximum efficiency and is inexpensive to install, but solvent entrainment, foaming, and localized freezing can occur. It is often used in emergencies, because vaporizing LIN can rapidly cool an unsafe or runaway reaction.

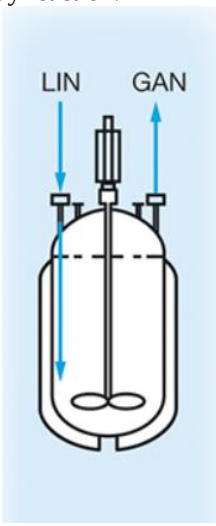

Figure 27. Cryogenic reaction cooling

Semi-indirect cooling

LIN flows through either a coil inside the reactor or a reactor cooling jacket. This simple method enables fast cooling and nitrogen recycle. However, drawbacks include lower cooling efficiency and higher costs for cryogenic construction and corrosion-resistant materials.

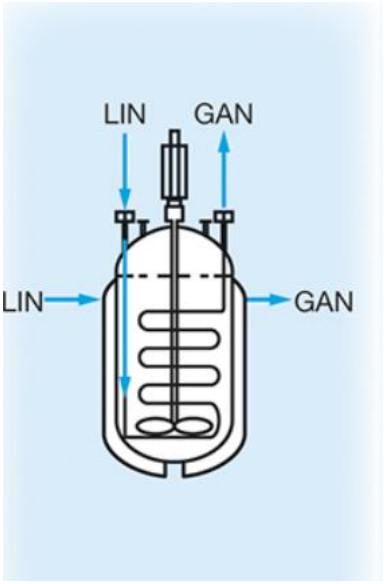

Figure 28. Semi-indirect cooling

Indirect cooling with HTF

In an external heat exchanger, LIN cools a heat-transfer fluid, which then flows through a secondary circuit to cool the reactor. This flexible approach provides accurate temperature control and accommodates large heat loads.

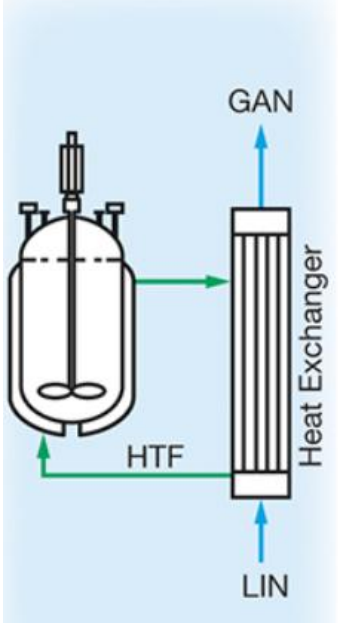

Figure 29. Indirect cooling with HTF

Cryogenic solvent and VOC recovery

Organic solvents and volatile organic compounds (VOCs) can be condensed with LIN and recovered. The ability to recover and reuse evaporated solvents reduces the amount of solvent that must be purchased. The cost savings is typically significant enough for recovery systems to pay for themselves in only a few years. Cryogenic VOC recovery is often a more environmentally friendly and cost-effective way to control VOC emissions than oxidation techniques.

The main component of a cryocondensation system is a heat exchanger, which provides LIN refrigeration, typically through secondary circuit cooling with a heat-transfer fluid or direct LIN injection cooling, to condense solvent vapors or VOCs. Direct surface cooling, which involves passing LIN through a traditional shell-and-tube heat exchanger, is generally not recommended for VOC recovery operations, especially those driven by environmental regulations. These applications

require a higher degree of temperature control and reliability than direct surface cooling can offer. Unstable VOC freezing or heat exchanger plugging can result in a breach in VOC compliance or an unplanned process shutdown, both of which can be serious and expensive incidents.

Secondary circuit cooling with a heat-transfer fluid is a more suitable method, as it allows precise temperature tuning to meet the desired VOC recovery efficiencies. The HTF is loaded into the shell side of the low-temperature condenser, where the temperature is precisely controlled via LIN heat exchange. Concurrently, the VOCs or solvent vapors are condensed inside the condenser by the refrigerated HTF.

Direct LIN injection cooling for VOC recovery is a newer technique that is still under development. LIN is directly injected into the VOC-laden vent streams to freeze the VOCs. A downstream filter collects and separates the frozen VOCs from the vent stream. This technique is especially useful for VOC streams that are subject to strict regulations.

Cryopreservation

Cryopreservation preserves biological samples at cryogenic temperatures for the purpose of prolonged or indefinite storage. The process operates on the principle that low temperatures exponentially reduce the rate of reactions associated with biological activity. Thus, the biological activity of samples at cryogenic temperatures is slowed to the extent that time is, in effect, stopped for the sample. The intention is that the stabilized sample can be warmed to ambient temperature at some point in the future - in some cases, up to 1,000 years later - to resume normal activity. Cryopreservation is a growing practice used to store many types of biological materials, including proteins, nucleic acids, cellular structures, single-cell or multicellular organisms, tissues, and organs.

For most samples, the most critical part of the cryopreservation process is the freezing step. If it is too slow, water freezing outside the cell draws out intracellular water molecules through osmotic pressure. The decrease in intracellular water increases the solute concentration inside the cell to potentially lethal levels. Also, slow freezing causes intracellular water molecules to arrange in large crystal structures that can pierce cell membranes and cause irreversible damage to the sample. In general, faster freezing forms smaller ice crystals, which are less damaging to cell structures. Typically, cryoprotectants and a cooling rate of 1°C per minute are standard protocols for cryogenic freezing of biological samples.

Vitrification is an approach for freezing samples for cryopreservation. Cryoprotectants reduce the freezing temperature, and additives increase the viscosity of the sample. The sample is then exposed to an extremely fast freezing regime to vitrify it in amorphous ice and prevent water crystal formation. It is critical that these samples be stored at a cryogenic temperature below the point at which water molecules begin to crystallize. A general rule of thumb for most cryopreserved samples is to store them below –130°C. The most effective and economical way to store samples is by immersing them in LIN or by cooling them with cold GAN vapor inside a specially designed cryochamber.

Refrigeration System

The Tundra refrigeration system is a patented, single-stage refrigeration system that can efficiently cool the chamber down to -45℃ (-50℉). It utilizes a common refrigerant and is able to operate continuously at -40℃. Since most low temperature environmental testing is done at -40℃, it is a good alternative to buying a cascade system. It uses up to 40% less energy and is less complex than a cascade system with fewer parts compared to the cascade system and lower maintenance & utility costs over time. At warmer temperatures, this system can also handle large live load conditions generated from testing electronics.

Humidity Range

This is probably one of the most misunderstood topics when it comes to environmental test chambers. This is due to the fact that Relative Humidity percentage is temperature specific. For example, the amount of moisture in the air at 20℃ (68°F) and 50% RH is not the same as it is at 10℃ (50°F) and 50% RH. As air temperature is reduced, its ability to hold moisture is also reduced. Thus, for a given amount of water vapor in the air , temperature decreases will lead to RH increases . The standard controllable temperature /humidity range for most manufacturers is 5℃ (41°F) to 85℃ (185°F) with 10% to 98% RH, limited by a 7℃ (44℉) dew point. The limitation of a 7°C (44°F) dew point can be very confusing. Since the amount of moisture varies at every temperature, the chamber manufacturers use dew point to describe the RH limitation. Inside the chamber there is a refrigerated coil that is controlled at a temperature very close to the freezing point of 0℃ (32°F). Moisture in the chamber will be attracted to the cold surface and condense, but not freeze. The accumulated water is drained out of the chamber thereby lowering the relative humidity. The refrigerated coil is never below freezing so frost will not develop. The chamber must be operated within the limits set by the manufacturer. Damage to the refrigeration system can occur if points outside of the standard range are attempted.

Types of Humidity Systems

There are various types of humidity systems used on test chambers today such as a water bath, boiler/steam generator and atomizing system.

- Water Pan - Very stable, but slow response
- Boiler - Standard on most CSZ chambers

The advantages of this system are that it can attain 98% humidity and has large capacity to work in any size unit. The disadvantage of this system is that live load from boiler can cause problems at lower temperatures when the DUT generates heat.

- Atomizer - This system sprays very fine drops of water into the air stream.

The advantage of this system are that it provides good control with live loads. This type of humidity systems is typically used for testing devices that are over 500 watts, with the exception of larger chambers.

Low Humidity (Dew Points below 7℃)

To achieve lower humidity levels down to 5% RH most manufacturers offer a low RH package. It normally includes a dry air purge system and refrigeration valves to allow the refrigerated coil to go below freezing. However, the dry air purge helps to offset this by maintaining a positive pressure in the chamber and sublimating some of the accumulating frost off the coil. Humidity Water De-ionized (DI) water is recommended for use with our humidity systems. Water should be provided that has a resistivity within a range of 0.05 to 2MΩ. Distilled water or reverse osmosis (RO) water exceeding of these limits may cause corrosion. For customers using tap water an optional Demineralizer Filtration System should be used to remove water impurities and minerals that can harm your test chamber. This is not needed for those customers that already have a de-ionized water supply. A Re-circulating Humidity Water Supply System is also a feasible option for those without a plumbed water supply to the chamber. The chamber should be filled with tap water along with a DI filter or with only DI water. This system is also collects condensate from the chamber, filters it, and stores it in a reservoir for reuse.

Note: If products being tested emit a harmful vapor or other contaminates, these can be picked up by the condensate and reused by the re-circulating system. This may damage your device under test.

Note: If using a city water line, a water pressure regulator is highly recommended to lower the water pressure to 25 PSIG for steam generator/boiler systems and 10 PSIG for atomizing humidity systems.

High water pressure may cause the top or bottom caps on the water filter to crack. This may result in water leakage that can damage the unit and/ or customer property.

If the water supply has a lot of particulate matter an additional inline pre-filter such as a 5 or 25-micron polypropylene pre-filter may be needed. Other filters are recommended if the water source has a lot of organic, free chlorine and chloramines, or phosphate complexes. The water supply should be checked occasionally for contaminants and resistivity.

How Much Water Does the Humidity System Need?

Many reach-in chambers typically use anywhere between 0.5 GPH to 3 GPH. Large chambers like walk-ins may require much more. The amount of water used will vary depending on the size of the chamber, conditions being run, and usage of the chamber humidity system.

Temperature Change Rate

The requirements for temperature change rates continue to get faster and faster. By incorporating faster change rates, total test time can be reduced. Products can also be thermally stressed at faster change rates which can identify reliability problems. However, be careful assuming the part temperature is changing at the same rate as the air. Every chamber manufacturer has different air flow volumes inside their chambers. The air flow must have enough volume to support the refrigeration system. The typical air velocity in most reach-in type chambers is approximately 100 ft/min on throughout the work space. This velocity works well for steady state and temperature cycling testing. However, the part temperature will lag behind air temperature with this air flow. Air velocity across part should be much higher to keep it closer to chamber air temperature during transitions. Typically 500 ft/min or more is required to move the part temperature at a similar rate to the

air temperature. It is a necessity in thermal shock applications to have air flow this high. For most temperature and humidity applications the air flow in reach-in type chambers is adequate for testing.

Product in Chamber

It is important to inform the chamber manufacturer of the type of product being test in the chamber. However, if all the details are not given to the chamber manufacturer, the resulting selection may not be best for the required applications and could cause safety risks. The chamber manufacturer should understand the test objectives. For example, hydraulic valves under pressure are being tested at various temperatures. Hydraulic lines enter and exit the chamber through an access port. Rarely, if ever, a fluid leak occurs in the chamber. This does not concern the operator since the warmest temperature achieved in the chamber is well below the auto -ignition point of the fluid . However, if a leak does occur the chamber will be at risk for an explosion . This is due to the fact that the standard nichrome wire heater used in most chambers can exceed 1000℉ surface temperature. For this type of application temperature limited sheath heaters must be used at a minimum. Depending on the application, a classified explosion proof chamber may be required. There are many scenarios which could be used for examples, but the bottom line is to make sure the chamber manufacturer all the details of the testing.

Product Load and Space Required

Many MIL-Standards specify approximately 1/3 product and 2/3 empty space around the product for adequate air flow. This may slightly vary with the design of the chamber. In some custom chambers, the work area is effectively an air duct and is almost 100% filled with product. Again, this is another area underlining the importance of the chamber manufacture understanding as much as there is to know of the test objectives.

Static (Dead) Load

The static load is any mass that is in the chamber that does not produce added heat. In the correct system to be correctly sized, we have to determine the dead load mass of the DUT along with any shelving, and fixtures. We would also need the type of material the DUT is made of to determine the specific heat. This will determine how easily your DUT gives up its heat during transitions from hot to cold and helps us accurately size the refrigeration system to meet your specific performance requirements.

Live Load

The live load is any mass that is in the chamber that produces heat. Any live load that is in the chamber will have to be measured (watts) to determine the correct refrigeration system to overcome that added load.
Some information needed for the design phase include: maximum dead load, maximum live load, type of material of the DUT, number of shelves for DUT support, and other fixtures needed for DUT mounting.

Chamber Construction

Chamber construction is a critical area that needs to be evaluated when making a chamber purchase. When looking at the various chamber manufacturers' brochures or products on-line, they all look very similar, they're typically boxes with doors and some may even be more attractive than others, but there is more to consider than just looks. Most have painted exteriors and stainless steel chambers. It is easy to believe they are all built the same way. However, when evaluating the details there are differences that can greatly affect the long term reliability of the chamber. Most of these differences relate to the way seams are constructed for the stainless steel liner. Are the seams welded, pop-riveted or screwed together? How are the ports fastened to the stainless steel liner and to the outer cabinet? Earlier in this document the topic of pressure within the chamber was addressed. Over the life of a test chamber the temperature is raised and lowered thousands of times. This stresses all the seams and connections in the chamber. The better the seams are bonded together the longer the chamber will operate dependably. When leaks occur in the stainless steel liner this opens a path for moisture to travel in and out of the chamber. The worse of these is when the chamber runs temperature and humidity test.
The humid air in the chamber finds the leak and condenses in the insulated area. Most chamber manufacturers use fiberglass insulation similar to what is installed in the walls of your house. When moisture condenses on the insulation it becomes saturated like a sponge and loses its insulating ability. The walls of the chamber then have less insulation which can affect the temperature and humidity performance. The water in the insulated space will eventually rust the outer sheet metal and allow water to leak on to the facility floor. A chamber with continuously welded seams is much less likely to develop leaks than a chamber assembled with other methods. Another point of consideration should be the access ports. As the pressure in the chamber goes up and down during temperature transitions the walls will deflect. The ports connect the inside chamber to the external cabinet. As the inside walls move from the expansion and contraction of air, the port

transfers that movement to the outer cabinet. Therefore, the connection between the port and the chamber must be extremely durable to withstand the frequent movement. There are several methods used to install ports by the chamber manufacturers. They range from pop-riveted and caulked to fully welded methods. Again, a welded port will hold up better than other fastening methods.

Another area that can be compromised over time is where the refrigeration lines penetrate the stainless steel chamber. The refrigeration lines are generally copper tubing. If any sharp edges touch the tubing a refrigerant leak will develop. A good method to eliminate the possibility of abrasion is to install the tubing in sleeves where it penetrates the chamber. The tubes should be stainless and continuously welded to the chamber linear. The copper refrigeration lines pass through the sleeves and the gaps filled with RTV which not only seals the penetration, but also provides a degree of resiliency to accommodate the movement generated as the chamber expands and contracts during temperature changes. As movement occurs the lines will not be exposed to sharp edges.

Cooling system

The refrigeration system removes heat from the product and the air which lowers the temperature in the chamber. The heat is moved through the refrigeration system and rejected at the condenser. There are two choices when it comes to condensers, air-cooled or water-cooled. Each one has its positives and negatives.

Integral Air-Cooled Chambers

Many small chambers come standard as air-cooled. The only utility connection required for temperature cycling chambers without humidity is power. This is very convenient for moving a chamber from one area to another. However, there are some items need to be considered with air- this additional load. For example, a chamber that has a 2 HP cascade system can reject 24,000 Btu/Hr or more into the room under full load. When the chamber is at set-point, it can reject between 12,000 to 15,000 Btu/Hr into the room. The smaller the room where the chamber is located, the more critical it is that the air conditioning system can handle the additional heat load. A general "rule of thumb" for heat of rejection is: 1Horsepower of refrigeration system is equal to 12,000 Btu/Hr. If a chamber is going to be installed in an area that is not air conditioned tell the chamber manufacturer. The chamber's performance will be reduced if the ambient environment where the chamber will be located exceeds 30°C. In some cases, the chamber will not operate. Condensers must be oversized to operate in high ambient room conditions.

Second item to consider for an air-cooled system is dirt. Large volumes of air are passed through the condenser constantly. Most condensers are located near the floor which allows them to pick up dirt easily. The condenser must be clean for the system to perform and work efficiently. This requires someone to clean the condenser at regular intervals. If the chamber is located in a dirty environment the condenser can become clogged very quickly. Restricted air flow will cause the refrigeration system to run at high pressure which will cause the high pressure safety to trip. If the environment described above is the destination for a test chamber, a remote air-cooled condenser) or water-cooled should be considered.

Remote Air-Cooled Chambers

Another type of air-cooled condenser is remote air-cooled. The air-cooled condenser is removed from the chamber and is placed in another location, normally outdoors. On the surface this sounds like the best option since the heat and noise is moved outdoors. However, this type of system is more complicated and expensive to install. This is due to several items: refrigeration piping must be sized and installed properly for the application, penetrations through the building roof or wall must be done by qualified personnel, a concrete pad or proper mounting (on roof) for the remote air-cooled condenser must be installed, and the roof must be able to support the weight of the remote air cooled condenser. This type of installation can become very involved as it will normally require bids from the following contractors: Refrigeration, Electrician and Roofer.

Water-Cooled Chambers

Larger chambers with refrigeration systems 6 horsepower or over are typically water cooled chambers. If your facility has process water that is pumped throughout the building and is routed to a cooling tower / dry cooler, a water-cooled chamber may be installed. A water-cooled unit is easy to install and maintain. Be sure to ask the chamber supplier for the water flow and pressure requirements for the unit. The capacity of the process water system should be verified before purchasing the chamber. Most problems with water-cooled systems are due to inadequate water flow and/or differential water pressure supplied to the chamber. If water cooled, provide and connect water supply and return lines to the inlet and outlet for the condenser. The line size should be equal to or larger than the inlet fitting provided on the chamber.

Note: Water cooled systems require a minimum of 40 PSI differential pressure (supply pressure minus return pressure) on the water system. Where water discharges to an open drain or non-pressurized return, supply must be 40 PSIG minimum. On systems using a closed loop cooling water system with a pressurized return, supply pressure must be at least 40 PSI greater than return pressure. Maximum water pressure should not exceed 80 PSI.

Water Usage

There are many applications where the refrigeration system demands fall into what is referred to as medium or high temperature applications. In these cases, the requirements identified below are inadequate. The chamber manufacture should supply these requirements when quoting so it will be known whether there is an adequate supply or not.

Ways to help prevent chamber condensation on parts

Air contracts as it cools. When a chamber is pulling down, it actually causes outside room air to be sucked into the chamber workspace. The moisture in the air will be drawn to and freeze on the cooling coil. The moisture will then vaporize into the air when the chamber is heated up and that moisture can end up as condensation on the test product. Dry Air Purge or Gaseous Nitrogen (GN2) may be used to minimize condensation. Purging the chamber with either of the two maintaining a slight positive pressure on the chamber and minimizes the moisture infiltration into the chamber. The dry air or GN2 contains very little moisture so the chamber air can stay "dry". To help avoid condensation on the walls and product with humidity chambers, bring up the air temperature first, let the walls and product stabilize, then raise humidity. If the chamber air temperature and humidity levels are raised faster than the wall and product temperature, moisture will condense on the cooler surfaces. By maintaining the dew point of the air below the surface temperature of the walls and product, moisture will not condense on the surfaces. In most cases you can run a characterization test or two first, to determine how long it takes the largest mass (be it product or wall) to stabilize. Many controllers offer cascade control and guaranteed soak capabilities. A separate sensor can be used to monitor, for example, the product. The controller can be programmed to enable a certain event, only after a certain condition has been met. In this case, we're telling the controller to delay the ramp up of humidity until the sensor placed on the product reaches a point within x number of degrees of set point.

LN2 Boost

LN2 Boost is designed to provide approximately 20,000 Btu/hr of additional cooling to -73°C (-100°F). The LN2 Boost function will only initiate if the controller is programmed with this option and the LN2 boost event is initiated. This event will allow the controlling solenoids to open during a programmed test profile. The controller will only turn on the LN2 solenoids)\ if the demand for cooling exceeds the refrigeration systems capacity. This is to ensure that there is no excess LN2 wasted during a profile. It is the customer's responsibility to supply the LN2 boost assembly with a maximum regulated pressure of 25 psig pressure from their supply tank.

How it works

LN2 is injected into the air stream through a small distribution tube located inside the plenum. As the LN2 is injected it immediately expands into a gaseous vapor. This expanding process absorbs heat,causing the cooling effect. The gaseous vapor is pure GN2 which can be dangerous if allowed to collect in a small area.

Safety Concerns

Venting the GN2 is ultimately the customer's decision but it is CSZ's recommendation that all systems with LN2 boost be vented to an outside environment. If GN2 is allowed to collect in small labs or areas around the chamber, the results can be very harmful or even fatal. GN2 will displace the oxygen in the environment, resulting in low levels of oxygen in or around the chamber making breathing difficult and even causing asphyxiation. GN2 should be vented directly to the outside environment through an insulated duct. This duct can be attached to the vented port located on the top of the chamber. Cincinnati Sub-Zero Products (2017) developed a list of considerations that new cold chamber purchasers would need to address as presented below:

- All necessary permits must be obtained and compliance to local and on site codes.
- Provide and coordinate rigging of equipment, uncrating and pallet removal, moving the chamber in the building and placing equipment at permanent location.
- Be sure to request a truck with a lift gate if there is not dock available.
- All chambers are shipped on pallets and a forklift is needed to remove it from the pallet. It is critical to know the exterior dimension of your chamber in order to move it into the building.
- Clearing doorways and hallways may be an issue.

- Installation of equipment.
- Proper power and voltage must be supplied for the chamber. The data plate label located in the back of the chamber describes the proper power information needed to operate the chamber.
- If the ambient environment of the area where the chamber will be installed exceeds 30°C (85°F), a chamber with a water cooled condenser should be used. Air-cooled chambers will lose capacity and damage can occur to the unit if the ambient room temperature is too high.
- A minimum of three feet clearance around the chamber is recommended for service and proper ventilation.
- If chamber is not on ground floor, make sure flooring can handle the weight of the chamber and its components.
- Provide electrical disconnect, if needed.
- Provide compressed air 80-110 psig, if needed, free of oil and entrained water.
- Provide water regulator (Humidity Chambers Only) and tap or de-ionized water.
- Connection of hose from chamber drains to either floor drain or a condensate pump.
- A qualified professional must make final connections, in accordance with local and on site codes.
- Anchor all chamber components to building floor where bolt down holes are present.
- If the chamber is an integral air-cooled unit, make sure the air-conditioning system in the area has enough capacity to remove that heat. The heat rejection information for the chamber will be listed in the chamber documentation and drawings located in the manual.
- For roof-mounted components, ensure that the building roof will support the added load of the components. Roof mounted components must meet local and on site codes.
- For roof-mounted components, provide all roof curbs and structures for their support.
- Provide all penetrations and sealing of penetrations through the roof for refrigeration and electrical runs.
- Location of air-cooled condenser must allow adequate space for free air circulation and maintenance.
- Ground level components must be mounted on customer supplied concrete pad or equivalent.

Computer Controlled Cooling Boxes

One of the most prevalent application of computer controlled cooling boxes is in the cryogenic field. By exploring this section it may be possible to use some of their skill and technology and apply it to material testing. One of the leaders in the industry since 2005 has been the Cryonics Institute (CI). They have set up two computer-controlled cooling boxes, a large one for human patients and a smaller one for pets & testing. These cooling boxes are designed to bring the temperature of patients or pets from above water-ice temperature after perfusion to liquid nitrogen temperature for long-term storage. The use of vitrification solution for perfusion mandates rapid cooling before solidification temperature ($\mathbf{T_g}$, near minus 120 degrees Celcius) to prevent ice formation. They have found that there should also be slow cooling below solidification temperature to liquid nitrogen temperature to prevent or minimize cracking. Other circumstances or testing may call for other cooling profiles. The computer-controlled cooling boxes provide the ability to control cooling rates with some precision in any temperature range using minimal manual supervision. It is also possible to obtain a log of the temperature changes that have occurred so that cooling curves can be generated and studied. From 2005 to 2009 computer control of the two cooling boxes was by a LabView/National Instruments system that was custom created for CI by Wineman Technology, Inc. The local (Clinton Township, Michigan) cryogenic engineer Marc McMaken built the small cooling box and provided the controlling hardware for both boxes.

The large cooling box is made of wood and extruded polystyrene foam insulation. The small cooling box is made of stainless steel and a type of foam insulation. Both cooling boxes have a long bar on the inside which is perforated with small holes that can shoot-out liquid nitrogen. Although the liquid nitrogen is quite cold, much of the cooling comes from heat absorbed when the liquid nitrogen vaporizes into gas. Thus the liquid nitrogen vaporization is considered to be an endothermic process. The heat of vaporization for liquid nitrogen is 5.57 kJ/mole.

Injection of liquid nitrogen into the cooling boxes is controlled by a Magnatrol Type-M normally-closed valve (10M61Z) which is rated for liquid nitrogen. A pressure regulator keeps the injection pressure at 45 PSI (Pounds per Square Inch). A 75 PSI pressure safety valve on the liquid nitrogen tank blows-off whenever pressure reaches 75 PSI in the tank. Too much pressure in the tank would hamper efficient operation of the 45 PSI pressure regulator. The Magnatrol valve is controlled by an electrical relay switch located in a power/relay box mounted on the cooling boxes, but only when a toggle switch on the power/relay box is in the up position. A +24 volt DC signal from the computer controller allows AC power from a wall socket to open the Magnatrol valve. No voltage (0 volt signal) comes from the computer controller when the Magnatrol valve is to be closed. An orange indicator light on the power/relay box is lit when the AC power is activating the Magnatrol valve. The signals received from the computer controller are based on temperature readings received from a thermocouple in the cooling box that has been placed in the patient or on the test object. T-type thermocouple beaded

probes are used which have an operating range of −200ºC to +350ºC. A new Omega 1/16 DIN CN96111TR-C2controller was purchased and wired into the system. The Magnatrol solenoid valve would noisily oscillate with the new controller, suggesting that the solenoid was defective. Eventually the root of the problem was found: the National Instruments controller required a DC relay, whereas the Omega controller required an AC relay. The system had been putting AC current into a DC relay. Replacing the DC relay with an AC relay stopped the noisy solenoid valve oscillations. Power consumption is very low for the Omega controller unit, about 45 watts. The next upgrade entailed obtaining an APC Smart-UPS XL1000Uninterruptible Power Supply (UPS) with an APC batterypack that could provide enough power during a blackout to keep the cooling box going for 16 hours. That would provide plenty of time to discover the problem and get the generator going and for the power to return.

The configuration screen on the laptop allows the operator to program a sequence of cooling steps, where each step specifies a target temperature. The rate at which the Magnatrol valve opens and the duration of the valve opening is determined by calculations in the computer based on the specifications in a cooling step and the temperature of the controlling thermocouple. A cooling curve will be displayed on the computer screen, which can be saved for future examination or for printing. One example of a sequence for cooling a patient from water-ice temperature to liquid nitrogen temperature might be the following:

(1)	cool	to	−130ºC	in	8	hours
(2)	hold	at	−130ºC	for	4	hours

(3) cool to −196ºC in 200 hours

The computer will calculate a cooling rate that is necessary to achieve the desired target temperature (ex, −130ºC) in the desired time (ex, 8 hours) for each step. When the program is started, the computer begins opening the Magnatrol valve at a rate required to achieve the desired cooling rate based on feedback from the controlling thermocouple. Typically that would involve the thermocouple in the throat used to approximate brain temperature.

The LabView/NI software/hardware allowed for four thermocouples, but the Omega software/hardware only allows for one thermocouple. With enough experience of the LabView/NI software/hardware it is possible to understand the relationship between ambient, body and brain temperature during the process of cooling. Cooling is controlled by ambient temperature, which results in the most gentle cooling of the patient, despite the fact that the temperature fluctuations at the thermocouple make it appear to be the least gentle. The Omega system can only apply a single temperature probe and has limited graphics capabilities, so it is less sophisticated than LabView. The Omega data from the single probe can be exported to a Microsoft EXCEL file. A chart can be created from EXCEL's charting capabilities.

Figure 30. Computer Controlled Cooling Box

Since its large-scale commercialization at the turn of the 20th century, nitrogen has become essential to the CPI. Its inerting capability enhances the safety of many operations and the quality of many products. Its use as a cryogen for extremely low-temperature refrigeration continues to grow as cryogenic processes are developed and improved.

The optimization of advanced process controls for liquid nitrogen cooling and freezing systems is an ongoing area of research. Precise control of temperature setpoints (e.g., ±0.5°C) and heat-transfer rates during extremely low-temperature operation (between –150°C and –196°C) is challenging because of heat leakage to the environment, even with vacuum insulation. Efforts are underway to develop more robust control systems capable of delivering extremely low-temperature liquid nitrogen refrigeration in a more precise, yet cost-effective, manner.

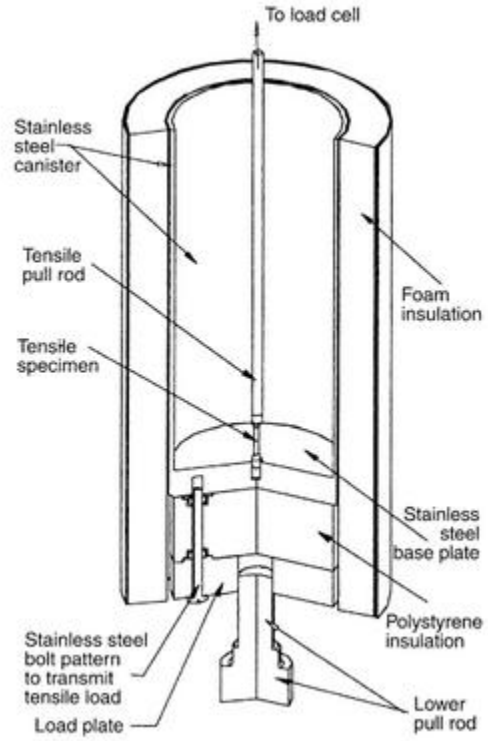

Figure 31. Cross Section of Cooling Box 1

Legacy cooling system component research analysis

Components

1) MiniPup Model 2000 Controller

The Series 2000 family of controllers possess extensive capability to control a multitude of different single and two loop systems. While temperature control is the most popular application, the Series 2000 Instruments can control any process or Machine that provides a current or voltage measurement. input signal, and can function from a relay or analog output signal in a variety of control forms. These output functions may be alarms, on-off, or PID. The model being used is a standard single loop microprocessor based PID process controller utilizing a 6 switch front panel keypad including a Start/Stop key. In general terms, there are three basic types of controllers: on-off, proportional and PID.

On/Off Control

An on-off controller is the simplest form of temperature control device. The output from the device is either on or off, with no middle state. An on-off controller will switch the output only when the temperature crosses the setpoint. For heating control, the output is on when the temperature is below the setpoint, and off above setpoint. One issue that arrises is that the temperature has to cross the setpoint to change the output state. This means the process temperature will be cycling continually, going from below setpoint to above, and back below. In cases where this cycling occurs rapidly, and to prevent damage to contactors and valves, an on-off differential, or "hysteresis," is added to the controller operations. This differential requires that the temperature exceed setpoint by a certain amount before the output will turn off or on again.

On-off differential prevents the output from "chattering" or making fast, continual switches if the cycling above and below the setpoint occurs very rapidly. On-off control is usually used where a precise control is not necessary, in systems which cannot handle having the energy turned on and off frequently, where the mass of the system is so great that temperatures change extremely slowly, or for a temperature alarm. One special type of on-off control used for alarm is a limit controller. This controller uses a latching relay, which must be manually reset, and is used to shut down a process when a certain temperature is reached.

Proportional Control

Proportional controls are designed to eliminate the cycling associated with on-off control. A proportional controller decreases the average power supplied to the heater as the temperature approaches setpoint. This has the effect of slowing down the heater so that it will not overshoot the setpoint, but will approach the setpoint and maintain a stable temperature. This proportioning action can be accomplished by turning the output on and off for short time intervals. This "time proportioning" varies the ratio of "on" time to "off" time to control the temperature. The proportioning action occurs within a "proportional band" around the setpoint temperature. Outside this band, the controller functions as an on-off unit, with the output either fully on (below the band) or fully off (above the band). However, within the band, the output is turned on and off in the ratio of the measurement difference from the setpoint. At the setpoint, the output on:off ratio is 1:1; that is, the on-time and off-time are equal. If the temperature is further from the setpoint, the on- and off-times vary in proportion to the temperature difference. If the temperature is below setpoint, the output will be on longer; if the temperature is too high, the output will be off longer.

PID Control

The third controller type provides proportional with integral and derivative control, or PID. This controller combines proportional control with two additional adjustments, which helps the unit automatically compensate for changes in the system. These adjustments, integral and derivative, are expressed in time-based units; they are also referred to by their reciprocals, RESET and RATE, respectively. The proportional, integral and derivative terms must be individually tuned to a particular system using trial and error. It provides the most accurate and stable control of the three controller types, and is best used in systems which have a relatively small mass, those which react quickly to changes in the energy added to the process. It is recommended in systems where the load changes often and the controller is expected to compensate automatically due to frequent changes in setpoint, the amount of energy available, or the mass to be controlled. There has also been a number of autotune controllers developed that have the ability to automatically tune themselves.

Brandt Instruments STD 5000 (I/P) Current to pressure transducer

Model: STD 5131

Immune to shock and vibration, the Brandt current-to-pressure (I/P) transducer is built for rugged, industrial environments. The field-proven E-Pi transducer technology is a revolutionary breakthrough that provided the industry with its first “solid state” I/P transducer.This advanced E-Pi technology uses a minimal amount of electrical energy and air consumption to convert a 4 to 20 mA input signal to a proportional pneumatic output signal (3-15 PSIG, 0.2-1 BAR, etc.). This pneumatic (backpressure) output is precisely modulated by a virtually weightless, low-mass membrane that is held in a continuously balanced position. The output of the E-Pi is fed into an integral volume booster to deliver a pneumatic output signal with an output capacity of 4.0 scfm. Overall performance, accuracy and repeatability are further enhanced via an internal feedback network that allows the transducer to quickly respond to input changes. These balanced supply and exhaust dynamics enhance stability while delivering accuracy of ±0.15% of span for superior process control. According to Figure 1 the model in use (STD 5131) is a device that functions only as a current to pressure with a 4-20 mA input and will produce a 3-15 PSIG standard output. Table 1 shows the device specifications.

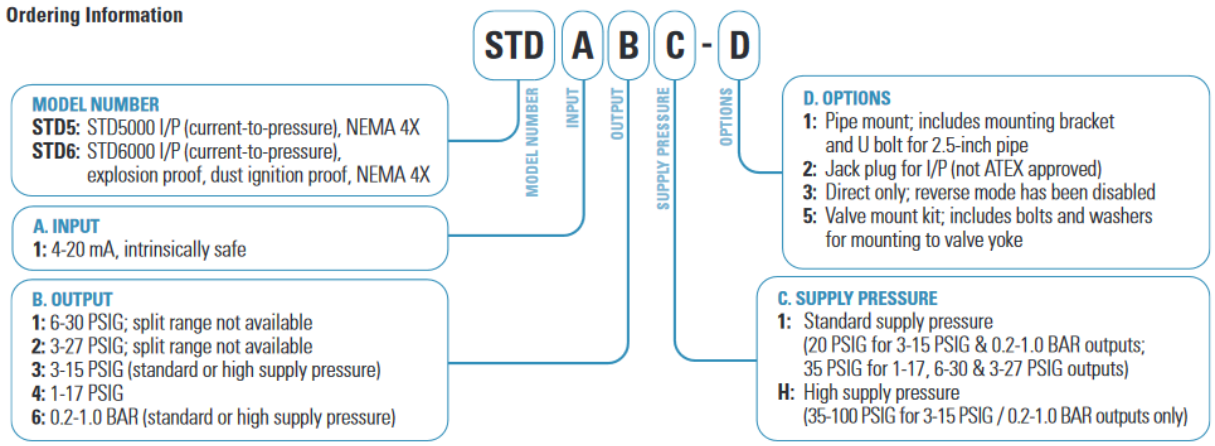

Figure 32. MiniPup Model Information

Thermo Scientific STD5000 & STD6000 Current-to-Pressure (I/P) Transducers

Functional Specifications	
Accuracy	±0.15% of span (3-15 and 1-17 PSIG output); ±0.25% of span (3-27 and 6-30 PSIG output)
Repeatability	0.05% of span
Deadband	0.02% of span
Stability/Reproducibility	0.5% of span/6 months
Output Capacity	Standard: 4.0 SCFM (supply and exhaust characteristics are balanced to within ±10%) High Pressure: 4-8 SCFM possible (dependent on air supply and tubing size)
Air Consumption	0.04 SCFM steady state average (0.06 SCFM maximum)
Position Effect	Not measurable
Vibration Effect	<0.25% from 1-200 Hz/1g
Frequency Response	-3 db at 5 Hz (per ISA-S26.4.3.1 Configuration A)
Loop Load	3.8 VDC + 5 ohm (195 ohm load at 20 mA)
Operating Current	3.7 mA min; 200 mA max; continuous at 120°F half cycle 70 amp 1/120 second at 68°F
Supply Pressure	Standard: minimum of 3 PSIG and maximum of 10 PSIG above the maximum calibrated output High Pressure: for outputs of 3-15 PSIG and 0.2 to 1.0 BAR, supply range is 35 to 100 PSIG or 2.4 to 6.9 BAR; Pressures below 35 may affect the output of the unit; Other output ranges may be possible (consult Thermo Fisher Scientific)
Air Supply	Clean, dry and oil-free instrument air
Operating Temperature	-40°C to +66°C (-40°F to +150°F)
Temperature Effect	Range of +18°C to +66°C (0°F to +150°F): ±0.02% / °F of span; Range -40°C to +66°C (-40°F to +150°F): ±0.04% / °F of span
RFI-EMI Effect	Less than ±1% effect on zero/span (26-1000 mHz @ 30V/m) when installed per product installation guidelines
Operational Modes	Field selectable direct, reverse and/or split range; see notes in model number description
Failure Mode	Mechanically direct (i.e., if the input current drops below 3.7 mA DC, the output will drop to 1 to 2 PSIG regardless of direct or reverse mode selection)
Physical Specifications	
Enclosure	Internally purged NEMA 4X/IP65; cast/machined aluminum with powder-coated epoxy
Connections	Supply port; ¼-in NPTF (1X) Pneumatic Output Port: ¼-in NPTF (2X) Electrical: ½-in NPTF conduit (2X); terminals 12-22 AWG wire
Weight	1.13 kg (2.5 lbs)
Certifications	
ATEX	STD5000: intrinsically safe, 4-20 mA models only; II 1G Ga Ex ia IIC T4 [Tamb -20°C to +60°C (-4°F to +140°F)]; II 1D Da Ex iaD 20 T+62°C (+144°F) STD6000: flameproof; II 2 G Ex d IIC T5 [Tamb -20°C to +50°C (-4°F to +122°F)];II 2 D Ex tD A21 IP6X T+100°C (+212°F)
CSA/US	STD5000: intrinsically safe, 4-20 mA models only; Class I, Div 2, Groups A, B, C & D; Class I, Div 1, Groups A & B; Class II, Div 1, Groups E, F & G; Class III, Div 1 when connected to CSA certified barriers rated 31.5V max, 463 ohms min, T3C; Class I, Div 1, Groups C & D; Class II, Div 1, Groups E, F & G; Class III, Div 1 when connected to CSA certified barriers rated 28V max, 120 ohms min, T3C; STD6000: Class I, Div 2, Groups A, B, C & D; Class I, Div 1, Groups B, C & D; Class II, Div 1, Groups E, F & G; Class III, Div 1
CE	Compliant

Figure 33. I/P transducer Initial Settings

The most common application of the I/P transducer is to obtain an electrical signal from a controller and produce a proportional pneumatic output for operating a control valve or positioner. The device can be mounted on the wall, pipe stand, or directly on the valve actuator depending on how well the device can withstand vibrations. If the transducer is able to withstand vibrations it should be placed on the valve actuator. If the vibrations are too bad then the instrument pipe should be used.

Most I/P converters are supplied instrument air around 20 PSIG above the required output. If the I/P transducer is not working or performing poorly, it may be having issues with its air supply. To troubleshoot the device, open the air set drain and check that the supply air is dry and there is no oil. The external bleed opening should also be examined to make sure it is venting properly and free from obstructions. The calibration is similar to the process for a pressure transmitter. Accurate inputs must be provided and the output should be tested with a test gauge or other output device. Also the Check Zero, Span, and Linearity should be adjusted as necessary. This calibration should use an accurate current generator or an accurate voltage generator with a compulsory precision resistor of 250 ohms and a .5 watt power rating.

I/P Transducer Calibration

I/P transducers are calibrated similar to analog DP transmitters. A DP transmitter senses signal process pressure and outputs a standard 4 -20 mA signal. During the calibration, pressure is applied within the range of the transmitter to confirm the output stays within the 4 – 20 mA range. The deviation is to be kept minimized by adjusting the ZERO and SPAN. The I/P transducer takes current in the 4 -20 mA range and converts it to a pneumatic output of 3 – 15 psig. Thus, the calibration would essentially be providing the transducer the 4 -20 mA and verifying that 3 -15 psig is being produced. The only things that would be adjusted are the ZERO and SPAN settings. By obtaining both 3 psig from a 4 mA input and 15 psig from a 20 mA input, it will be proved that the device is operating within the required range. The necessary equipment setup is shown in Figure 2.

Safety Precaution

The steps and guideline provided here are meant as a general guide. Before embarking on an actual calibration, consult your manufacturer's manual for the I to P converter. It should be your **de facto guide**. Make sure you are wearing all the necessary safety gear and that you are complying with all the requirement for Hazardous Area classification and any other requirement that will ensure the exercise is done safely.

Materials Required:

- Current Source - capable of delivering 150% (30m A) of maximum output of transducer with the required compliance voltage.
- Supply pressure of at least 20psig.
- A milliammeter (In the absence of a milliammeter, a 0 - 10VDC voltmeter with a 250 ohm resistor connected across it can serve the same purpose - 1VDC indication for 4m A and 5VDC indication for 20m A)

Figure 34. I/P transducer safety info

Connect the equipment setup as shown below:

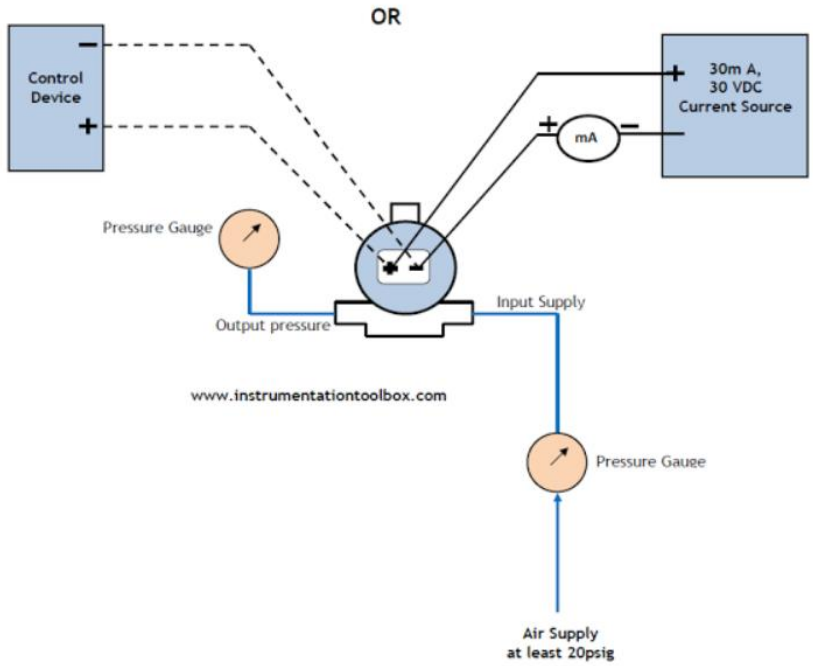

Figure 35. I/P transducer wiring setup

Research Control Valve Mod No: 1002GCN36EVOSOLN36

The Type 755 actuator is a pneumatically operated, spring opposed diaphragm actuator designed specifically to fit the Research Control Valve body-bonnet assembly. The unit is available in two sizes: one to fit the 1/4 in. (6 mm) valve and a larger version to fit the 1/2...1 in. (12...25 mm) valves. It provides smooth linear extension of the valve stem upon an increasing instrument signal. A decrease in instrument signal causes the stem to retract and open the valve. Downward closing force is generated by instrument air on top of the diaphragm. An increasing pressure in the diaphragm cavity opposes the force of the spring and extends the stem, closing the valve. The unit is designed to retract the stem, opening the valve, should the instrument signal fail.

The 1/4 in. (6 mm) size 755 actuator normally operates in response to a 3-15 psi change in instrument signal, or a 12 psi range. This signal range causes the valve to stroke a distance of approximately 7/16 in. The standard spring has a deflection rate of 25 pounds per 1/8 in. and operates against an effective diaphragm area of approximately 7 square inches. The 1/2 in. size 755 actuator also normally operates in response to the same psi change in instrument signal, or a 12 psi range. This signal range causes the valve to stroke a distance of approximately 9/16 in. The standard spring in the 1/2 in. unit has a deflection rate of 30 pounds per 1/8 in. and operates against an effective diaphragm area of approximately 11 square inches.

Figure 36. Research Control Valve Actuator

DIMENSIONS

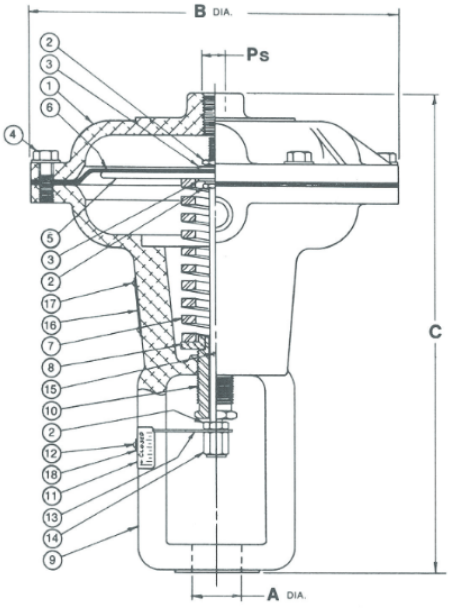

Dimensions	Actuator Size	
	1/4 in. (6 mm)	1/2 in. (12 mm)
Ps	1/8 in. (3.2 mm) NPT	1/4 in. (6.4 mm) NPT
A	0.625 in. (15.9 mm)	0.875 in. (22.2 mm)
B	5.12 in. (130.0 mm)	6.43 in. (163.3 mm)
C	6.62 in. (168.1 mm)	8.40 in. (213.4 mm)

Description of Items

Item	Description	Standard Material	Material Size	
			1/4 in. (6.4 mm)	1/2 in. (12.7 mm)
1	Pressure case	Aluminum	—	—
2	Stem nut	300 stainless steel	1/4 in. (6.4 mm) hx	3/8 in. (9.5 mm) hx
3	Washer (2 ea.)	300 stainless steel	—	—
4	Rim screw (6 ea.)	300 stainless steel	5/16 in. (7.9 mm) hx	3/8 in. (9.5 mm) hx
5	Diaphragm plate	Steel-Zn/Pl	—	—
6	Diaphragm	Buna or Nylon	—	—
7	Spring	Steel	—	—
8	Spring seat	Aluminum	—	—
9	Spring case & yoke	Aluminum	—	—
10	Spring adjuster	300 stainless steel	5/16 in. (7.9 mm) hx	5/8 in. (15.9 mm) hx
11	Travel scale	300 stainless steel	—	—
12	Screw	300 stainless steel	—	—
13	Travel pointer	300 stainless steel	—	—
14	Stem connector	300 stainless steel	1/4 in. (6.4 mm) hx	3/8 in. (9.5 mm) hx
15	Stem	316 stainless steel	1/8 in. (3.2 mm)	3/16 in. (4.8 mm)
16	Nameplate (2 hole)	Stainless steel	—	—
17	Drive screw (2 ea.)	Stainless steel	—	—
18	Washer	Stainless steel	—	—

Figure 37. Research Control Valve Parts

SPECIFICATIONS

Diaphragm Effective Area	1/4 in. (6.4 mm) unit; 7.3 in.^{2} (4709.7 mm^2) 1/2 in. (12.7 mm) unit; 11.25 in.^{2} (7258.1 mm^2)
Pressure Rating	Max. pressure 60 psi (4.1 bar)
Temperature Limit	With Buna diaphragm at < 30 psi (2.1 bar) –20…160° F (–28.9…71.1° C) (Consult factory for higher temperatures)
Spring Ranges	Standard: 3…15 psi (0.2…1.0 bar), throttling Optional: 6…30 psi (0.4…2.1 bar), throttling Optional: 3…27 psi (0.2…1.9 bar), throttling Optional: 0…15 psi (0…1.0 bar), On/Off Optional: 0…30 psi (0…2.1 bar), On/Off

Figure 38. Research Control Valve Specs

The USB to RS-232 converter facilitates the connection of legacy RS-232 products to the modern USB-equipped host PCs for the purposes of configuration and test. Peripherals used with the USB to RS-232 converter include the host PC and the connected valve actuator. The USB to RS-232 converter is typically only connected during the configuration of the valve actuator.

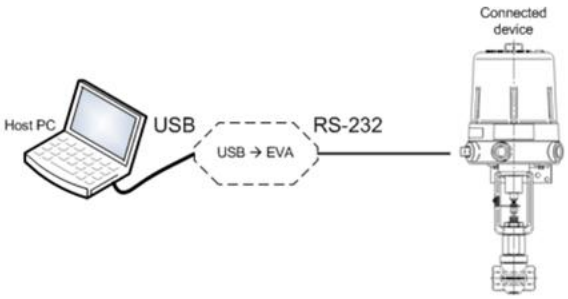

Items Required

- USB to RS-232 converter module (1)
- Badger Meter product featuring an RS-232 serial interface
- USB cable with ferrites and A connector to mini-USB (1)
- Terminal emulator with VT52 emulation
- Access to FTDI drivers (within the Windows® driver base, or on the included CD/DVD, or from the FTDI site *http://www.ftdichip.com/FTDrivers.htm)*

Figure 39. Research Control Valve Setup

Actuators are a method of automating a valve so that no human interaction is needed to cycle it. Actuators can be remotely operated and can act as a shutdown during an emergency, where human interaction would be dangerous. At a basic level, an actuator is a control mechanism that is operated by an energy source. This energy can be hydraulic pressure, pneumatic pressure, or electric current which moves the internal mechanical parts of the actuator. They can be designed to fail-open (in the case of actuator failure, the valve will stay open) or fail-close (in the case of actuator failure, the valve will stay closed). They also are distinguished by whether they are for quarter-turn (e.g., ball valves, plug valves) or linear (e.g., gate valves) valve operation.

Types of Actuators

Double Acting – Actuators in a double acting configuration have air/liquid supplied to both sides of the piston, with one side being higher pressure which achieves the movement required to actuate the valve. This configuration uses the air/liquid as energy to both open and close the valve.

Spring Return – Actuators in a spring return configuration have air/liquid supplied to only one side of the piston, and the energy to move the mechanisms comes from a spring on the opposite side. This configuration uses the air/liquid as energy to open or close the valve, while the spring acts to affect the opposite motion.

Pneumatic– Pneumatic actuators utilize compressed air to generate the operating energy. These actuators are quick to respond, but are not ideal for environments under high pressures, as gas is compressible. Pneumatic actuators can be either spring return or double acting.

- Piston Style – Piston style actuators generate linear force by the air acting on the piston. The conversion of this linear force to torque (for use in rotary valves) is achieved by specific actuator designs.
  - Scotch Yoke – A scotch-yoke actuator includes a piston, connecting shaft, yoke, and rotary pin. The yoke is offset 45 degrees from the axis of the piston at the two ends of travel and at 90 degrees to the piston shaft when in the mid travel position. The canted scotch-yoke design is ideal for offset butterfly valve actuation.
  - Rack and Pinion – Unlike traditional actuators, which produce a 90-degree turn of the pinion, rack, and pinion, actuators output a 180-degree turn. This style of actuator is particularly suitable for actuating plug valves.
- Diaphragm Style – The diaphragm-style actuator includes a rubber diaphragm and stem in a circular steel housing. This style of actuators is ideal for valves requiring shorter travel, such as diaphragm valves and globe valves.

Brandt Filter Flow

Pneumatic Instrumentation requires well regulated, clean, dry, oil-free air to assure a long trouble free life. Brandt Instruments FAS Series of Filter Regulators offers combinations of regulators and high-efficiency filters designed to regulate supply air and remove contaminates, oil and water vapor. The FAS2022: I/P Filter Regulator is recommended for use with Brandt's CPT and STD Series of Current to Pressure Transducers. It features a powder coated zinc body and metal bowl with manual drain and 5 micron filter. It features an integral 0-60 psig supply gauge with no exposed fittings. It can also be mounted directly to the STD Series of Current To Pressure Transducers. The supply pressure regulators are used to provide pneumatic measuring and control equipment with a constant air supply. The supply pressure regulator reduces and controls up to a maximum pressure of 150 psi in a compressed air net-work to obtain the pressure required.

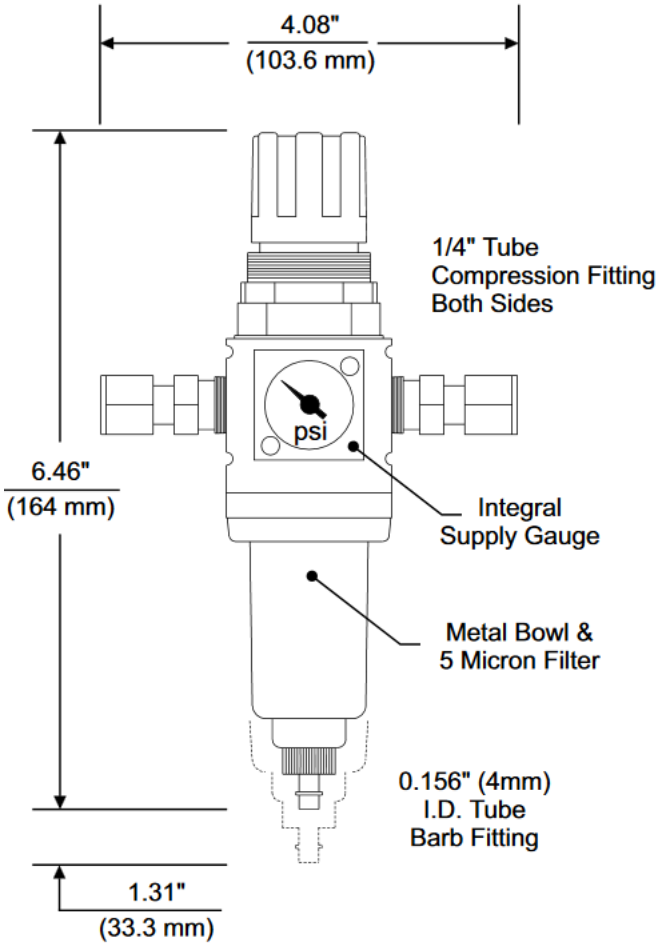

Figure 40. FAS2022 Filter Regulator

SPECIFICATIONS

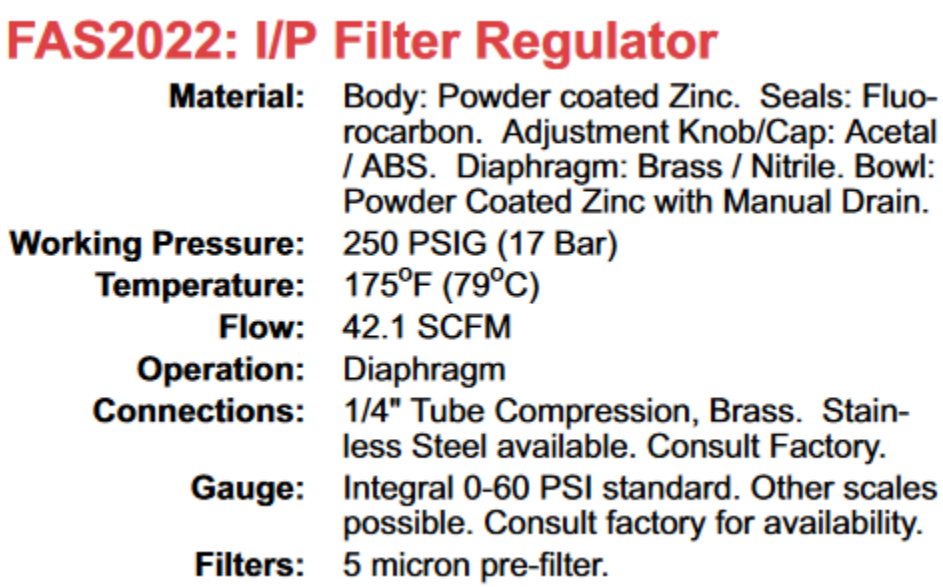

Figure 41. FAS2022 Filter Regulator Specs

The cold boxes at this lab were designed to use the existing nitrogen cooling system and have room for different attachments. They also include a wire port for strain gages, and easier access to the samples with a broad empty surrounding area. The boxes are constructed of an alumninum base and walls with tape and Amaflex being used for additional insulation. There is also a cooling radiator system that was assembled near one of the walls and shock absorber covers were placed over the radiator after being measured and cut and attached for added protection. Upon testing the shock absorbers were limiting the temperature decreases so they were replaced with ¼ inch polyethylene plates with additional bar port holes to allow for easier movement of the bar. Stoops (1987) found that the addition of a thermocouple switch box to the system would reduce the time needed to change the thermocouple sensor from one cold box to another to just a little above 30 minutes. Other discoveries include only needing 10 minutes to arrive at a stable cold air temperature inside the box. If the box is already closed it will take about 3 hours to warm back up. This is due to the boxes not leaking nitrogen. The boxes were redesigned for extra space to maneuver the samples as well as to increase visibility and video monitoring. Extra space was also given for the thermocouples, strain gauges, and their wiring that will prolong their lifespan by not having to be crushed by the box lids. The design now makes it possible to use the boxes in either room temperature or cold temperatures. Further modifications would be necessary for testing at high temperatures.

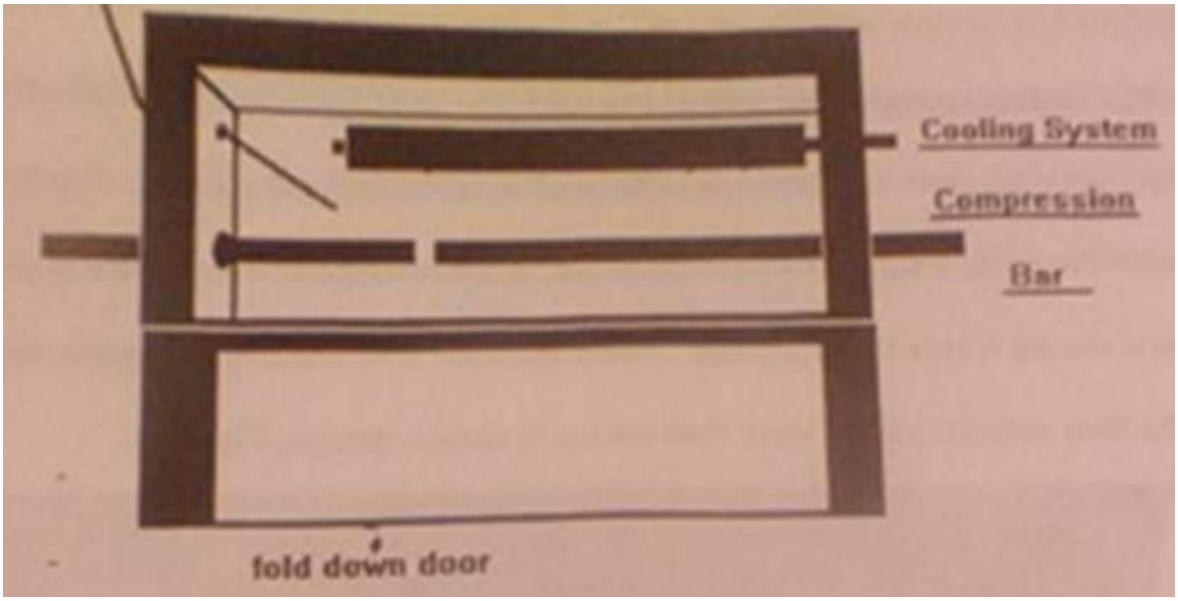

Figure 42. CRREL cold box design

The standard operating procedure for the cooling system shown in Figure 44 consists of several necessary elements. First the air supply needs to have a minimum of 30 psig. The next step is to adjust the controller to the desire set point and then turn it off. The LN2 tank valve then needs to be turned to fully open and then the controller is turned back on. The final step is to adjust the SVOF fine tune control so that the controller reaches a steady state. To shutdown the system there are a few steps as well. First the LN2 tank valve needs to be closed. Then a sufficient time must pass for the LN2 to drain from the lines into the chamber. If the Liquid Nitrogen gets trapped between the tank and the valve the nitrogen will expand and the tubes will explode. The final step is to turn off the controller.

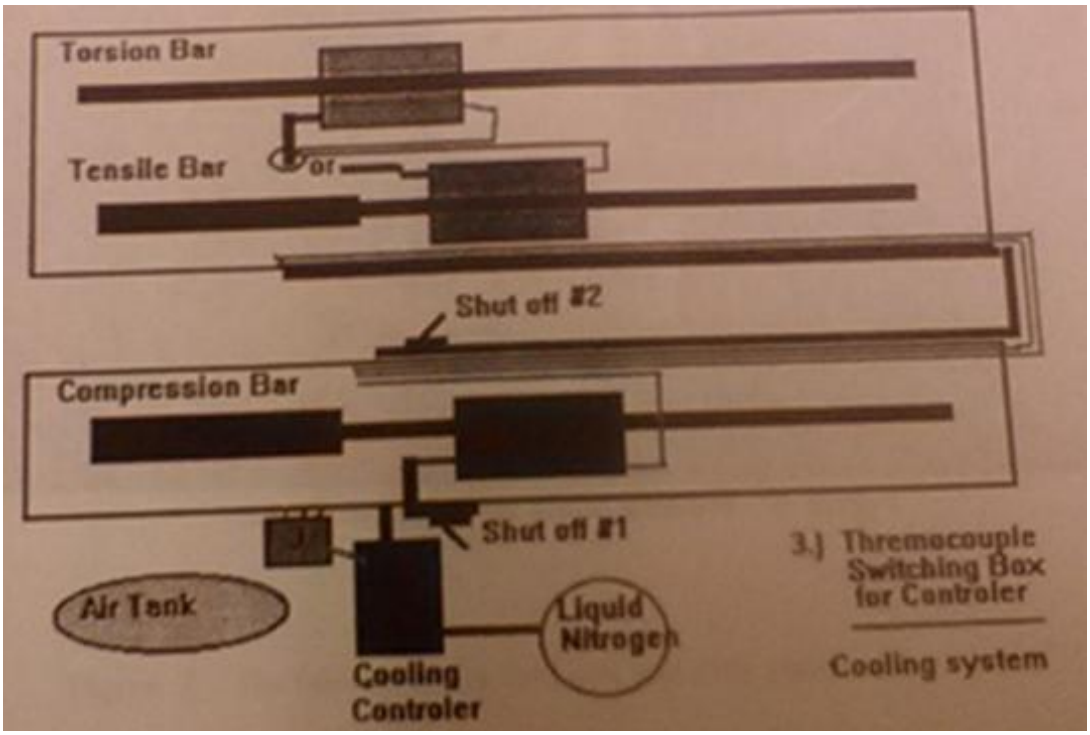

Figure 43. CRREL cooling system design

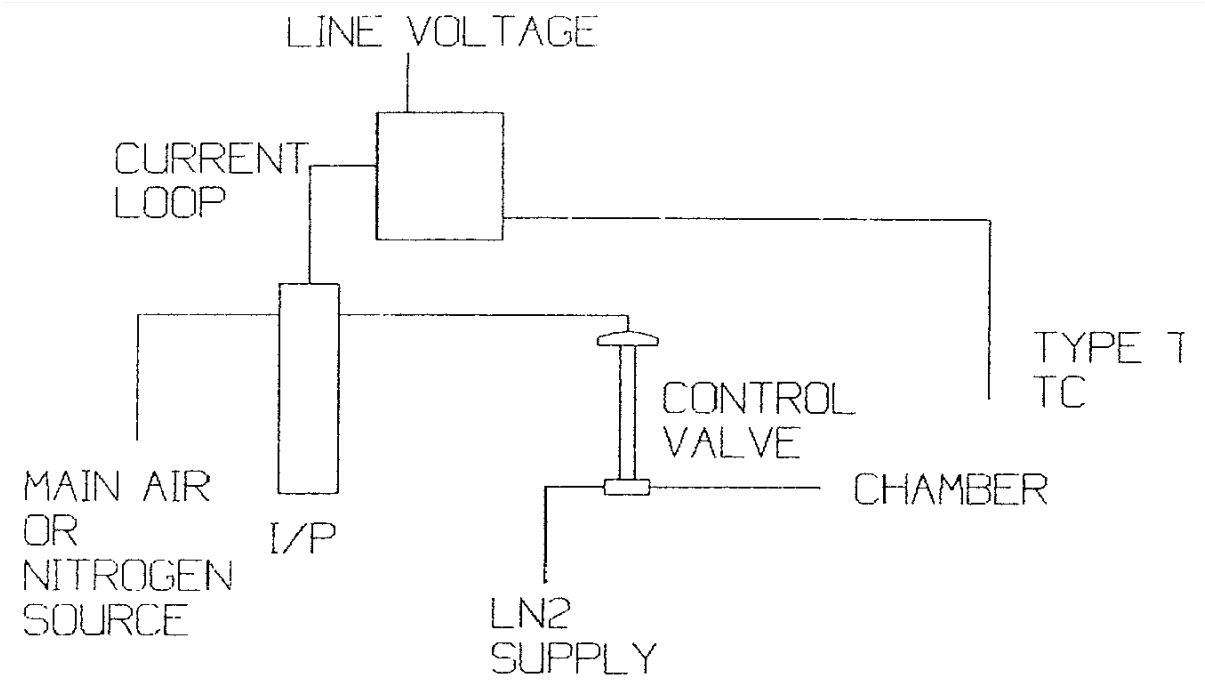

Figure 44. CRREL cooling system control

Strain Gauges

There are five main types of strain gauges: mechanical, hydraulic, electrical resistance, optical, and piezoelectric. Mechanical strain gauges are sometimes known as a crack monitors. They are composed of two separate plastic layers that have a layer of tough, plexi-glass plasticsandwiched in between. The bottom layer has a ruled scale on it and the top layer has a red arrow or pointer. One layer is attached to one side of the crack and one layer to the other so, as the crack opens, the layers slide very slowly past one another and the pointer will move over the scale. Some mechanical strain gauges can be even more crude in nature. The most simple setup is to glue a piece of plastic or glass across a crack and wait for it to shatter when the material is force to move(Follansbee and Murr, 1986). Figure 45 shows an example of a mechanical strain gauge.

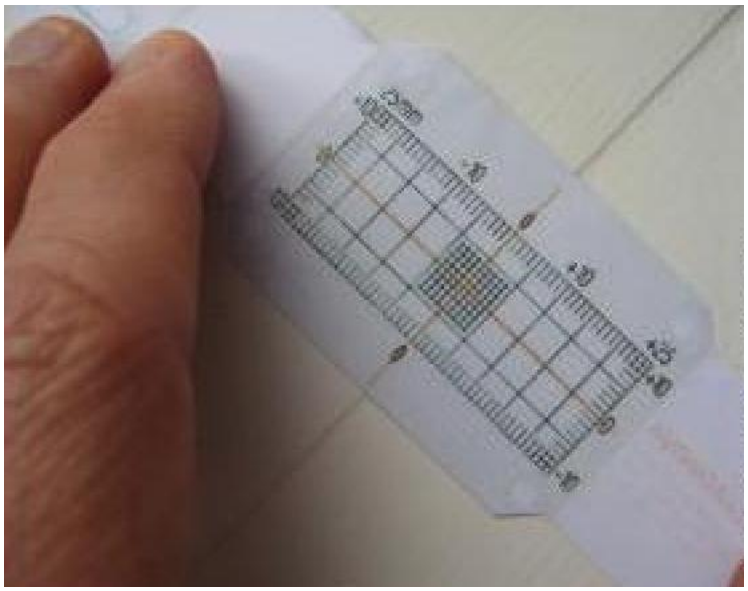

Figure 45. Mechanical strain gauge

One of the problems with mechanical strain gauges is detecting very small strains. An example of this would be a situation where a house is slowly subsiding but the amount of movement is so small that it won't register as a problem until serious damage occurs. With a simple crack detector, it would take 1mm of building movement to produce 1mm of movement on the surface of the crack detector (Malvernand Harding, 1984). If the goal is to detect smaller movements smaller that don't show up on the scale a strain gauge with leverage to amplify the strain is needed. In that case, even a tiny movement of the detecting element produces a very large and easily measurable movement of a pointer over a scale.

Hydraulic detectors a solution to this problem and function like simple syringes. Syringes are essentially hydraulic pistons where a small movement of fluid in a large piston will produce a much larger movement of fluid in a small piston attached to it. This is measurable at the needle where the fluid comes out. This can be applied to a strain gauge by connecting a large piston to whatever it is that's producing the strain and use a smaller piston in a smaller tube, marked with a scale, to indicate how much movement has occurred (Kato et al.,1972). The relative size of the pistons determines how much the movement that is trying to be detected can be scaled up. Typically, hydraulic strain gauges will multiply movement by a factor of 10 or so and are most commonly used in geology related activities (Field and Walley, 2013)

If the object to be measured is very large such as an airplane wing, there will be a need to have far more sophisticated measurements and in greater quantity than a simple mechanical strain gauge will allow. It would be desired to measure the strain during takeoff, when the engines are producing maximum thrust. It would be very impractical and dangerous to attach little plastic strain gauges onto the wing and then go out to measure them during a flight. The application of electrical strain gauges will be able to record the measurements safely from a flight recorder in the cockpit. Figure 46 shows a close up view of two electrical strain gauges. One of their primary benefits is the maze-like wiring patterns attached to a foil backing. As the design changes shape it will force the wires to change their resistance as the foil gets bend by stresses and strains.

Figure 46. A close up view of two electrical strain gages.

The most common electrical strain gauge design results in thin, rectangular-shaped strips of foil with maze-like wiring patterns on them leading to a couple of electrical cables. The foil gets attached to the material to be measured and then cables are wired to a computer or monitoring circuit. When the material is placed under strain, the foil strip will get very slightly bent out of shape and the maze-like wires are either pulled apart and stretched slightly thinner or pushed together and become slightly thicker. Changing the width of a metal wire changes its electrical resistance, because it's harder for electrons to carry electric currents down narrower wires. The resistance is typically measured using a Wheatstone bridge and the strain is thencalculated from those values. If the forces involved are small, the deformation will be elastic and the strain gauge will eventually returns to its original shape (Kato et al., 1972). That would mean that the strain gauge would be well suited for making many measurements over a period of time.

Resistance-type strain gauge were first invented in 1938 by MIT professorArthur Ruge to help with earthquake detection. Figure 47 shows his circuit design. It consists of a conducting metal filament that is shown in yellow stretched back and forth between a pair of comb-like supports (blue) and connected to contacts (red) that can be wired into a circuit (Samanta, 1971). As the strain changes, the filament is distorted and its resistance rises or falls. This means that measuring the resistance is a way of indirectly measuring the strain. The gauge also includes a second, similar filament (orange) that can be used behind the yellow filament to compensate for any changes in resistance caused purely by changes in temperature. The idea is to choose different materials for the two filaments so that their temperature changes cancel one another out. Ruge made his filaments from strain-sensitive alloys such as Advance (copper-nickel) and Nichrome (nickel-chrome).

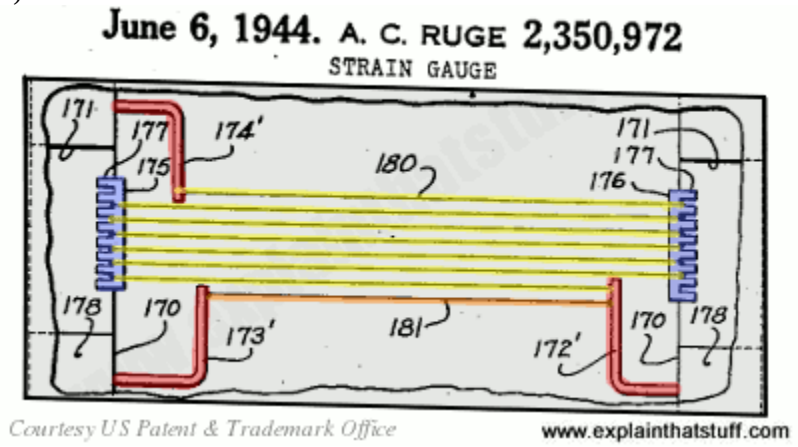

Figure 47. Ruge's original electrical resistance strain gauge design.

The final type of strain gauge is the optical strain gauge. This is necessary due to the fact that some materials change their optical properties or how they transmit or reflect light when they are impacted by stresses and strains. Glass and plastics are good examples. Glass is very useful and a versatile material, but it also is fragile and brittle. This makes it potentially very dangerous as it can suddenly crack or shatter without warning if it undergoes too great of a straining force. That could become problematic for some applications such as a plate-glass window for a store or a car windshield. One way to detect strain in glass is to shine a polarized light onto it at an angle. Some of the light will be reflected and some will be transmitted. The relative amounts of transmitted and reflected light will change according to how much strain the glass is under (Usui and Shirlrosnl, 1982). By measuring the amount of reflected light, the strain on the glass can be precisely measured. An early design from 1938 of one of these created by Samuel Gray is shown in Figure 48.

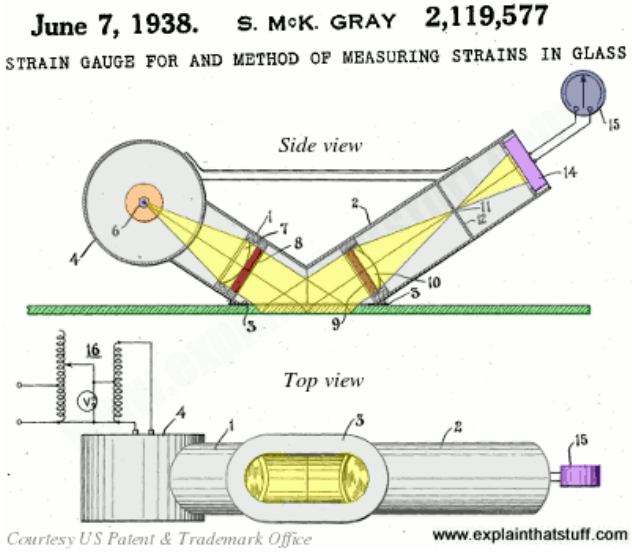

Figure 48. Strain gauge design for measuring strains in glass.

There is one additional unofficial type of strain gauge that is considered to be piezoelectric. It came into being due to the fact that there are some types of materials(quartz crystals and various types of ceramics) that are able to function effectively as natural strain gauges (Samanta, 1970). When placed in either tension or compression, they will generate tiny electrical voltages between their opposite faces. This phenomenon is known as piezoelectricityand is considered to be the way of generating a timekeeping signal in quartz watches.By measure the voltage changes from a piezoelectric sensor, the strain can be easily calculated. Piezoelectric strain gauges are extremely sensitive (1000 times more than manual strain gauges) and reliable and can withstand years of repeated use. They are sometimes called piezoelectric transducers, due to their ability to convert mechanical energy into electrical energy.

Hopkinson Bar Application

Atypical Hopkinson bar configuration will use metal foil strain gauges on the incident and transmitted bars to measure the elastic strain wave pulses generated by a projectile impact. The signals from the strain gages are then used to calculate the dynamic plastic stress and strain in the rapidly deforming sample by applying the straight forward wave theory. There is sometimes an issue of uncertainty of the strain gage signals when using the classic Wheatstone bridge output circuit with the parallel resistor calibration method. The overall uncertainties of these results are dependent on many factors. One starting point in understanding the uncertainty of the stress–strain results is to examine the uncertainty of the strain gage signals themselves.

The historical development of the use of the Kolsky bar for dynamic material property measurements is very much interconnected with the historical development of the metal-foil variable-resistance strain gage. The prime period of development was the mid-twentieth century which was a time of rapidly expanding experimental mechanics work in the US. This work was primarily motivated by the rapidly advancing aircraft industry and the development of the space program. The Society for Experimental Mechanics (SEM), which was originally named the Society for Experimental Stress Analysis (SESA), was and continues to be, a leading publisher of advances in the measurement of strain with traditional strain gages as well as many new advanced measurement systems. SEM conferences have also been a leading community in reporting new developments for Split Hopkinson Pressure bars over the previous decades.

The bonded variable resistance strain gaugeswere the first to be inventedin 1930. The variable resistance strain gage (SR-4 gage) consisted of a fine metal wire formed into a grid pattern and glued to the test surface. New strain gage innovations over the next several years led eventually to the etched metal foil gages being developed during the 1950s. The metal foil gages of the late 1950s became extremely important in stress analysis for all kinds of structures and systems. The strain gages in use today are still similar in appearance to the gages of the 1950s. However many innovations have been made in signal processing and data recording.

Strain Gauges at CRREL

At CRREL the strain was measured at the midpoint of each half of the split Hopkinson bar using two strain gauges (CEA-09-125 SUR-350) with a length of 0.125 in and a 350 Ohm resistance at each location. A small gauge radius of 0.60 in was chosen so that the strain averaging would only occur over the smallest possible physical area of the bar. The gauges were compensated for stainless steel and aligned at opposite ends of the bar to take into account the bending moment. An AE-10 epoxy was used and was cured at room temperature. A three wire technique was used to connect the gauges in a bridge configuration. Each gauge cable was individually shielded and the gauges were wired into opposite sides of a two-active-arm, four-arm bridge. Micro Measurement M Coat D was used over the gauge system to protect against moisture. Each gauge was connected to the bridge completion and balance circuit by 15 ft wires while the four-arm bridge was completed with 350 Ohm resistors.

The bridge balance circuit is similar to the one designed by Stein (1967). Bridge balance was obtained with a 500 kOhm potentiometer and bridge excitation was obtained at 15V with a HP 6218B power supply. Each bridge needed its own power source. Both amplifiers were set on a gain of 10, which corresponded with a bandwidth of 100 kHz and 120 dB of common mode rejection at the differential inputs. Each amplifier output was single ended can connected to the positive input terminal of the scope channel. Measurements were than taken and recorded using the +/- 100 mV and digitized at 0.5 us per point, meaning the record length was around 4 ms. Both oscilloscope channels were used as Channel 1 recorded the incident and reflected strain and Channel 2 recorded the transmitted strain. The oscilloscope was set to begin recording when the hammer impacts the first bar. It was found that this contact then applied a 3V battery voltage directly to the external trigger output of the scope. Calibration was done by using the gauge shunt technique using a 349, 650 Ohm resistor which ensured each active gauge would give 250 microstrain at the oscilloscope input. Table 1 shows the materials previously used for strain measurement at CRREL.

Table 1. Instrumentation Components			
Quantity	Description	Manufacturer	Model Number
4	Strain gauge	Micro Measurements	CEA-09-125 Ur-350
4	Calibration resistors	Micro Measurements	W-349650-02
4	Bridge completion resistors	Micro Measurements	S-350-01
1	Bridge completion and balance unit	CRREL In-house	None Provided
2	Power supply	Hewlett-Packard	HP 6218B
1	Graphics plotter	Hewlett-Packard	HP 7470A
1	Interface board	Captial Equipment Co.	PC<>488
1	Digital oscilloscope with dual amplifiers and dual disk drives	Nicolet Instrument Co.	4099A, 4562, XF44
1	External scope trigger (3V battery)	Union Carbide Corp	W-356
	Gauge epoxy	Micro Measurements	AE-10
	Gauge cable	Beldun	8723

Wiring Process

The first step in getting the split Hopkinson bar ready for wiring is to clean the bar with Wet and Dry. Phosphor bronze with a grain size of 280 is used to rub back and forth along the bar until it gets very shiny being sure to remove any layers of corrosion (Brotrob, 2012a). Then, a finer grain of 600 can be rubbed up and down the bar a smaller number of times. The next step is to use a paper towel or piece of paper to remove all of the dust and oils. The final cleaning step involves using a small amount of acetone that is sprayed on another paper towel. Several pieces of paper should be used until no more dirt or oil is coming up from the bar. The focus should be in the area of the bar where the strain gauges might be attached.

Next the bar needs to have soldering pads attached to it. There are matrices available which will guide the positioning of the strain gauges around the circumference of the bar (Brotrob, 2012a). Large soldering pads should be used and they should be compared to the matrix to see how long they should be cut. After the pad is cut to size it should also be cleaned with acetone as there may be some dust or oil. A piece of tape will then be cut and the soldering pad will be attached to it using pliers or tweezers. It is an excellent idea to preplan where the soldering pad will be positioned and align the soldering pads carefully so the end of the soldering pads and the beginning of the strain gauges will line up. The strain gauge lead wires must be prevented from coming in contact with the Hopkinson bar. Some superglue is then added to the exposed side of the soldering pad. Then the pad will be attached to the bar at roughly where the strain gauge will be attached. The soldering pad is placed on top of the bar and rolled around with light pressure. The tape should be stretched so it thins out and any leftover tape should be cut off (Brotrob, 2012b). Once the superglue dries the tape can be removed. Any excess superglue should be scraped off by a knife. Then restart the Wet and Dry cleaning process for both the bar and soldering pads. This is done so that it will be easier to solder the strain gauge lead wires later on. It is important to make sure there is not the slightest bit of superglue left. If the soldering pad was not positioned correctly relatively to the bar all is not lost. A layer of tape can be wrapped around it and cut to shape so there is a nice clear corner at the beginning of the soldering pads (Brotrob, 2012b). Clean the area again as necessary.

Two sided tape should be cut and applied to the one section of the strain gauge wiring print out. Then that section of the printout should be cut out as straightly as possible. The other side of the tape should be uncovered and something should be used as a temporary weight to hold it stable. Four strain gauges are then selected (Phosphor Bronze FLK 217) and attached to the double sided tape using a small tool (Brotrob, 2012b). Care should be taken not to touch the side of the strain gauge that will be attached to the bar. The right side of the strain gauge should be fit up against the corner of the tape so that the majority of the gauge is extended beyond the tape (Brotrob, 2012c). This should be done for all four strain gauges. It is important to measure the distance between the edge of the paper and the centerline of each strain gauge. This will define where the strain gauge sits with respect to the start of the bar. Once that is finished then the process of attaching the strain gauges can be started. A very small amount of superglue should be applied to each strain gauge. The gauges can then be attached to the bar using the line that was made earlier. Using tweezers the tape can be positioned to the right of the soldering pad. Apply a little bit of pressure in tension, the tape should be rolled up along the line (Brotrob, 2012c). Once that is done apply additional pressure.

Once the strain gauges are attached the next step is to prepare the lead wires for soldering. In order to do that each lead wire needs to be positioned using tweezers over one single section of the soldering pad. One thing to avoid is bending the lead wire around a sharp corner (Brotrob, 2012d).This is done using very slight movements with the lead wire being

supported at one side. Grabbing it with the tweezers should be avoided due to the possibility of introducing a sharp bend which will likely lead to it breaking over time. Any straight lead wires should be very slightly bent to introduce a bit of compliance for the impact (Brotrob, 2012d). Turn the bar around to prepare all of the lead wires in this manner. After this is done cut a bit of tape and apply it to fix the lead wires in place.

Then next portion needed is the preparation for the soldering. One of the cables should be cut off and open up the shielding on one end of the cable. On the end of the cable 5 mm of insulation should be cut off and set aside. Two more additional wires of the same approximate length should be prepared in the same method. Soldering flux is then applied in the areas that required soldering including the strain gauge cable, the two additional wires, and most importantly over the soldering pad on the bar and the strain gauge lead wires (Brotrob, 2012d).Be careful of the amount applied with minimal amount as too much could affect the connection and readings.

The last step is to perform the soldering. That is done by placing the soldering tip on the soldering pad for a while to let the soldering gun warm up. The soldering flux liquid will change in color as the temperature increases. When it becomes sufficiently hot enough the soldering wire is added and the solder will flow out over the soldering pad and embed the strain gauge lead wire. The other strain gauge wires are to be attached to the soldering pad in the same manner. After this is finished the superfluous bits of each strain gauge lead wire can be cut using a small knife so that they do not get connected with the bar itself (Brotrob, 2012e). Once the wires are cut the tape can the be unwound and removed from the bar. The strain gauge cable can then be attached temporarily to the bar with another piece of tape. The wires at end of the cable are typically different colors (green, yellow, red, blue) and will be soldered to connect with the strain gauge lead wires on the soldering pad(Brotrob, 2012e). The short black wires that were cut previously are then attached to the soldering pad in the same manner with both ends attaching to the soldering pad to create a horseshoe shaped loop. The connections are the next item to check to make sure they are correct and working using a digital multi-meter. The final step is to protect the strain gauge station. This is accomplished by adding some tape and rolling it up to cover the strain gauge station and the lead wires with some slight tensile force (Brotrob, 2012e). The purpose of this is to prevent any movement of the soldering wires when the bar is impacted. Care should be taken with the strain gauge wires so that no bends are created and not break during any bar impacts. Any previous temporary tape can now be removed from the bar especially the tape used to hold the strain gauge cable into place for soldering to the lead wires (Brotrob, 2012e). After that step everything should be placed into the final position typically between two of the soldering pads. More tape is then applied to hold it into place. One key step is to now introduce a bend into the cable so that it becomes easier to fully tape the cable to the bar over the soldering pad. This then completes the strain gauge station.

Wiring process for CRREL bars

The installation of the strain gauges for the incident bar system is shown in Figure 49. The strain gauge wires are connected into the data acquisition system for the initial pulse readings and also connected to the Wheatstone bridge in Figure 50. The difference between the two measurements becomes the estimated strain value. The diagram color codes the wires for easy installation.

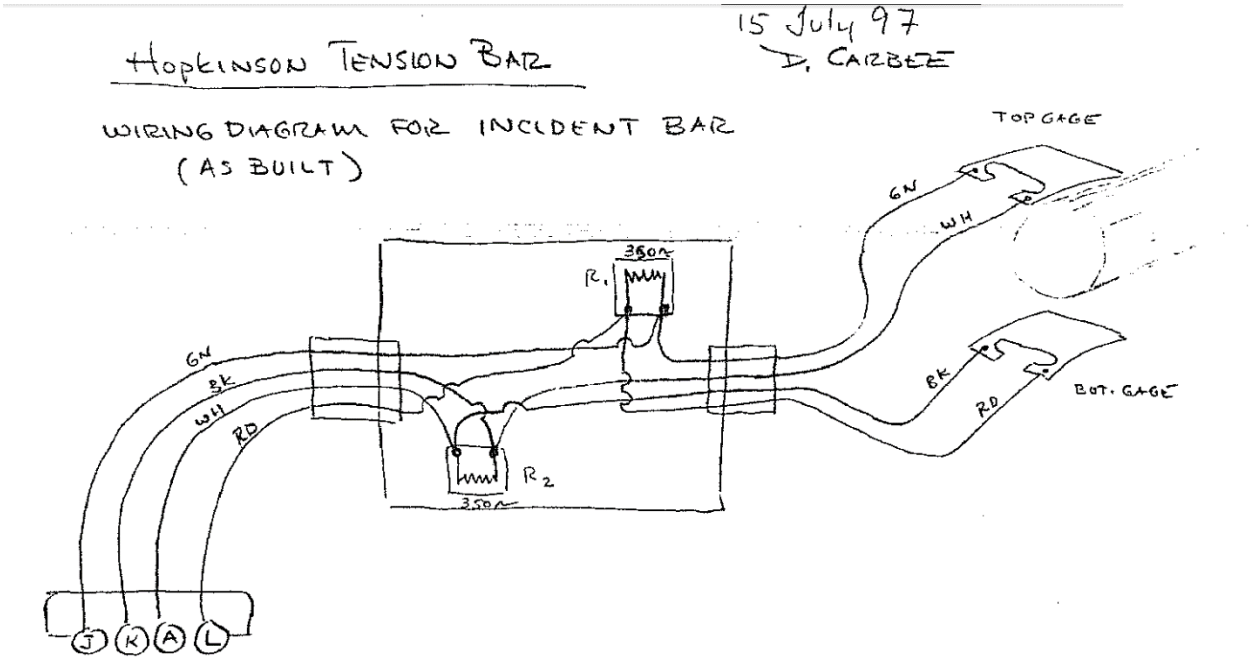

Figure 49. Strain gauge design for the incident bar.

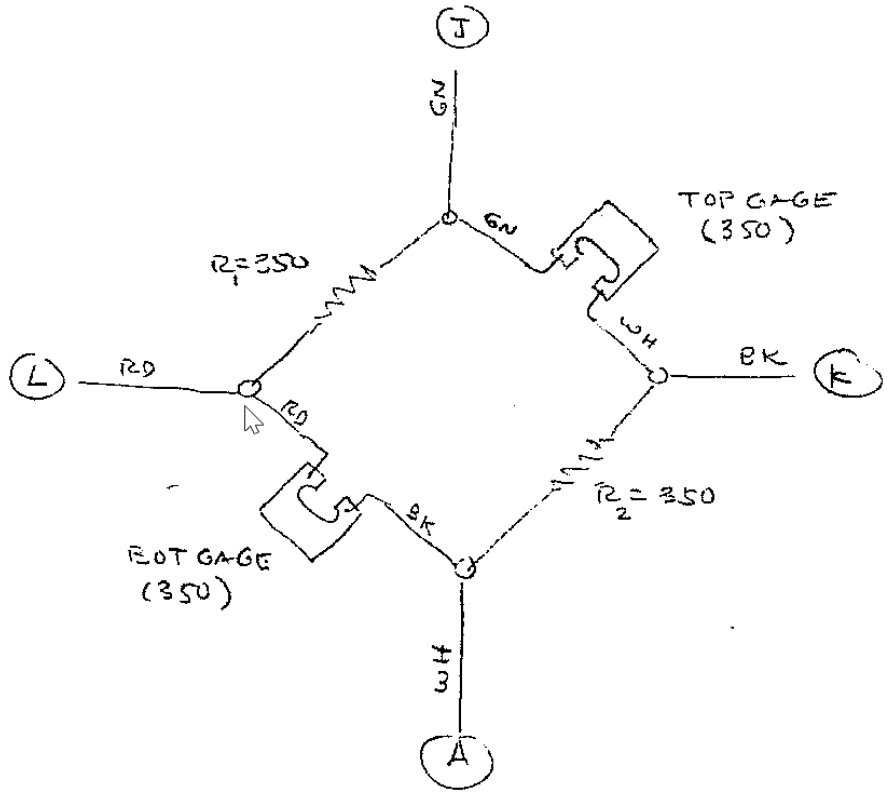

Figure 50. Strain gauge design of Wheatstone Bridge in CRREL Hopkinson Bar system.

The CRREL Hopkinson bar was first calibrated using a dummy sample to guarantee the accuracy of the relationship between the loading torque and the strain voltage, the duration of the pulse and the elimination of the loading reverberation. This was done through the addition of another pressure bar called a preloading bar and having the dummy

specimen implemented. The dummy specimen was recommended to be made of the same material as the tested specimen. The pulse transmitted through the dummy specimen becomes the actual incident pulse for the real specimen. Under this arrangement, the profile of the incident pulse is very similar to that of the transmitted pulse measured behind the specimen. This incident pulse produces a plateau in the reflected pulse, representing a constant strain rate in the specimen The incident pulse was dictated by the dummy specimen's elastic-plastic response. This elastic-plastic response is very similar to that for the actual specimen because they are made of the same material. Figure 51 illustrates what the calibration configuration will likely appear to be. It is good procedural practice to begin the calibration and initial testing with using dummy samples until all of the testing details and calibrations have been worked out. The strain gages for the incidental bar and the transmitted bar should be connected in a half bridge configuration for the Wheatstone bridge as in Figure 52. The dummy gages should be in a quarter bridge configuration as shown in Figure 53.

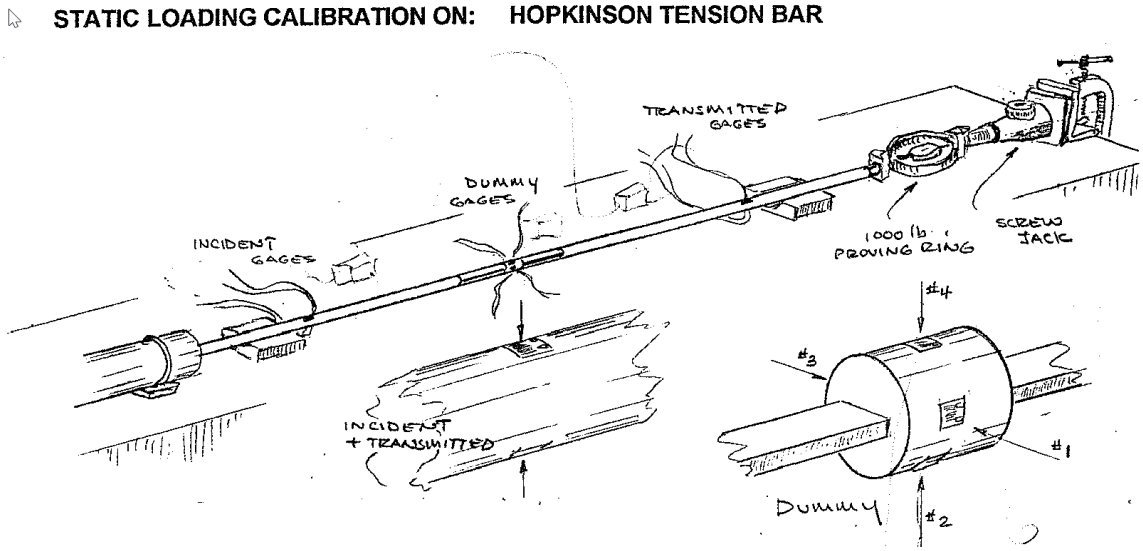

Figure 51. Strain gauge design for CRREL Hopkinson Bar system.

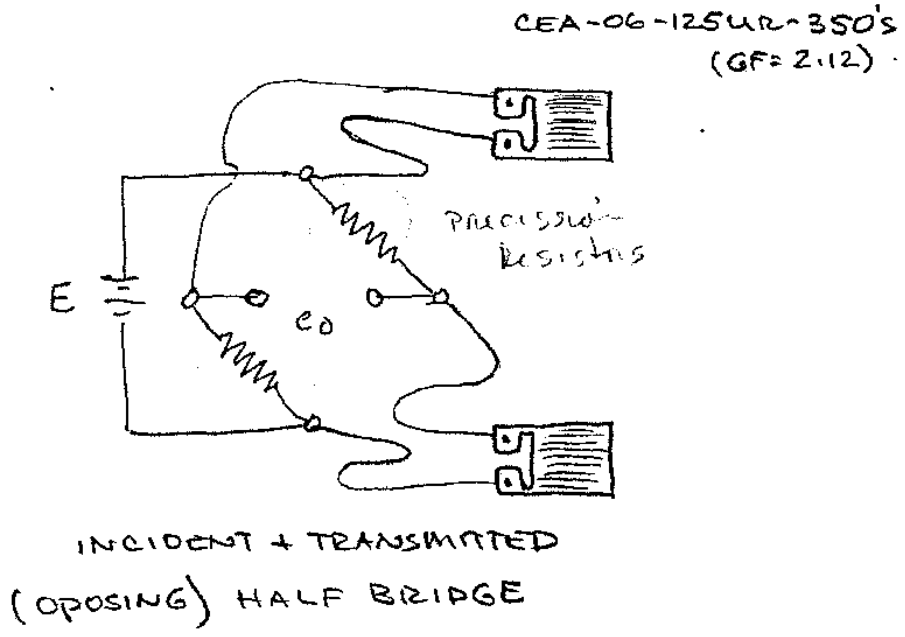

Figure 52. Wheatstone bridge design for CRREL Hopkinson Bar system.

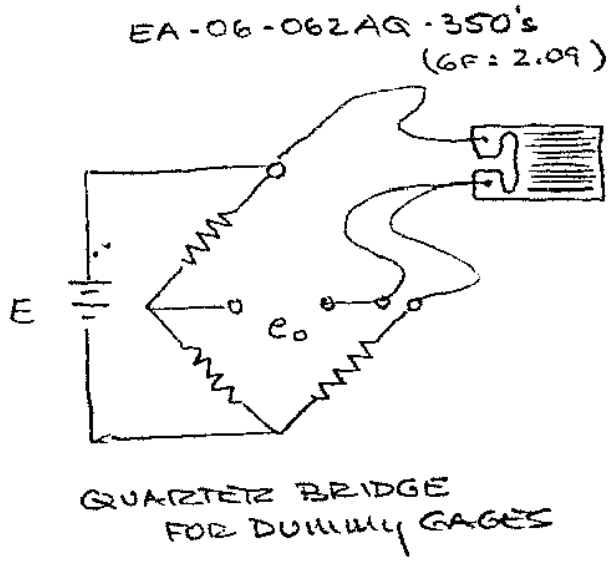

Figure 53. Wheatstone bridge design for dummy gages.

One additional change that was looked at by CRREL was equipping the system with a calibrated proving ring for determining the applied testing load. A flow meter for was also used in conjunction for determining the amount of strain at the maximum load in the test. Loading during the calibration procedure was applied through a previously calibrated piezoelectric proving ring. A special fixture was manufactured to facilitate the calibration and to ensure that both the point and line of application of the load simulated that which occurred in the orthogonal machining operation. In these calibration tests five signals were monitored: one from the proving ring applying a load (normal or shear), and one from each of the active load cells. It was found that through the loading ring a known load could be applied to the front portion of the dynamometer in the normal direction. The signal from the shear load cell indicated the cross sensitivity effect while the signals from the other two load cells on the top portion of the dynamometer provided a measure of the cross coupling effect. A centered ball seat adapter was used to protect the end of both the proving ring and transmitted bar and provide the system additional stability. Figure 54 displays how the connection between system components is to be handled. Figure 55 shows the entire Hopkinson bar system and where the strain gauges should be placed. One unique feature is that a P-3500 portable strain indicator was used to manually take strain gage readings.

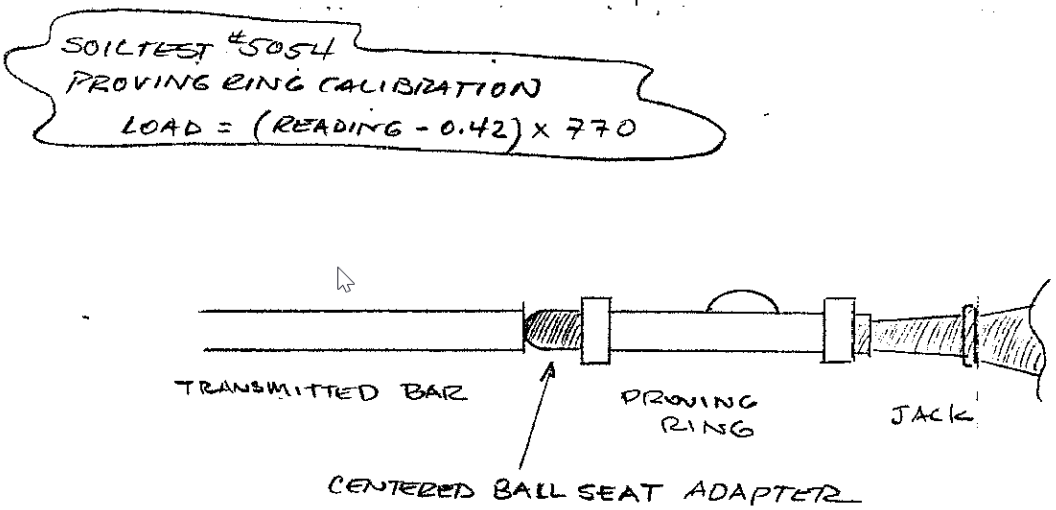

Figure 54. Addition of Ball Seat Adapter and Proving Ring for Enhanced Stability.

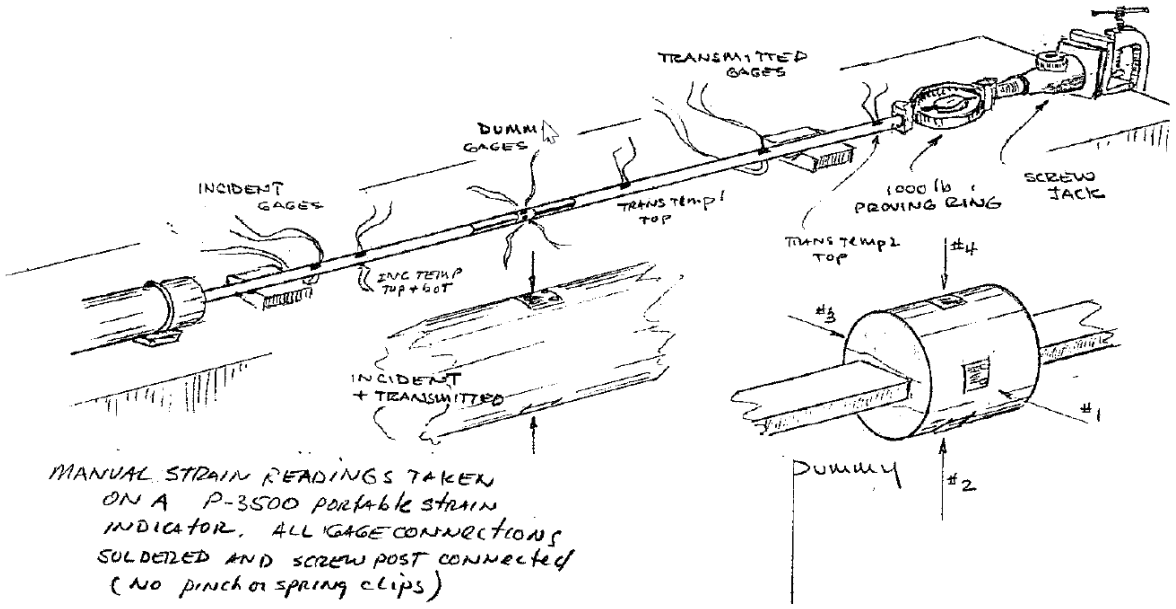

Figure 55. Strain gage placement for entire Hopkinson bar system during calibration.

The P-3500 strain gage indicator is used in conjunction with the various dummy samples and the strain gages that have been placed at various locations on the two bars. An example of what the experimental calibration measurements may look like is displayed in Table 2. By comparing what the strain gages read from the previous known values of the dummy samples, adjustments in the way of constants and additional values to the equations may then be made to bring the measured values within the known range and can then be applied to future Hopkinson bar measurements.

The final step in the calibration of the strain gages and Kolsky bar system is to obtain measurements for the system and compare them against known values. Strain readings should be taken on both the transmitted and incident bars at several locations as well as for the dummy specimens. Table 2 shows a previous example of the measurements taken for system calibration. Measurements were taken at initial start up and then as force was applies to the impact projectile. From this it can been determined where the forces are affecting the system and by comparing the values of the dummy specimens, changes to the initial parameters and instrument sensitivity can be applied to bring the system to within the range of the known values.

Table 2. Previous strain gage reading and their format.

Manual strain readings. 29 July 96

Gage	Zero			load 1 (444 lb.)				load 2 (671 lb.)			
	initial	final	avg	reading	strain	load	%	reading	strain	load	%
Inc top	465	464	464.5	456	-8.5	302	-31.9	446	-18.5	658	-1.9
Inc bot	536	536	536.0	524	-12.0	427	-3.8	514	-22.0	783	16.7
						avg.	-17.9			avg.	7.4
Trans top	232	231	231.5	213	-18.5	658	48.3	201	-30.5	1085	61.7
Trans bot	183	182	182.5	156	-26.5	943	112.4	150	-32.5	1156	72.3
						avg.	80.3			avg.	67.0
Dummy 1	-1496	-1492	-1494.0	-1519	-25.0	890	100.4	-1517	-23.0	818	22.0
Dummy 2	-980	-979	-979.5	-997	-17.5	623	40.2	-1011	-31.5	1121	67.0
Dummy 3	-933	-932	-932.5	-942	-9.5	338	-23.9	-947	-14.5	516	-23.1
Dummy 4	-856	-854	-855.0	-855	0.0	0	-100.0	-865	-10.0	356	-47.0
						avg.	4.2			avg.	4.7
Inc temp top	-1292	-1290	-1291.0	-1302	-11.0	391	-11.8	-1309	-18.0	640	-4.5
Inc temp bot	-714	-713	-713.5	-733	-19.5	694	56.3	-742	-28.5	1014	51.1
						avg.	22.2			avg.	23.3
Trans temp1 top	-1064	-1075	-1069.5	-1075	-5.5	196	-55.9	-1084	-14.5	516	-23.1
Trans temp2 top	-1641	-1643	-1642.0	-1663	-21.0	747	68.3	-1676	-34.0	1210	80.3
						avg.	6.2			avg.	28.6

Optimizing strain gauge excitement levels

In working with the strain gage calibration one important piece of information needed is to know the recommended value of bridge excitation voltage for a given size and type of gauge. There are many factors beyond the gauge itself that enter into this so there is no simple formula that can be applied. The issue becomes even more difficult when the optimal level of excitation level is desired. Too much excitation will hardly ever damage the strain gauge; instead it will cause performance degradation (Zorev, 1963).Thus the goal is to meet the total requirements of each particular system component.

The primary considerations are of the thermal variety. This is due to the fact that as the voltage is applied to a strain gauge bridge, it will create a power loss in each arm. All of these power losses must be dissipated in the form of heat. This means that only a negligible fraction of the input power becomes available at the output circuit and the sensing grid of every strain gauge will operate at a higher temperature than the substance to which they are bonded. The heat generated within a strain gauge must be transferred by conduction to the mounting surface and this relationship is a function of the substance heat-sink capacity and strain gauge power level (Measurement Group, 2010). One of the drawbacks of this is that both the substance and sensing grid operate at higher than normal temperatures. Gauge performance is greatly affected by excessive temperature rise through a loss of self-temperature compensation (STC), magnified hysteresis and creep, and variations of heat-sink conditions between the gauges and bridge circuit. STC data can be looked up from the manufacturer to best obtain low excitation levels. Hysteresis and creep are most dependent on backing and glue-line temperatures. A gauge with a backing normally rated at +250 F in transducer service would likely be forced to be down rated by 20 to 50 F to avoid high excitation conditions (Measurement Group, 2010). Another method of avoiding excessive excitation is through the use of zero or no-load stability. The emergence of hot spots, areas of the gauge or grid that are subject to higher temperatures will also restrict the allowable excitation levels (Samanta, 1971).These hot spot are susceptible to creep and instability due to either imperfections on the gauge or voids or bubbles on the glue-line. Factoring in these variables it is usually determined that the power-dissipation of a gauge will be proportional to the size and area of the grid. It is preferable to use high-functionality adhesives that leave thin, void-free glue-lines with a thickness ranging from 0.0001 to 0.0003 inches.

There are several factors that affect the optimum excitation level for a strain gage that include: strain gage grid area, gage resistance, heat-sink properties of the mounting surface, temperature range of the surrounding environment, static vs. dynamic strain loads, and the insulation and wiring process (Measurement Group, 2010). The material makeup of the mounting surface makes a huge difference. Metals such as aluminum or copper will serve as a heat sink while plastic materials will act as thermal insulators. The shape of the gage part may also contribute to additional thermal stresses due to self-heating. Damage during installation to the gage, solder tabs, or glue-line will also cause high levels of excitation to be an issue. One key issue that needs addressing is the use of strain gages under direct submersion of liquefied gasses. The excitation voltage must be kept sufficiently low to avoid grid self-heating which will lead to gas bubbles developing in the grid lines (Measurement Group, 2010). The bubble sizes will increase with the temperature increases and break lose to rise to the surface which will appear on the output signal as additional noise. They solution to avoid this is to either have very small excitation levels or apply protective coatings on the grid to minimize direct contact.

Strain gage excitation calculation

There are three principle equations that are used to determine the optimum excitation level. The first necessary equation determines the power dissipated in the grid.

$$P_G = \frac{E_B^2}{4R_G} \quad (1)$$

where: E_B is the bridge excitation in volts
R_G is the gage resistance in ohms
P_G is the power dissipated in the grid in watts
One key assumption is that the bridge voltage E_B is based upon an equal arm bridge arrangement where the voltage across the active arm is half of the bridge voltage. The second equation is used to calculate the power density in the grid.

$$P_G' = \frac{P_G}{A_G} \quad (2)$$

where: A_G is the grid area (active gage length * grid width) in inches
P'_G is the grid power density in watts per square inch
P_G is the power dissipated in the grid in watts

The third equation is created by substituting P_G from the first equation into the second equation and solving for E_B. When the grid area A_G, gage resistance R_G, and grid power density P'_G are known, the equation becomes:

$$E_B = 2\sqrt{(R_G * P_G' * A_G)} \quad (3)$$

Grid power density curves

With the values obtained from the three previous equations it is then possible to determine the optimum excitation level. This is done by first determining the necessary heat sink condition from Table 3. For the Hopkinson bar system at CRREL it is necessary to have a high accuracy requirement under static conditions. Using one of theavailable resistors under normal testing conditions require a heat sink range of 0.01-0.002 watts/in^2. In most testing a value of 0.002 watts/in^2 is recommended(Measurement Group, 2010).

Table 3 — Heat Sink Conditions

watts/in² *kilowatts/m²*

	Accuracy Requirements	EXCELLENT Heavy Aluminum or Copper Specimen	GOOD Thick Steel	FAIR Thin Stainless Steel or Titanium	POOR Filled Plastic such as Fiberglass/Epoxy	VERY POOR Unfilled Plastic such as Acrylic or Polystyrene
STATIC	High	2 — 5 *3.1 — 7.8*	1 — 2 *1.6 — 3.1*	0.5 — 1 *0.78 — 1.6*	0.1 — 0.2 *0.16 — 0.31*	0.01 — 0.02 *0.016 — 0.031*
STATIC	Moderate	5 — 10 *7.8 — 16*	2 — 5 *3.1 — 7.8*	1 — 2 *1.6 — 3.1*	0.2 — 0.5 *0.31 — 0.78*	0.02 — 0.05 *0.031 — 0.078*
STATIC	Low	10 — 20 *16 — 31*	5 — 10 *7.8 — 16*	2 — 5 *3.1 — 7.8*	0.5 — 1 *0.78 — 1.6*	0.05 — 0.1 *0.078 — 0.16*
DYNAMIC	High	5 — 10 *7.8 — 16*	5 — 10 *7.8 — 16*	2 — 5 *3.1 — 7.8*	0.5 — 1 *0.78 — 1.6*	0.01 — 0.05 *0.016 — 0.078*
DYNAMIC	Moderate	10 — 20 *16 — 31*	10 — 20 *16 — 31*	5 — 10 *7.8 — 16*	1 — 2 *1.6 — 3.1*	0.05 — 0.2 *0.078 — 0.31*
DYNAMIC	Low	20 — 50 *31 — 78*	20 — 50 *31 — 78*	10 — 20 *16 — 31*	2 — 5 *3.1 — 7.8*	0.2 — 0.5 *0.31 — 0.78*

0.02

Once the heat sink condition is found either the bridge excitation level or the grid density can be found using the charts in Figures 56 through 58. They function as plots of bridge excitation voltage vs the grid area for constant power density levels based upon gage resistances of 120, 350, and 1000 ohms respectively(Measurement Group, 2010). The power density value is approximated to the nearest curve and will be intersected by the known value. From this the other value can be determied from following the intersection and estimating the axis value. Further information about a strain gage can be looked up in a manufacture's chart that would be similar to the one shown in Figure 59. This would include the resistance, nominal gage factor, temperature range, strain limits, soldering temperature, and thermal output based upon the ambient temperature.

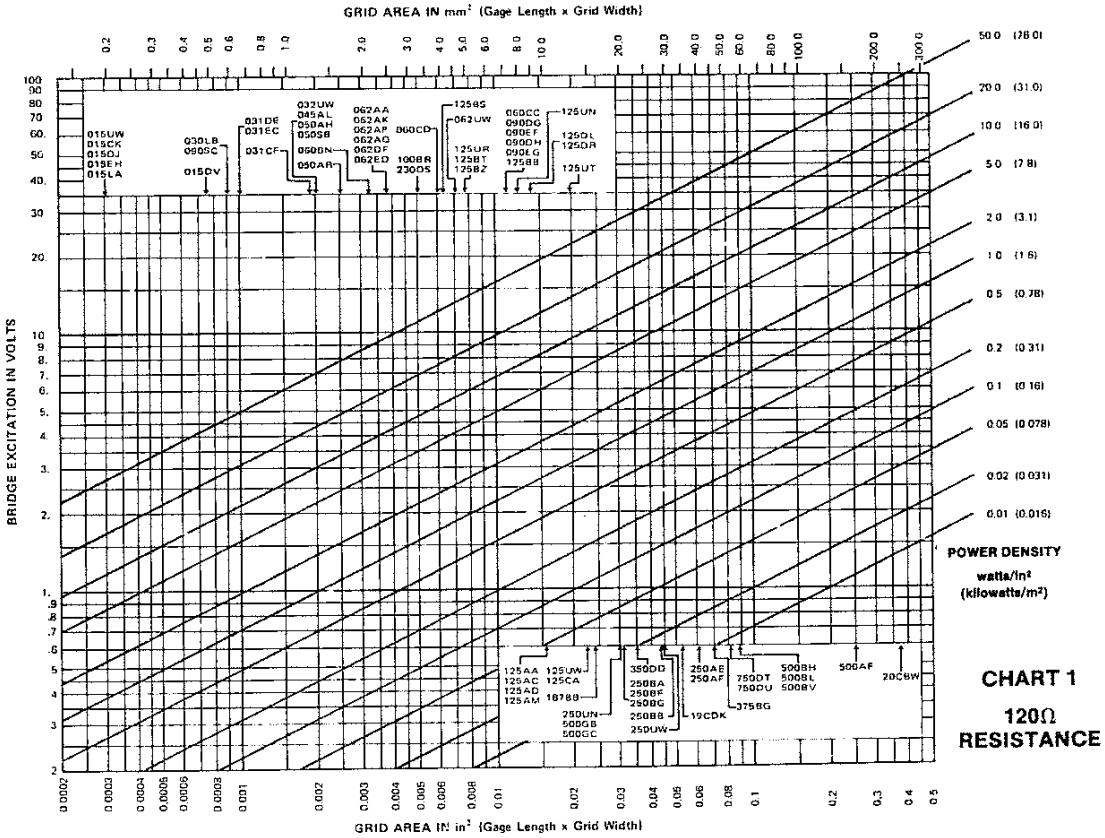

Figure 56. Power density curves for 120 ohm resistor.

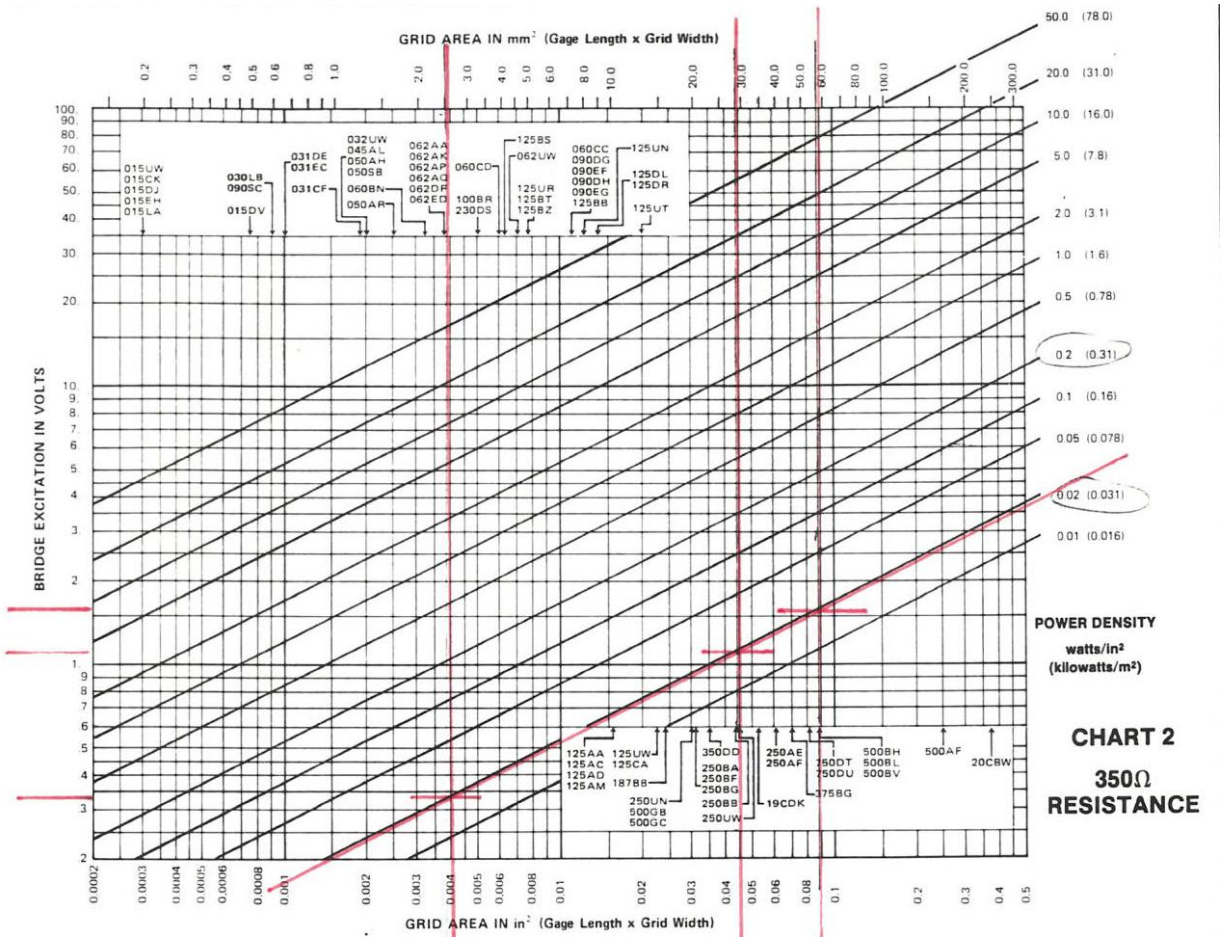

Figure 57. Power density curves for 350 ohm resistor.

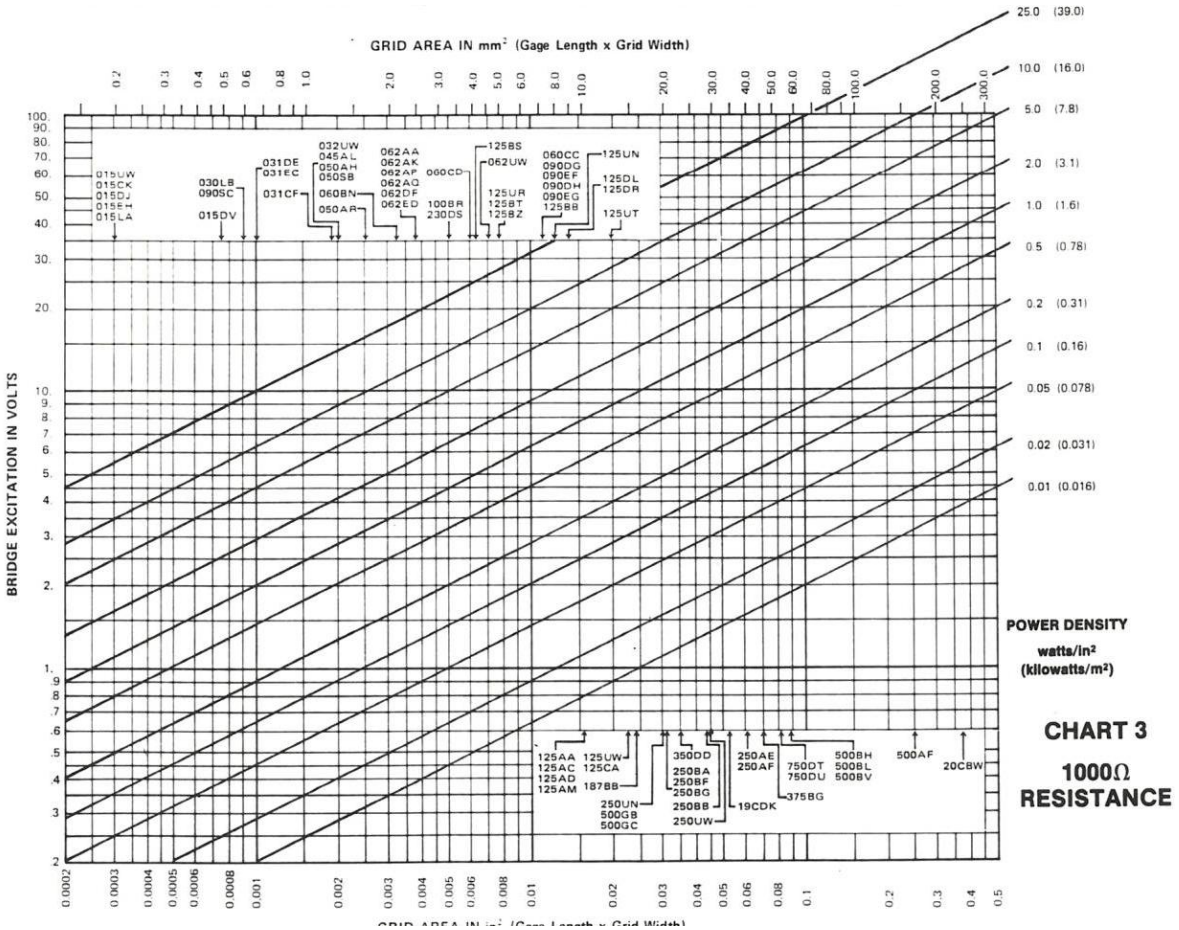

Figure 58. Power density curves for 1000 ohm resistor.

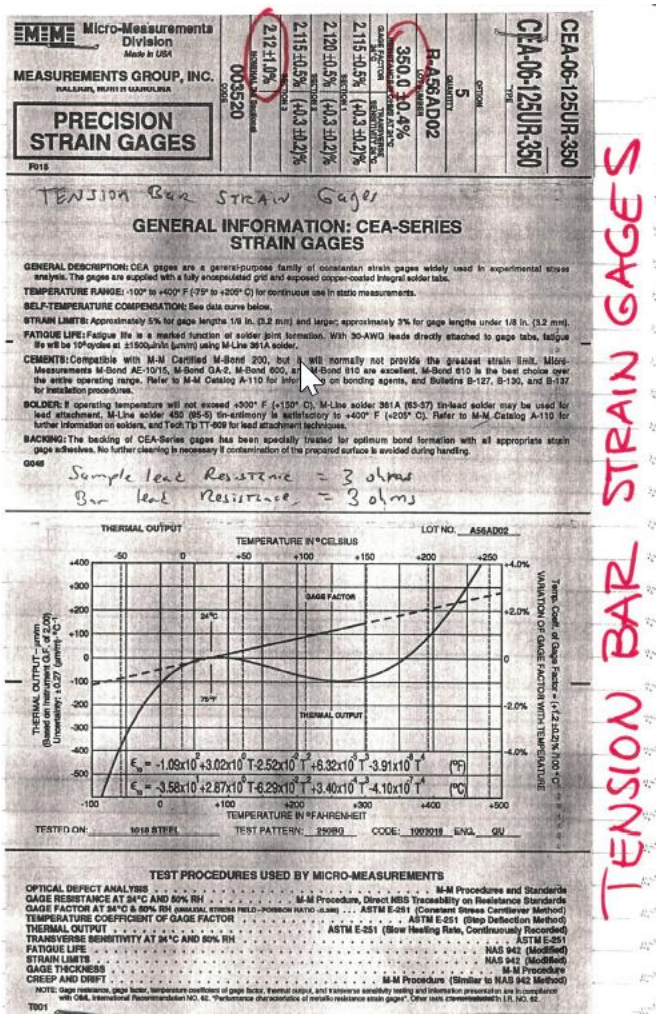

Figure 59. Strain gage information chart.

Strain Gauge Rosettes

Strain gage rosettes are an arrangement of two or more gage grids that are oriented independently to measure the normal strains along different directions of the surfaces of the test specimen. They are a key component in experimental stress analysis especially in general biaxial stress states. In cases where the principle directions are unknown, three independent strain measurements in different directions are necessary to determine the principle stresses and strains(Measurement Group, 1990). Even if the principle directions are known in advance, two independent strain measurements are still needed to determine the principle stresses and strains. There are three basic types of strain gage rosettes: tee, 45º-Rectangular, and 60º-Delta as shown in Figure 60. A tee rosette consists of two grids that are mutually perpendicular. The 45º-Rectangular rosette consists of three grids with the second and third grids being angularly displaced from the first grid by 45º and 90º respectively. The 60º-Delta rosette also contains three grids with the second and third grids being angled away from the first grid by 60º and 120º respectively. The 45º-Rectangular orientation is the most popular in CRREL designs. The tee rosette should only be used if the principle strain directions will be known ahead of time. Other stresses such as bending or axial stress must be avoided as they will interfere with the principle strain measurement(Measurement Group, 1990). They should also be avoided when cases of geometric irregularities (holes, ribs, shoulders) as they will cause error measurements due to the misalignments from the primary axes. If the strain directions are unknown then a rectangular or delta rosette using three elements becomes necessary. The benefit of these designs is that there is no difference in orientation (Follansbeeand Kocks, 1988). Delta rosettes are typically able to give the optimum sampling of strain distributions due to their maximum 120º angular separation of the gage axes. Rectangular rosettes have

a simpler data-reduction relationship that had been popular in the past but are being rendered not as important due to advances in computing power(Measurement Group, 1990).

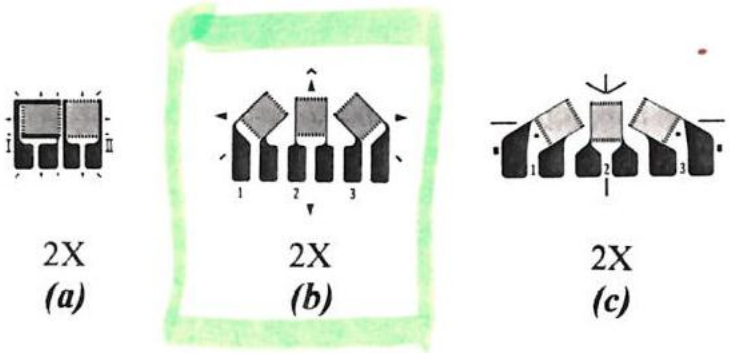

Figure 60. Basic rosette types by grid orientation: (a) Tee; (b) 45º-Rectangular; (c) 60º-Delta

Rosettes are often created using different combinations of grid alloy and backing materials to meet different requirements for various applications. Another parameter that can vary is in the gage lengths which is classified by the active length of each individual grid within the rosette (Davis, 1971). The rectangular and delta rosettes may be placed in different geometric shapes and yet have the same functional equivalency as shown in Figure 61.

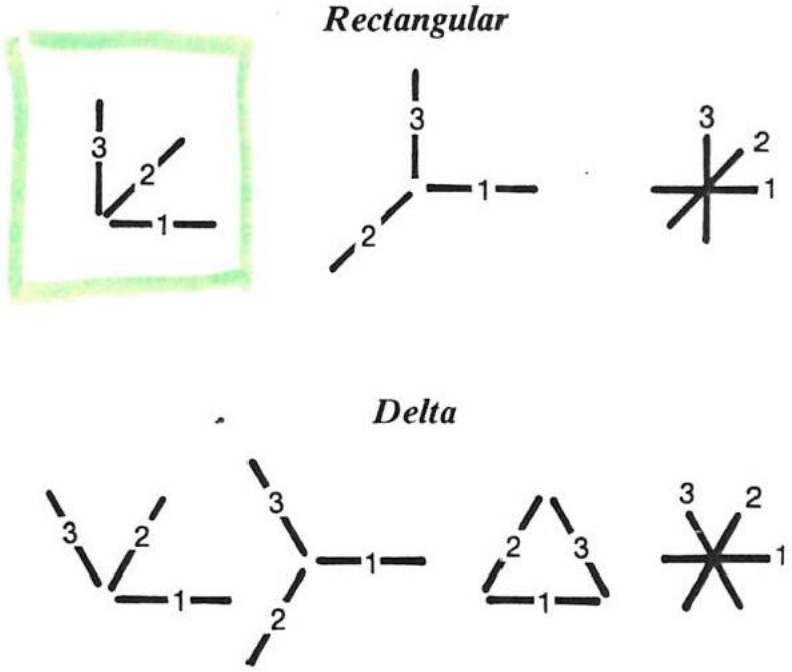

Figure 61. Geometrically different but functionally equivalent configurations of rectangular and delta rosettes.

All three rosette types (tee, rectangular, and delta) are constructed in both stacked and planar configurations. Examples of each are shown in Figure 62. Planar construction is limited to one flat level while stacked construction has layers built upon each other (Follansbeeand Kocks, 1988). Planar rosettes are typically chosen when the strain gradients on the material surface will not be severe. They have several advantages in that they are thin and flexible with conformability to curved surfaces, require minimal reinforcing, provide a good deal of heat dissipation, have optimal stability, and give a great deal of freedom for the installer in terms of wire placement and attachments(Measurement Group, 1990). The main drawbacks for the planar construction are that it needs a great deal of surface area for the sensitive portion of the gage, and in cases of

severe strain gradients it may detect multiple strain fields and magnitudes. Overall the stacked construction will use the least surface area and will have the centroids of all grids laying over the same part of the material surface. Troke (1967) found that all grids in a stacked rosette will have the same gage factor while the grids in a planar rosette will differ slightly due to different orientations relative to the direction of the strain. Another point of difference is that the stacked rosette is stiffer than the planar rosette which plays a factor in heat dissipation. This is due to some of the heat conduction paths being longer in the upper grids of the stacked rosette. Stacked rosettes have also been found to produce errors when the material is subject to bending in cases where the highest grid level is higher than the material surface (Nicholas, 1981).

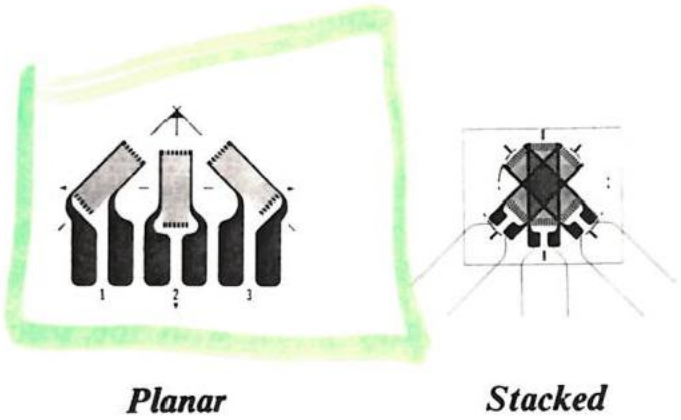

Figure 62. Rectangular rosettes of equal gage length in planar and stacked alignment

Often it becomes necessary to differentiate the members of a rosette for strain measurement. A system of gage numbering is an essential component of rosette measurements. This is especially true for rosettes with three elements where an incorrect numbering will lead to erroneous principal strain directions. The problem is even more significant with rectangular rosettes where not only will the strain directions be wrong but also the strain magnitudes as well(Davis, 1971). Perry (1989) discovered that three rectangular element rosettes have an optimal numbering system when grid numbers 1 and 3 are set such that they are perpendicular to each other as any other alignment will produce incorrect strains. Grid number 2 should then be set so that it is 45º away from grid 1. In the delta rosette configuration, the axes of grids 2 and 3 should be 60º and 120º away respectively, in the same direction, away from grid 1. A counter clockwise direction of numbering is preferable due to it being consistent with the measurement of angles in that direction as positive (Stevenson and Harding, 1984). Examples of this numbering system can be seen in Figure 63 which depicts a counter clock wise numbering system for various types of rosettes.

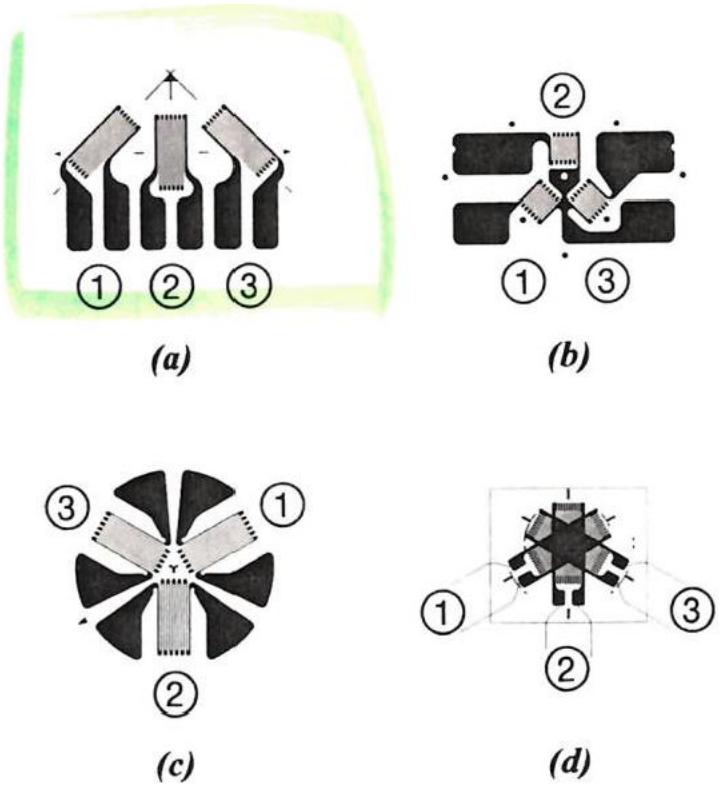

Figure 63. Counterclockwise numbering of gage grids of various rosettes.

Once the rosette strain measurements are obtained the next logical step is to calculate the principle strains through the strain transformation relationship. In simple terms it is the expression of the relationship between the normal strain of a test surface and the two principle strains including the angle from the principal axis in the direction off the strain (Usui and Shirlrosnl, 1982). This can be most easily observed when the Mohr's circle for strain is transposed upon the forces as Figure 64 shows. This principal strain can then be calculated for any angle θ using the following equation:

$$\epsilon_o = \frac{\epsilon_P + \epsilon_Q}{2} + \frac{\epsilon_P - \epsilon_Q}{2}\cos 2\theta$$

Figure 65 demonstrates the alignment that the rectangular rosette should be placed in. When the Mohr's circle is superimposed upon it as in Figure 66, the strain determined by each grid can then be calculated using the following set of equations:

$$\epsilon_1 = \frac{\epsilon_P + \epsilon_Q}{2} + \frac{\epsilon_P - \epsilon_Q}{2}\cos 2\theta$$
$$\epsilon_2 = \frac{\epsilon_P + \epsilon_Q}{2} + \frac{\epsilon_P - \epsilon_Q}{2}\cos(2\theta + 45^o)$$
$$\epsilon_3 = \frac{\epsilon_P + \epsilon_Q}{2} + \frac{\epsilon_P - \epsilon_Q}{2}\cos(2\theta + 90^o)$$

One interesting feature is that by using measured values for each grid direction they can be plugged back into the above set of equations and obtain both the principle strains and the angle with the following set of equations:

$$\epsilon_{P,Q} = \frac{\epsilon_1 + \epsilon_3}{2} \pm \frac{1}{\sqrt{2}}\sqrt{((\epsilon_1 - \epsilon_2)^2 + (\epsilon_2 - \epsilon_3)^2)}$$
$$\theta = \frac{1}{2}\tan^{-1}\frac{(\epsilon_1 - 2\,\epsilon_2 + \epsilon_3)}{(\epsilon_1 - \epsilon_3)}$$

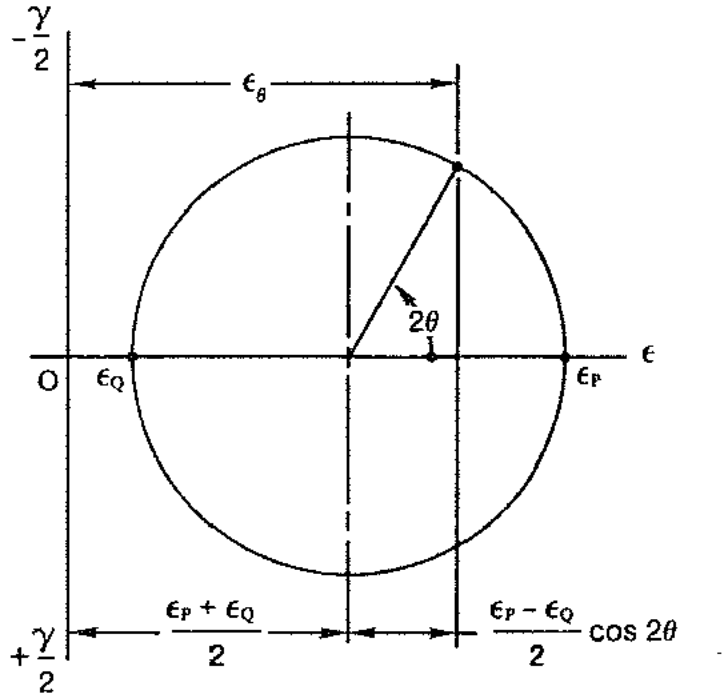

Figure 64. Strain transformation of principle strain ϵ_o into directional strains ϵ_P and ϵ_Q using Mohr's circle for strain.

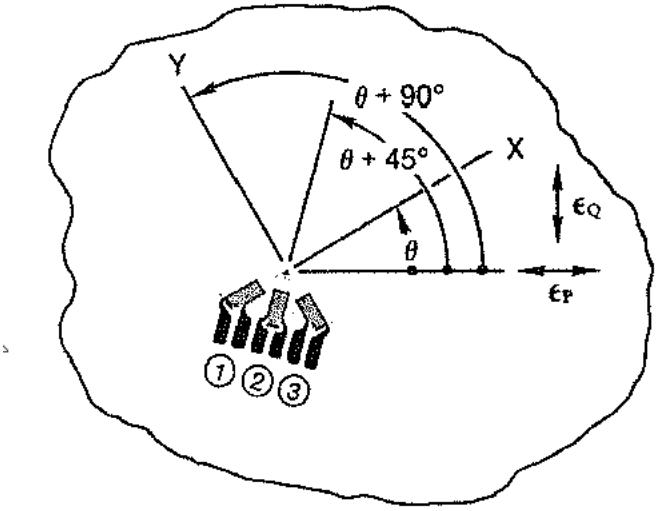

Figure 65. Rectangular rosette placed on surface with Grid 1 at angle θ from principle axis.

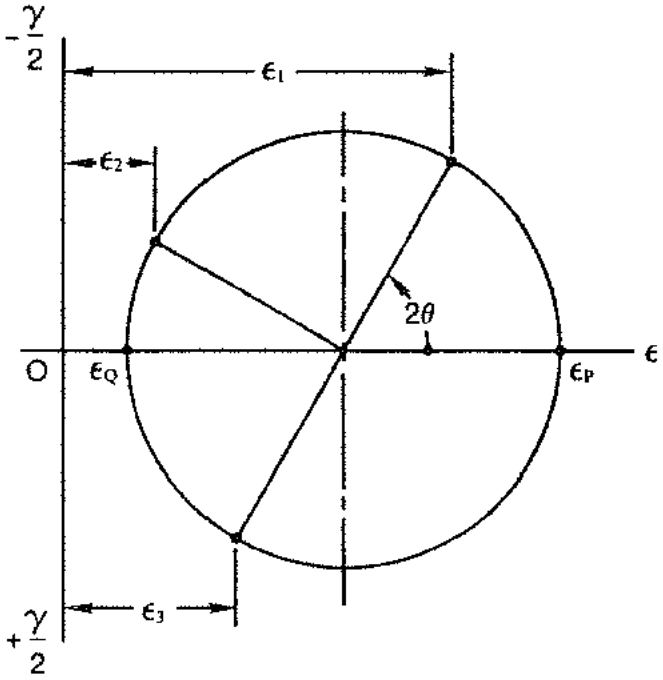

Figure 66. Axes of rectangular rosette placed on Mohr's circle for strain.

When using a delta rosette the process is very similar with the only alteration being that the grid angles will change for grid 2 and grid 3. Figure 67 displays the different alignment and angular changes while Figure 68 shows these changes upon the Mohr's circle. The equations for calculating the strain sensed by each grid then become:

$$\epsilon_1 = \frac{\epsilon_P + \epsilon_Q}{2} + \frac{\epsilon_P - \epsilon_Q}{2}\cos 2\theta$$
$$\epsilon_2 = \frac{\epsilon_P + \epsilon_Q}{2} + \frac{\epsilon_P - \epsilon_Q}{2}\cos(2\theta + 60^o)$$
$$\epsilon_3 = \frac{\epsilon_P + \epsilon_Q}{2} + \frac{\epsilon_P - \epsilon_Q}{2}\cos(2\theta + 120^o)$$

One interesting feature is that by using measured values for each grid direction they can be plugged back into the above set of equations and obtain both the principle strains and the angle with the following set of equations:

$$\epsilon_{P,Q} = \frac{\epsilon_1 + \epsilon_2 + \epsilon_3}{3} \pm \frac{\sqrt{2}}{3}\sqrt{((\epsilon_1 - \epsilon_2)^2 + (\epsilon_2 - \epsilon_3)^2 + (\epsilon_3 - \epsilon_1)^2)}$$
$$\theta = \frac{1}{2}\tan^{-1}\frac{\sqrt{3}(\epsilon_3 - \epsilon_2)}{(2\,\epsilon_1 - \epsilon_2 - \epsilon_3)}$$

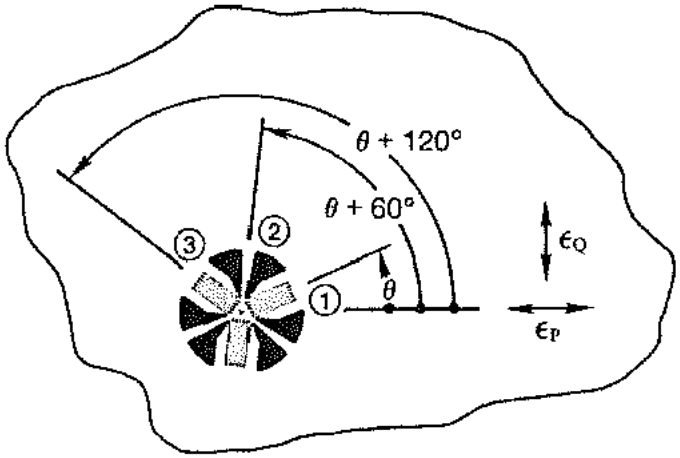

Figure 67. Delta rosette placed on surface with Grid 1 at angle θ from principle axis.

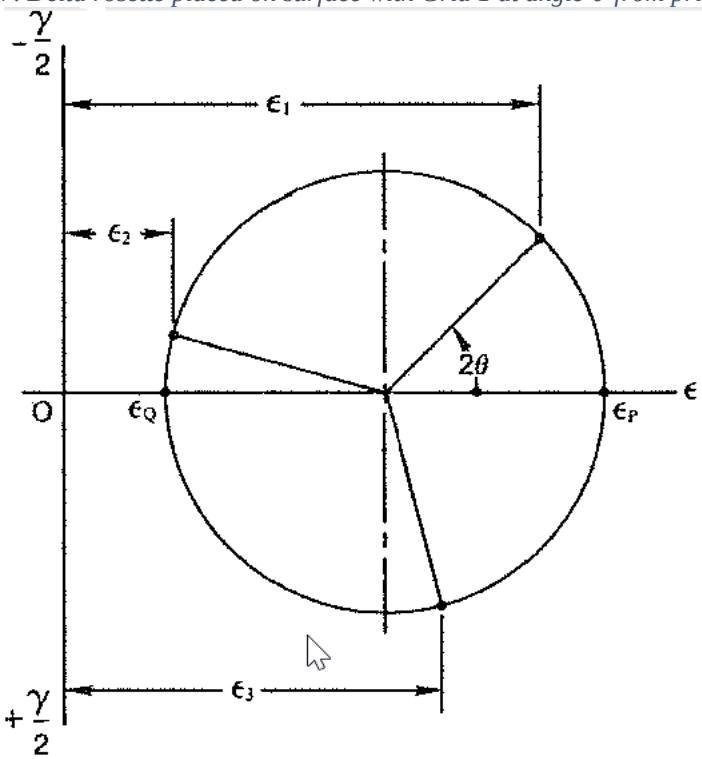

Figure 68. Axes of delta rosette placed Mohr's circle for strain.

It is important to keep in mind that positive angles must be interpreted as counter clock wise. It is key for the three main steps of obtaining the principal stresses. First the measured strain on the sample surface is obtained from the strain gage rosette. The measured strains are then transformed to principle strains. From these principle strains, the principle stress can be calculated using Hooke's law in cases where both the elastic modulus (E) and Poisson's ratio (γ) are known for the sample being tested using the following equations:

$$\sigma_P = \frac{E}{1-\gamma^2}\left(\epsilon_P + \gamma\epsilon_Q\right)$$

$$\sigma_Q = \frac{E}{1-\gamma^2}\left(\epsilon_Q + \gamma\epsilon_P\right)$$

One key component in the formula is that there needs to be a linear relationship between stress and strain over the range of testing stresses. This means that the equations are likely not going to be able to be used for composite materials and alloys as they have a tendency to produce non-linear stress and strain ratios(Measurement Group, 1990). Errors in the elastic modulus will impact the calculations in a much greater manner that Poisson's ratio due to its position in the numerator so care should be taken to get the most accurate value. Another issue with composite materials is that generally they employ directional fiber reinforcement which means that the Hooke's law equations would not be applicable.
Some of the most common possible places where error may occur include strain gage measurements, thermal sensitivity, leadwire resistance effects, and incorrect shunt calibration(Measurement Group, 1990). Additional error will often occur if several individual single element strain gages are wired together to form a rosette instead of purchasing a commercially produced rosette as it is often very difficult to install at the precise alignment due to their small size.

CONCLUSION

The split Hopkinson bar is a device for material testing that is used to determine the material properties of a specimen at very high strain rates.The split Hopkinson bar operates by using a launched striker to impact a set of bars and a suspended sample to create unidirectional stress waves. The measurement and recording of their propagation reveal the material properties of the specimen. There are many factors that must be considered in designing and operating a Hopkinson bar system. A key requirement for getting accurate results from the Hopkinson bar system is that the bars and specimen must remain firmly in place without causing any vibrations. It is also important to know some of the properties of the materials being tested as it will determine what bar size to use and whether a pulse shaping technique will be required.

REFERENCES

[1] *Al-Juaid, A.A. and R. Othman. (2016). Modeling of the Strain Rate Dependency of Polycarbonate's Yield Stress: Evaluation of Four Constitutive Equations. Journal of Engineering, Cairo*
[2] *Bagchi, A. and P. K. Wright, (1987). Proc. Roy. Soc. Lon. A409, 99-107.*
[3] *Bagom, A. (1983). Ph.D. thesis, Carnegie-Mellon University, Pittsburgh, Pennsylvania.*
[4] *Baranowski, P., R. Gieleta, J. Malachowski, K. Damaziak, and L. Mazurkiewicz. (2014). Split Hopkinson pressure bar impulse experimental measurement with numerical validation. Metrology and Measurement Systems; Warsaw 21.1 (2014): 47-58.*
[5] *Beteta, O. and S. Ivanova. (2015). Cool down with liquid nitrogen. Chemical Engineering Processes. September 2015. 30-35*
[6] *Brotrob. (2012a). How to strain gauge a Split Hopkinson bar part 1: Preparation and Cleaning. Accessed at: https://www.youtube.com/watch?v=LOKXZbZTx4s*
[7] *Brotrob. (2012b). How to strain gauge a Split Hopkinson bar part 2: Attaching Soldering Pads. Accessed at: https://www.youtube.com/watch?v=9I56wGYoUDA*
[8] *Brotrob. (2012c). How to strain gauge a Split Hopkinson bar part 3: Attaching Strain Gages. Accessed at: https://www.youtube.com/watch?v=sDFC6PG0YB0*
[9] *Brotrob. (2012d). How to strain gauge a Split Hopkinson bar part 4: Preparation and Soldering. Accessed at: https://www.youtube.com/watch?v=_x6WWbjeeqc*
[10] *Brotrob. (2012e). How to strain gauge a Split Hopkinson bar part 5: Soldering and Final Steps. Accessed at: https://www.youtube.com/watch?v=oCwEUD6X7JA*
[11] *Chakraborty, T., Mishra, S., Loukus, L., Halonen, B., and B. Bekkala (2015). Characterization of rocks through large diameter split hopkinson pressure bar and achieved force equilibrium. International Journal of Impact Engineering, 27: 118-130.*
[12] *Childs, T.H. and K. Maekawa, (1988). Proc. 1st lnt. Conf. Behaviour of Materials. Stratford, Inst. Metals, London.*
[13] *Christman, D.R., W.M. Isbell, S.G. Babcock, A.R. McMillan and S.J. Green (1971) Measurement of dynamic properties of materials. Report No. DASA 2501-2 , MSL 70-23, vol. II, Arlington, Va.*
[14] *Clarke, S. D., S. D. Fay, S. E. Rigby, A. Tyas, J. A. Warren, and J. J Reay. (2016) Blast Quantification Using Hopkinson Pressure Bars. J. Vis. Exp. (113), e53412, doi:10.3791/53412.*
[15] *Cincinnati Sub-Zero Products, LLC. (2017). Points to Consider when Purchasing & Installing Environmental Chambers. 95018. 1-16.*
[16] *Davies, R.M. (194 8) A critical study of the Hopkinson Pressure Bar. Phil. Transactions of the Royal Society, London, Series A, 240: 375.*
[17] *Davies, E.D.H. and Hunter, S.C. (1963) The dynamic compression testing of solids by the method of the Split Hopkinson Pressure Bar. Journal of Mech. Physical Solids, ll: 155.*
[18] *Davis, C.E. (1971). Int. J. Mach. Tool Des. Res. 11-31.*
[19] *Diemand, D. and M. Moritz. (1990). In-House Laboratory Independent Research Program-FY88. CRREL Special Report 90-34*
[20] *Duffy, J. and J. Harding. (1979). Proc. 2rid Conf. Mech. Prop. High Rates of Strain. Inst. of Physics, London.*

[21] Duffy, J., J.D. Campbell and R.H. Hawley (1971) On the use of a torsional Split Hopkinson Bar to study rate effects in 1100-0 aluminum . Journal of Applied Mechanics, Transactions of the ASHE, 38: 83-91.
[22] Dutta, P. K. (2001). The Fracturing Processes of Freezing Composites. Proceedings of the Eleventh International Polar Engineering Conference 118-123.
[23] Dutta, P. K. and K. Kunsoo. (1993). High-strain-rate tensile behavior of sedimentary and igneous rocks at low temperatures. CRREL Report: 93-16.
[24] Dutta, P. K. and D. Hui. (1991). Energy absorption of graphite/epoxy plates using Hopkinson bar impact. CRREL Report: 91-20.
[25] Dutta, P.K., D. Farrell and J. Kalafut (1987) The CRREL Hopkinson bar apparatus. USA Cold Regions Research and Engineering Laboratory, CRREL Special Report 87-24.
[26] Field, J.E. and S.M. Walley (2013). Review of the dynamic properties of materials; history, techniques, and results. Rock Dynamics and Applications. 8: 3-21
[27] Follansbee, P.S. and U. F. Kocks, (1988). Acta Metall. 36, 81-88.
[28] Follansbee, P.S. and L.E. Murr (1986). Metallurgical Aspects of Shock Wave and High Strain Rate Phenomena. Marcel Dekker, New York.
[29] Follansbee, P.S., Regazzoni, G. Harding, J., and U. F. Kocks. (1984). Proc. 3rd Conf. Mech. Prop. High Rates of Strain. Inst. of Physics, London.
[30] Hadjuck, D.A. (1987) Computer Manual – CRREL Hopkinson Bar Laboratory
[31] Harding, J., E.O. Wood and J.D . Campbell (1960) Tensile testing of materials at impact rates of strain. Journal of Mechanical Engineering Science. 88.
[32] Hauser, F .E. (1966) Techniques for measuring stress-strain relations at high strain rates. Experimental Mechanics. 395.
[33] Hopkinson, B. (1914) A method of measuring the pressure produced in the de tonation of high explosives or by the impact of bullets. Philosophical Transactions of the Royal Society, London, Serie s A, 213(10): 437-456.
[34] Kang, P., K. Gao, J. Liu, Y. Liu, and Z. Zhang. (2017). Experimental and Numerical Evaluation of Rock Dynamic Test with Split-Hopkinson Pressure Bar. Advances in Materials Science and Engineering; New York.
[35] Kato, S., Yamaguchi, K. and M. Yamada. (1972). Trans. ASME, J. Engng Ind. 94, 683-696.
[36] Kececioglu, D. (1958).Trans. ASME 80, 158-179.
[37] Kim, Y. S. and S. Young. (2015). A Parameter Study for the Test Condition of Kolsky Bar Experiment Applied Mechanics and Materials 752-753.Advanced Engineering and Technology (20150400): 477-480.
[38] Klepaczko, J. (1980) In Mechanical properties at high rates of strain. (J. Harding, Ed.) London: Institute of Physics, p. 201.
[39] Kolsky, H. (1949) An investigation of the mechanical properties of mate rials at very high rates of loading. Proceedings of the Physical Society, 62 :676-700.
[40] Kruszka, L., M. Mariusz, and Z. Mariusz. (2014). Experimental analysis of visco-plastic properties of the aluminum and tungsten alloys by means of Hopkinson bars technique.Applied Mechanics and Materials; Zurich 566 : 110-115.
[41] Lau, K.T., P.K. Dutta, L.M. Zhou, and D. Hui. (2001). Mechanics of bonds in an FRP bonded concrete beam. Composites Part B 32: 491-502.
[42] Li, X., T. Zhou, Tao, D. Li, and Z. Wang.(2016). Experimental and Numerical Investigations on Feasibility and Validity of Prismatic Rock Specimen in SHPB. Shock and Vibration; Cairo.
[43] Lindholm, U.S. and Yeakley, L.M. (1968) High strain rate testing: Tension and compression. Experimental Mechanics. (1): 1-9.
[44] Liu, W.,R.Q. Shen,X.X. Sun, and Y.H. Ye. (2013). Effect of Acceleration Pulse Shape on Damage of the Specimen under Hopkinson High-G Loading.Applied Mechanics and Materials; Zurich 455: 236.
[45] Mahdi, M.I. and T.H. Childs (1989). Ann. CIRP 38-55.
[46] Malvern, L.E. and J. Harding. (1984) Experimental and theoretical approaches to characterization of material behavior at high strain rates of deformation, in Mechanical Properties of High Rates of Strain. London: Institute of Physics, 1-17.
[47] Measurement Group.(2010). Optimizing Strain Gage Excitation Levels. Tech Note TN-502
[48] Measurement Group.(1990). Strain Gage Rosettes – Selection, Application, and Data Reduction. Tech Note TN-515
[49] Merchant, M.E. (1945). J. Appl. Phys. 16, 267-272.
[50] Meyer, M.L. (1963). Interpretation of Surface-Strain Measurements in Terms of Finite Homogeneous Strains. Experimental Mechanics. 294-301.
[51] Nicolaescu, G.I., G.A. Stefan, C. Enache, Constantin, and M. Valeriu. (2015). Torsional testing at high strain rates using a Kolsky bar. Land Forces Academy Review; Sibiu 20.2: 233-242.
[52] Nicholas, T. (1975) Air Force Materials Laboratory Report AFML-TR-75-54. Ohio : Wright Patterson AFB.
[53] Nicholas, T. (1981) Tensile testing of materials at high rates of strain. Experimental Mechanics, (5): 177-185.
[54] Panowicz, R. and J. Janiszewski, (2016). Tensile Split Hopkinson Bar Technique: Numerical Analysis of the Problem of Wave Disturbance and Specimen Geometry Selection. Metrology and Measurement Systems; Warsaw 23.3 : 425-436.
[55] Panowicz, R, J. Janiszewski, and M. Traczyk,(2017). Strain measuring accuracy with splitting-beam laser extensometer technique at split Hopkinson compression bar experiment. Polska Akademia Nauk. Bulletin of the Polish Academy of Sciences: Technical Sciences; Warsaw 65.2 : 163-169.
[56] Paul, Jastin V. (2015). Development of a miniature tensile Kolsky bar for dynamic testing of thin films. New Mexico Institute of Mining and Technology, ProQuest Dissertations Publishing,

[57] Ramalingham, S. and K. J. Trigger, (1976). J. MTDR 16, 335-351.
[58] Rhorer, R.L., M. A. Davies, M.l D. Kennedy, B. S. Dutterer, and T. J. Burns. (2002). CONSTRUCTION AND ALIGNMENT OF A KOLSKY BAR APPARATUS. Journal of the International Societies for Precision Engineering and Nanotechnology. (8):534-562.
[59] Ross, C.A., W.H. Cook and L.L. Wilson (1984) Dynamic tensile tests of composite materials using a Split Hopkinson Pressure Bar. Experimental Techniques, 30: 30-33.
[60] Samanta, S.K. (1970). Proc. 11th Int. MTDR Conf.University of Birmingham.
[61] Samanta, S.K. (1971). J. Mech. Phys. Solids 19, 117-135.
[62] Shin, H.H., H.Y. Lee, J.B. Kim, and Y.H. Yoo. (2015).A Numerical Verification of the Reliability of a Split Hopkinson Pressure Bar with a Total Bar Length of 3 m and a Diameter of 1 Inch Applied Mechanics and Materials 799-800.Mechanical and Electrical Technology VII : 681-684.
[63] Sokovikov, M., D. Bilalov, V. Oborin, V. Chudinov, and S. Uvarov, Sergey. (2016).Structural mechanisms of formation of adiabatic shear bands. Frattura ed Integritá Strutturale; Cassino 38 : 296-304.
[64] Song, B., K. Nelson, R. Lipinski, J. Bignell,, and G.B. Ulrich. (2015). Dynamic high-temperature Kolsky tension bar techniques.EPJ Web of Conferences; Les Ulis 94 Les Ulis: EDP Sciences.
[65] Stevenson, M.G. and J. Harding. (1984). Proc. 3rd Conf. Mech. Prop. High Rates of Strain. Inst. of Physics, London.
[66] Stoops, R.L. (1997). Fabrication of Temperature Control Cold Boxes for the Hopkinson Bars.
[67] Troke, R.W. (1967). Flat vs Stacked Rosettes, Experimental Mechanics 24-28.
[68] Tsai, S.W. and H.T. Hahn. (1980). Introduction to Composite Materials. Technomic Publishing Company.
[69] Usui, E. and T. Shirlrosnl, (1982). ASME PED 7-13
[70] Zorev, N. (1963). ASME Proc. Int. Prod. Engng Res. Conf., Carnegie Institute of Technology, Pittsburgh. 42-51.
[71] Zou, C. and L. Wong, and Y. Ngai; (2016).Size and Geometry Effects on the Mechanical Properties of Carrara Marble Under Dynamic Loadings. Rock Mechanics and Rock Engineering; Wien 49.5 : 1695-1708.